

RESCON '09

Research Student Conference

22 - 24 June 2009

**BOOK OF
ABSTRACTS**

Brunel
UNIVERSITY
WEST LONDON

SCHOOL OF ENGINEERING AND DESIGN



Welcome Note from the School of Engineering and Design (SED)

It is my pleasure to welcome you to ReSCon'09, the Second SED Research Student Conference. This follows the success of the first ReSCon, organised by the School of Engineering and Design at Brunel University in 2008, which consisted of 35 oral and 31 poster presentations. ReSCon'09 is a larger, three-day event consisting of 49 oral and over 32 poster presentations, aimed at giving our research students an opportunity to practice their presentation skills and present their findings to their colleagues, academics and industrial collaborators.

The abstracts contained in this book focus on a particular aspect of the students' research, selected to appeal to a diverse audience rather than attempting to describe their entire doctoral project. They have all been peer-reviewed by academics and fellow research students.

The ReSCon Committee, composed entirely of research students, have invested considerable time and effort to ensure the success of the event. They deserve our appreciation in organising every aspect of the conference. The School is also grateful to Dr Rhys Morgan for his academic support and to the SED Research Office, particularly Mrs Carole Carr, whose administrative support was crucial in making this event successful.

I trust you will enjoy the conference and will find these three days interesting and informative.

A handwritten signature in black ink, appearing to read "Luiz C. Wrobel". The signature is written in a cursive, flowing style.

Professor Luiz C. Wrobel

Deputy Head of School (Research)

School of Engineering and Design

Brunel University, UK



Welcome Note from ResCon09 Committee

Dear Participant,

On behalf of the School of Engineering and Design (SED), the affiliated research institutes and ResCon09 committee members, it is our great pleasure to welcome you to the second SED Research Student Conference (ReSCon2009) being held 22-24th June 09 in the Lecture Centre.

This year's Rescon09 conference consists of three full days of technical presentations, along with a poster session and social event. We are confident that you will find the events this year to be rewarding both professionally and personally.

The committee members will be available at registration to introduce themselves, welcome you to the conference and hand out the conference packs (including the Book of Abstracts, the conference programme and other useful information).

We would like to express our great thanks to Prof Luiz Wrobel, Deputy Head of School (Research), for his constant support, along with Dr Rhys Morgan, in helping to make this conference possible. Our special thanks also goes to Carole Carr, Research Office Manager and her great team, including Karen (the temp), for their help and guidance when ever needed. They have been the driving force behind many successful SED events and we are certain that they will ensure that ReSCon continues to play a key role in contributing to research and innovations in the School of Engineering & Design.

We would also like to thank the Vice Chancellor Prof Chris Jenks, for his valued time and support, our supervisors and all the academic staff providing talks during the sessions.

Finally we would like to thank the Heads of the School of Engineering & Design and the Graduate School for sponsoring the conference and providing the prizes.

Thank you for attending Rescon09. We hope you will enjoy the conference and look forward to welcoming you.

The ReSCon Committee 2009

RESCON '09

SED Research Student Conference

Brunel University

22-24th June 2009



(Back row from left to right: A Cifter, A Khamsehnezhad, J Azizi, S Hume-Chignell, R Swash. Front row from left to right: S Memon, A Umar, Ritwik, M Silva)

Committee Members 2009

Sally Home-Chignell	<i>Chair</i>
Abubakar Umar	<i>Vic-Chair</i>
Manjula Silva	<i>Abstract and Presentation Coordinator</i>
Mohammad Rafiq Swash	<i>Website Coordinator</i>
Abduesselam Cifter	<i>Graphics Coordinator</i>
Jawid Azizi	<i>Registration Coordinator</i>
Ritwik	<i>Poster Coordinator</i>
Amir Khamsehnezhad	<i>Events Coordinator</i>
Shahzad Memon	<i>Advertising Coordinator</i>

Advisory Panel

Prof. Luiz Wrobel	<i>Deputy Head of School (Research)</i>
Mrs. Carole Carr	<i>Research Office Manager</i>
Dr. Rhys Morgan	<i>Lecturer</i>

Table of Contents

Welcome note from the School of Engineering & Design	i
Welcome note from ResCon09 Committee	ii
List of ResCon09 Committee Members	iii
Conference Programme	vii
Day One Sessions	1
Evaluation of a Commercial Programmable Floating-Gate MOSFET as a Radiation Dosimeter for In-Vivo Dosimetry	2
Understanding Mobile phone users by Cognitive style and concept map	5
Novel Cross-Layer Scheduling for Single-Cell OFDMA Systems with Heterogeneous QoS and Partial CSIT	8
Determining Aircraft True Airspeed in Straight and Level Flight for Handicapped Air Racing	12
Grain Refinement of Wrought Al Alloy by Intensive Melt Shearing.....	15
Hardware Implementation and Power Modelling of 2D Haar Transform for Medical Imaging	20
Non-Newtonian Behaviour in Molten Lead	24
Grain Growth Simulation Using Cellular Automata.....	27
Effect of Ultrasonic Vibrations on Processing Parameters of Polyethylene and Thermal Mechanical Properties of Extrudate	30
FPGA Implementation of Image and Signal Processing IP cores Using Dynamic Partial Reconfiguration	33
Use of Metallic Resonant Sensors in Torque Measurement transfer standard	36
Materials from Renewable Resources for Packaging Applications: Polylactic Acid and Starch	39
A Novel Design for a Reconfigurable Micro-processing Cell.....	40
A Comprehensive Bandwidth Requesting Method for IEEE 802.16 WiMax Networks using piggyback Requests	46
Monoclonal antibody purification using robotic phase system selection coupled with counter current chromatography (CCC).....	49
Load Flow Analysis with Voltage and Reactive Power Optimization in Distribution Networks using NEOS Solvers.....	52

Day Two Sessions	55
Various Delay Channel Access Algorithms for the IEEE 802.11n	56
Effects of the Interaction between Physical and Mental Workload on Human Performance	59
Smart implants for measurement of strain during fracture healing.....	62
Fingerprint Sensing: Issues and Solutions	65
Simulating of graphane's epitaxial growth on SiC surface.....	69
Content based Image Retrieval with Semantic Annotations: A Review and Evaluation.....	73
The Collection, Communication and Inclusion of User Data in Design.....	77
Grid Connection Oriented Modelling of Full Converter with turbines: Provision of frequency response	80
Investigating Factors affecting Loss of Control of General Aviation Aircraft	84
Dynamic Metadata Synchronization for Multimedia Retrieval	89
3D Video Transmission over Wireless Networks.....	92
Coordinated Active Voltage Control for Distribution Networks with Distributed Generation	96
Sketch-Based Clothing 3D Virtual Humans	99
Neuro-Fuzzy System and Particle Swarm for Optimizing Metals Heat Treatment Process.....	102
Efficient Implementation of Wavelet Packet for Medical Image Segmentation and Analysis.....	106
Anthropometrics without Numbers!: An Investigation of Designer's Use and Preference of People Data.....	109
Quality of Service Management for Real-Time Rich-Media Applications and Development of Related Software.....	113
Day Three Sessions	116
An Intelligent System for Pet Tumour Detection and Quantification.....	117
Simulation of a Novel, Toroidal-Type, CVT.....	120
Efficient Low Power Reconfigurable Architectures for 3D Medical Image Compression	123
Robustness of Complex Networks to Link Damage.....	127
Designing Medical Devices for Lay Use	129

Forecasting Routing Techniques using Location information for wireless adhoc networks (FORTEL)	132
Liquid-Vapour Visualization of an evaporating diesel spray using Laser Induce Exciplex Fluorescence Technique	135
Performance of a Transparent Polymer Film UWB Antenna Under Varying Radius of Curvature.	139
Inclusive Design for Air Travel	142
Pre-Clinical Assessment of a Smart Piezo-Actuated Limb Lengthening Device	145
A Review of Short-term Electricity Price Forecasting Techniques in Deregulated Electricity Markets	144
Elastohydrodynamic Film Thickness in Variable Conditions	148
Reconfigurable Patch Antenna for Cognitive Radio and Wireless Mobile Applications	155
Operational Analysis of Security Constrained Optimal Reactive Power Flow Solutions	158
An Analysis of organisations that have purchased BS8887-1(2006).....	160

Day 1 Registration 8:30 – 8:50			
Welcome/Opening Speech	9:00 – 9:10	Prof. Chris Jenks, Vice Chancellor and Principal, Brunel University	
		Prof. Savvas Tassou, Head, School of Engineering and Design	
Conference Chair	9:10 – 9:15	Ritwik ReSCon 09 Committee Member	
Session 1	9:15 – 10:35	Rajiv Bose	Evaluation of a Commercial Programmable Floating-Gate MOSFET as a Radiation Dosimeter for In-Vivo Dosimetry
		Wen-Chia Wang	Understanding mobile phone users by cognitive style and concept map
		Charilaos Zarakovitis	Novel Cross-Layer Scheduling for Single-Cell OFDMA Systems with Heterogeneous QoS and Partial CSIT
		Sally Hume-Chignell	Determining Aircraft True Airspeed in Straight and Level Flight for Handicapped Air Racing
Break	10:35 – 11:00	Tea/Coffee	
Introduction	11:00 – 11:05	Prof. Zhongyun Fan Head of the Brunel Centre for Advanced Solidification Technology	
Session 2 <i>Session Chair: Abubakar Umar</i>	11:05 – 12:25	Hu Tian Li	Grain Refinement of Wrought Al Alloy by Intensive Melt Shearing
		Abdul Naser Sazish	Hardware Implementation and Power Modelling of 2D Haar Transform for Medical Imaging
		Ritwik	Non-Newtonian Behaviour in Molten Lead
		Fahad M. Almohaisen	Grain Growth Simulation Using Cellular Automata
Break	12:25 – 13:55	Lunch/ Poster Session	
Introduction	13:55 – 14:00	Prof. Jack Silver Head of The Wolfson Centre for Materials Processing	
Session 3	14:00 – 15:20	Amir Khamsehnezhad	Effects of Ultrasonic Vibrations on Processing Parameters of Polyethylene and Thermal and Mechanical Properties of Extrudate
		Benjamin Krill	FPGA Implementation of Image and Signal Processing IP cores Using Dynamic Partial Reconfiguration
		Jittakant Intiang	Use of Metallic Resonant Sensors in Torque Measurement transfer standard
		Kodikara Manjula Dilkushi Silva	Materials from renewable resources for packaging applications: Polylactic acid and Starch
Break	15:20 – 15:45	Tea/Coffee	
Introduction	15:45 – 15:50	Dr. Rhys Morgan Advanced Manufacturing and Enterprise Engineering	
Session 4	15:50 – 17:10	Rakan Alsharif	A Novel Design for a Reconfigurable Micro-processing Cell
		Usman Ahmed Ali	A Comprehensive Bandwidth Requesting Method for IEEE 802.16 WiMax Networks using Piggyback Requests
		Samantha Fernando	Monoclonal antibody purification using robotic phase system selection coupled with counter current chromatography (CCC)
		Jan Veleba	Load Flow Analysis with Voltage and Reactive Power Optimization in Distribution Networks using NEOS Solvers
Social Event Mead/Cavendish Rooms (Hamilton Centre) 17:30 - 20:30pm			

Day 2 Registration 9:00– 9:30			
<i>Welcome/Opening Speech</i>	9:30 – 9:40	Prof. Luiz Wrobel <i>Deputy Head of School (Research), School of Engineering and Design</i>	
<i>Conference Chair</i>		Ritwik <i>ReSCon 09 Committee Member</i>	
Session 5	9:40 – 11:00	Dionysios Skordoulis	Various Delay Channel Access algorithms for the IEEE 802.11n
		Abdulrahman Basahel	Effects of the Interaction between Physical and Mental Workload on Human Performance
		Jaya Luxshmi Nemchand	Smart implants for measurement of strain during fracture healing
		Shahzad Memon	Fingerprint Sensing: Issues and Solutions
Break	11:00 – 11:20	Tea/Coffee	
<i>Introduction</i>	11:20 – 11:25	Prof. Kai Cheng <i>Head of Advanced Manufacturing & Enterprise Engineering</i>	
Session 6	11:25 – 13:05	Nikolai Issakov	Simulating of graphene's epitaxial growth on SiC surface
		Nasullah Khalid Alham	Content based Image Retrieval with Semantic Annotations: A Review and Evaluation
		Chris McGinley	The Collection, Communication and Inclusion of User Data in Design
		Dominic Banham-Hall	Grid Connection Oriented Modelling of Full Converter wind turbines: Provision of frequency response
		Michael Bromfield	Investigating Factors affecting Loss of Control of General Aviation Aircraft
Break	13:05– 14:05	Lunch/ Poster Session	
<i>Introduction</i>	14:05 – 14:10	Prof. Abdul Sadka <i>Head of Electronic and Computer Engineering</i> <i>Director of Centre for Media Communications Research</i>	
Session 7	14:10 – 15:30	Rafiq Swash	Dynamic Metadata Synchronisation for Multimedia Retrieval
		Umar Abubakar Sadiq	3D Video Transmission over Wireless Networks
		Maciej Fila	Coordinated Active Voltage Control for Distribution Networks with Distributed Generation
		Hui YU	Sketch-Based Clothing 3D Virtual Humans
Break	15:30 – 15:50	Tea/Coffee	
<i>Introduction</i>	15:50 – 15:55	Prof. John Sumpter <i>Head of Institute for the Environment</i>	
Session 8	15:55 – 17:15	Tawfeeq Al-kanhal	Neuro-Fuzzy System and Particle Swarm for Optimising Metals Heat Treatment Process
		Shadi Mahmoud Al-Zu'Bi	Efficient Implementation of Wavelet Packet for Medical Image Segmentation and Analysis
		Farnaz Nickpour	Anthropometrics Without Numbers: An investigation of designers' use of people size data
		Sivanantharasa Panchadcharam	Quality of Service Management for Real-Time Rich-Media Applications and Development of Related Software
End of Second Day			

RESCON '09

School of Engineering and Design

Research Student Conference

Brunel University

22nd – 24th June 2009

Venue: Lecture Theatre D, Registration: LC206/208

Day 3 Registration 9:00- 9:30			
<i>Welcome/Opening Speech</i>	9:30 – 9:35	<i>Dr. Kate Hone</i> <i>Director of the Graduate School</i>	
<i>Conference Chair</i>		<i>Ritwik</i> <i>ReSCon 09 Committee Member</i>	
Session 9	9:35 – 11:00	Mhd Saeed Sharif	An Intelligent System for Pet Tumour Detection and Quantification
		Colin Bell	Simulation of a Novel, Toroidal-Type, CVT
		Afandi Ahmad	Efficient Low Power Reconfigurable Architectures For 3D Medical Image Compression
		Emil Gegov	Robustness of Complex Networks to Link Damage
Break	11:00 – 11:20	Tea/Coffee	
<i>Introduction</i>	<i>11:20 – 11:25</i>	<i>Prof. David Harrison</i> <i>Head of Brunel Design</i>	
Session 10	11:25 – 13:05	Abdusselam Cifter	Designing Medical Devices for Lay Use
		Hadi Noureddine	Forecasting Routing Technique using Location information for wireless ad hoc networks (FORTEL)
		Mohammad Reza Herfatmanesh	Liquid-Vapour Visualization of an evaporating diesel spray using Laser Induced Exciplex Fluorescence Technique
		Thomas Peter	Performance of a Transparent Polymer Film UWB Antenna Under Varying Radius of Curvature
		Laura Baird	Inclusive Design for Air Travel
Break	13:05-14:05	Lunch/ Poster Session	
<i>Introduction</i>	<i>14:05-14:10</i>	<i>Prof. Tadeusz Stolarski</i> <i>Head of Mechanical Engineering</i>	
Session 11	14:10 – 15:10	Rhona MacInnes	Pre-Clinical Assessment of a Smart Piezo-Actuated Limb Lengthening Device
		Linlin Hu	A Review of Short-term Electricity Price Forecasting Techniques in Deregulated Electricity Markets
		Konstantinos Kalogiannis	Elastohydrodynamic Film Thickness in Variable Conditions
Break	15:10 – 15:30	Tea/Coffee	
Session 12	15:30 – 16:30	Hattan AbuTarboush	Reconfigurable Patch Antenna for Cognitive Radio and Wireless Mobile Applications
		Peter Macfie	Operational Analysis of Security Constrained Optimal Reactive Power Flow Solutions
		Alexander Plant	An analysis of organisations that have purchased BS 8887-1 (2006)
<i>Closing Ceremony</i>	<i>16:30 – 16:45</i>	<i>Prof. Luiz Wrobel</i> <i>Deputy Head of School (Research), School of Engineering and Design</i>	
End of Final Day			

RESCON '09

DAY ONE: SESSIONS



SED Research Student Conference

Brunel University

22-24th June 2009

Evaluation of a Commercial Programmable Floating-Gate MOSFET as a Radiation Dosimeter for In-Vivo Dosimetry

R. Edgecock¹, J. Matheson¹, M. Weber¹, E. G. Villani¹, R. Bose², A. Khan², D. R. Smith², I. Adil-Smith², and A. Gabrielli³.

¹STFC Rutherford Appleton Laboratory Particle Physics Dept., Chilton, Didcot, UK

²Centre for Sensors and Instrumentation, Brunel University, Uxbridge, UK

³University of Bologna, Physics Dept., Viale Berti Pichat 6/2, Bologna, Italy

Contact Author: rajiv.bose@brunel.ac.uk

Keywords (3): Dosimetry; In-Vivo Dosimetry; Radiation

Introduction

Dosimetry is the measurement of absorbed radiation, and *In-Vivo Dosimetry* (IVD) is the measurement of the absorbed radiation a patient's cancer receives during radiotherapy. The recommended use of IVD as standard practice for independent dose verification of tumour exposure during *External Beam Radiation Therapy* (EBRT) has long since been proposed [1].

The aim of this research project is two fold, to enhance the functionality of the currently available dosimeters used for IVD, and to design that dosimeter to also be sensitive in *HADRON THERAPY*. Functionality includes an implantable wireless dosimeter that provides real-time measurement of radiation exposure. Hadron therapy represents the next generation of radiotherapy (currently most EBRT exploits X-ray beams, but hadron therapy uses protons, neutrons, or heavier ions).

The *Floating-Gate MOSFET* (FGMOSFET) as a dosimeter has previously been investigated [2]. The scope of this paper is to highlight the suitability of the FGMOSFET for IVD based on completed research [3].

Although the effect of radiation on a FGMOSFET is similar to a standard MOSFET [4] there are some important differences. With both MOSFET and the FGMOSFET based dosimeters, the amount of absorbed radiation is inferred by measuring a shift in *threshold*

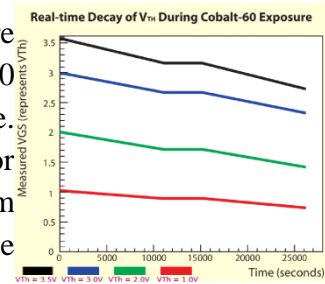
voltage (V_{Th}). However the radiation sensitive regions that cause this V_{Th} shift between a MOSFET and a FGMOSFET are different.

Methodology/Approach

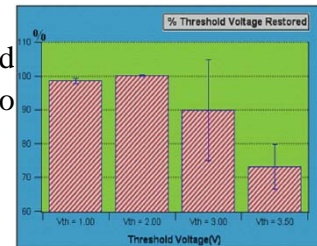
The experiment was to test the suitability of the FGMOSFET device as a dosimeter, specifically at radiation fluences comparable to those a patient would experience when undergoing radiotherapy. To do this, a PCB was fabricated to house an array of FGMOSFET devices (16 in total). The FGMOSFET devices were characterised initially, and in groups of 4 had their V_{Th} set from 1.0 V to >3.5 V. The array was exposed to a Cobalt-60 radiation source at a fixed distance of 10cm for a specific length of time with an absorbed radiation dose-rate 0.33 rad/s. A total received dose of 90 Gy was given to the array. The devices were then characterised again after radiation exposure, and finally recalibrated to test recoverability of the threshold voltage.

Results and discussion

The first plot illustrates the effect of radiation on V_{Th} , where V_{Th} reduces linearly with applied fluence. The total dose of 90 Gy is split into two clear phases separated by a rest phase. There is a visible difference in the rate of decay of V_{Th} for devices programmed with a higher initial V_{Th} . The maximum sensitivity reached is approximately 9.0 mV/Gy for the FGMOSFET with the V_{Th} .



The reprogramming results are summarised in the second figure. The highest threshold devices recovered up to approximately 73% of its pre-irradiated V_{Th} .



Further work for optimising the FGMOSFET includes designing a customised FGMOSFET specifically engineered with radiation sensitivity in mind.

Conclusion

The work presented results of gamma irradiation with Cobalt-60 of commercial programmable FGMOSFET devices. An interesting feature of these devices is their threshold programming capability with a resolution of the order of 1 mV. Under radiation exposure, the real-time shift in threshold voltage was measured for devices programmed at different thresholds. Sensitivity of up to approximately 9.0 mV/Gy was measured, along with excellent linearity and little sensitivity spread. The total noise measured with

the setup was low enough to allow a resolution of approximately 20 mGy. A room temperature annealing of approximately 8 mV was found for all devices.

After irradiation it was possible to restore the devices biased at the highest V_{Th} to approximately 73% of their initial value. The small size ($75 \times 200 \mu m^2$), sensitivity and programmable characteristics of these devices suggest that this technology would be very suitable for applications in the field of in-vivo dosimetry.

References

- [1] Donaldson, L. (2006) 2006 Annual Report of the Chief Medical Officer. Available at: <http://www.dh.gov.uk/en/Publicationsandstatistics/Publications/> [Accessed 8th November 2008].
- [2] M.N. Martin, D.R. Roth, A. Garrison-Darrin, P.J. McNulty and A.G. Andreou, FG MOS dosimetry: Design and implementation, IEEE Trans. Nucl. Sci. 48 (2001) 2050.
- [3] R. Edgecock *et al* (2009) 'Evaluation of commercial programmable floating gate devices as radiation dosimeters', JINST 4 P02002
- [4] G. Shani (2001) Radiation Dosimetry: Instrumentation and Methods. 2nd edn. CRC Press.



SED Research Student Conference

Brunel University

22-24th June 2009

Understanding Mobile Phone Users by Cognitive Style and Concept Map

Wen-Chia Wang, Mark Young, Joseph Giacomini

Human-Centred Design Institute, School of Engineering and Design, Brunel University,
Uxbridge, Middlesex, UK

wen-chia.wang@brunel.ac.uk

Keywords: easy to use, concept maps, cognitive style

Understanding users is an essential principle for designing an interface. However, designers, system programmers, and users have different definitions regarding 'easy to use'. This study attempts to understand users by their concepts about how to use a mobile phone by concept maps and to categorize users by their cognitive styles. The result will provide a clearer direction toward how to improve users' satisfaction by providing a suitable interface on mobile phones which are individually coherent with the user's concept of how to operate a mobile phone.

Introduction

In the past 50 years, people have learned how to create and program computers; 'the next frontier is in actually making computers serve and adapt to human needs rather than forcing humans to adapt' [3]. Based on this concept, how to make computers (and relevant electronic products which need an interface) easy to use by fitting the user's needs individually has become an important issue. Cognitive style is defined as 'a person's typical mode of perceiving, thinking, remembering, and problem solving' [2]. It is 'stable, relatively enduring consistencies in the manner or form of cognition' [4]. This study anticipates obtaining users' cognition instead of demographical information to categorize users and explore the relationship between their cognitive styles and concepts by concept maps, carding sorting, and the Group Embedded Figures Test (GEFT).

Methodology

This study will execute interviews, concept maps, card sorting and GEFT to obtain participants' cognitions of how to use a mobile phone.

Concept maps-The aim of concept maps is to organize and represent knowledge by graphical tools [7]. It includes concepts and shows the relationship between two concepts by a connect line and words or phrases to specify their relationship. An important characteristic of concept maps is the cross-links; it helps to present the relationship or links between different segments or domains [7].

Card sorting-Card sorting is a low tech method to discover users' mental models by sorting a bunch of cards (with the description of concepts) into groups and to name those groups. It provides the investigator with information about the participant's insights and the information space and their inspiration of the names [6]. According to an analysis of mobile phones' functions from Nokia, Samsung, LG, and Sony Ericsson, the terms of functions vary; card sorting might help to understand users' categorization of the menu of a mobile phone.

Cognitive style-The definition of cognitive style has been quoted by [1] as 'consistent individual differences in preferred ways of organizing and processing information and experience' [5]. One of the dimensions of cognitive style is field independence /dependence (FI/FD). The instruments of the Group Embedded Figures Test (GEFT) can be conducted for FI/FD to examine the relationship between cognitive perceptual ability and learning ability individually [8].

Plan

1. Interview: to understand users' opinions of how to judge whether a mobile phone is easy to use or not. The results which relate to interface and operation behavior might be helpful for further discussion and analysis.
2. Concept maps: based on the participant's oral description about how to use a mobile phone to draw a concept map and compare it with standard operation steps on current mobile phones to find out the differences.
3. Card sorting: for understanding user's categories of mobile phone functions. The terms of functions of Nokia, Samsung, LG and Sony Ericsson will be used on cards; the participant will only be given relevant functions that they mentioned for concept maps.
4. Cognitive style: the GEFT will be used to define whether the participant's cognitive style tends towards field independence or field dependence.

Discussion

The anticipation of the result of this study is to categorize mobile phone users by different aspects which can reflect their cognitive style and needs more precisely.

References

- [1]Allinson, C. W., Lassing, & Hayes, J. (1996). The cognitive style index: a measure of intuition-analysis for organizational research. *Journal of Management Studies*, 33(1996), 119-135.
- [2]Green, K. E. 1985. Cognitive style: a review of the literature. *Technical Report*.
Chicago, United States. May 1985.
- [3]Jacob, R., Feiner, S., Foley, L., Mackinalay, J., Olsen, D. :UIST'007: Where will we be ten years from now? In: Proceedings of ACM UIST'97 Symposium on User Interface Software and Technology, pp.115-118. Addison-Wesley/ACM Press, Banff, Canada, Panel statement (1997).
- [4]Messick, S., 1969. Measure of cognitive styles and personality and their potential for educational practice. In K. Ingendamp (Ed.), *Developments in educational testing*. London: University of London Press.
- [5]Messick, S. (1976). Personality consistencies in cognition and creativity. In Messick, S. and associates (Eds), *Individuality in Learning*. San Francisco, Cal.: Jossey-Bass, 4-22.
- [6]Nielsen, J. (1995). *Card sorting to discover the users' model of the information space*. [Online]. Useit.com. Available at: <http://www.useit.com/papers/sun/cardsort.html> [accessed 11 March 2009].
- [7]Novak, J.D., Cañas, A.J. (2006). *The Theory Underlying Concept Maps and How to Construct Them*. [Online]. Institute for Human and Machine Cognition. Available at: <http://cmap.ihmc.us/Publications/ResearchPapers/TheoryUnderlyingConceptMaps.pdf>. [accessed 03 February 2009].
- [8]Wook-Sung Yoo; Chi-Yeon Park, "Online Group Embedded Figures Test," *Information Technology Based Higher Education and Training, 2006. ITHET '06. 7th International Conference on* , vol., no., pp.267-271, 10-13 July 2006.



SED Research Student Conference

Brunel University

22-24th June 2009

Novel Cross-Layer Scheduling for Single-Cell OFDMA Systems with Heterogeneous QoS and Partial CSIT*

Charilaos Zarakovitis¹, Qiang Ni¹

1. Electronic Engineering, School of Engineering & Design
Brunel University, Uxbridge, Middlesex, UK

Charilaos.Zarakovitis@brunel.ac.uk

Keywords: OFDMA, cross-layer analysis, resource allocation

Introduction

We propose a novel cross-layer scheduling scheme for a single-cell orthogonal frequency division multiple access (OFDMA) wireless system with partial channel state information at transmitter (CSIT) and heterogeneous user delay requirements. Previous research efforts on OFDMA resource allocation [2], [3] are typically based on the availability of perfect CSIT [4] or imperfect CSIT but with small error variance [5]. Either case consists to typify a non tangible system as the potential facts of channel feedback delay or large channel estimation errors have not been considered. In order to attain a more pragmatic resolution and to achieve additional system performance our proposed cross-layer design determines optimal subcarrier and power allocation policies based on partial CSIT and individual user's quality of service (QoS) requirements using a novel robust power-bit loading (PBL) algorithm.

Methodology/Approach

As shown in Figures 1a and 1b, our system model includes the channel model, CSIT model, physical layer model, queuing system model and media access control (MAC) layer model. After performing minimum mean square error (MMSE) estimation at the base station (BS) we maximize the mutual information between the BS input and output, given the CSIT realization $\hat{h}_{ij} \in \hat{\mathbf{H}}_{K \times N_F}$, subject to a target outage probability P_{out} under the power constraint $N_F P_{TOT}$. By using matrix theory [5] we maximize channel's capacity and result a PBL scheme that allows the data transmission rate to be higher than the traditional Shannon capacity based formulas. The queuing system is modelled as an M/G/1 queue, where packets arrive at the j^{th} user's buffer according to a Poisson arrival

* This work is funded by a UK Engineering and Physical Sciences Research Council (EPSRC) CASE Award under Grant No 07000486 in collaboration with Motorola Ltd.

process with independent rate λ_j and variant packet size F . We introduce K tuples $[F, \lambda_j, T_j^{\max}]$ to describe the QoS parameters that K users require, where T_j^{\max} denotes the maximum delay of the j^{th} user. The queue state information (QSI) of each user can then be denoted by the vector $\mathbf{B}_{K \times 1} = [B_1, \dots, B_j, \dots, B_K]$ with the j^{th} component indicating the number of packets remaining in user's buffer. The MAC layer is responsible for the cross-layer scheduling at each system state, $state = (\hat{\mathbf{H}}_{K \times N_F}, \mathbf{B}_{K \times 1})$, that characterizes system's dynamics. The cross-layer scheduler determines the subcarrier allocation from the policy $\mathcal{S}_{N_F \times K}[\hat{h}_{ij}, B_j]$, the power allocation policy $\mathcal{P}_{N_F \times K}[\hat{h}_{ij}, B_j]$ and the corresponding data rate allocation policy $\mathcal{R}_{N_F \times K}[\hat{h}_{ij}, B_j]$. A convex optimization problem has been formulated from the adaptation of the delay constraints and physical layer parameters, which after relaxation gives the optimal subcarrier j^* , power \tilde{p}_{ij}^* and rate allocation r_{ij}^* solutions. The resulted \tilde{p}_{ij}^* policy has a multi-user water-filling structure and has been produced by an adaptive power allocation (APA) algorithm. On the other hand the j^* strategy is based on a linear low complexity dynamic subcarrier allocation (DSA) greedy algorithm. A novel offline mechanism has been also introduced that calculates fast and efficient the Lagrange multipliers of DSA and APA algorithms by using the secant combined with the bisection root-finding methods.

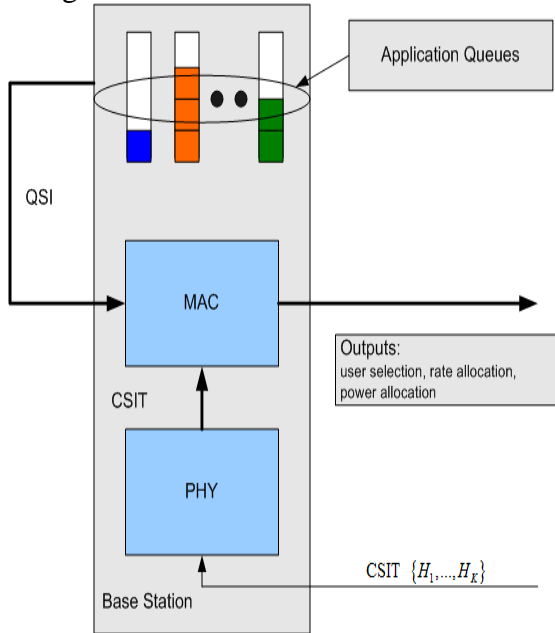


Figure 1a: System model (plain view)

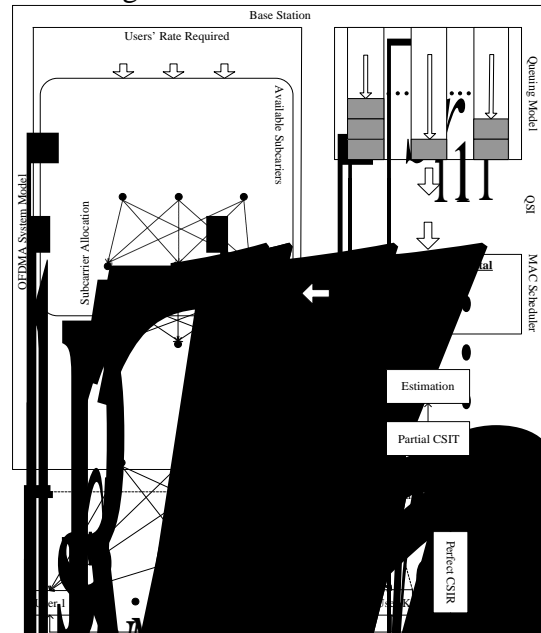


Figure 1b: System model (extended view)

Results and discussion

Various simulation scenarios have been performed by using Monte Carlo simulation methods and show that the proposed cross-layer scheduler maximizes system's throughput while simultaneously satisfies the heterogeneous delay requirements with

significant low overall system's power consumption. Indicial, Figure 2 shows that the delay requirements of the users are satisfied even when the channel error variance increases. For high CSIT error variance $\sigma_h^2 = 0.1$ the delay of the sensitive users is steady without overcoming their maximum delay tolerance while the delay of the insensitive user increases dramatically since the scheduler gives priority to the sensitive users.

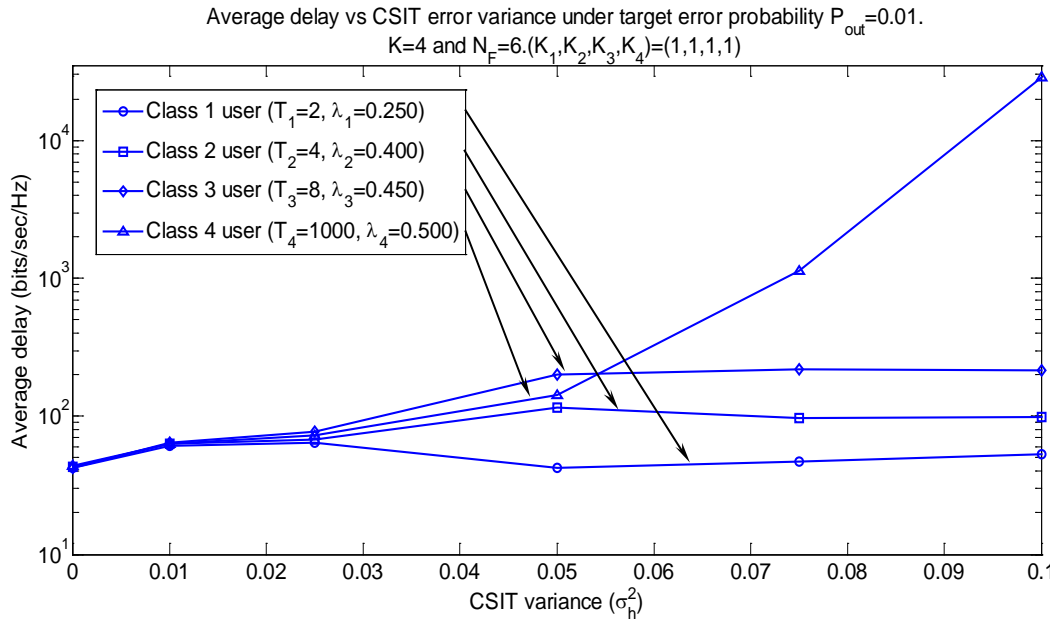


Figure 2: Average delay vs. CSIT error variance σ_h^2 of a system consisted by $N_F = 6$ subcarriers and $K = 4$ users with different classes $(K_1, K_2, K_3, K_4) = (1, 1, 1, 1)$.

Conclusion

The proposed cross-layer scheduler provides maximization of the overall system's throughput and efficiently serves the QoS differentiation of the mobile users, with real-time and robust performance having low power consumption even at large CSIT error. The proposed scheduler has been designed concerning realistic systems' characteristics and can be adopted by the next generation wireless standards. The extended version of this paper has been accepted by the IEEE WCNC'09 conference [1], and a journal version is under construction.

References

- [1] C. C. Zarakovitis, Q. Ni, D. E. Skordoulis "Cross-Layer Design for Single-Cell OFDMA Systems with Heterogeneous QoS and Partial CSIT", IEEE WCNC'09 proceedings, Budapest, Hungary, Accepted in Nov 2008.
- [2] R. Berry and E. Yeh. "Cross-layer Wireless Resource Allocation", IEEE Signal Processing Magazine, Vol. 45, pp. 59-68, September 2004.
- [3] E. Yeh and A. Cohen. "Information Theory, Queuing, and Resource Allocation in Multi-User Fading Communications", Proc. Information Sciences System Conference, Mar. 2004, pp. 1396-1401.
- [4] A. Goldsmith and P. Varaiya. "Capacity of Fading Channels with Channel Side Information" IEEE Transactions on Information Theory, 43:1986-1992, November 1997.
- [5] D. Hui, and V. K. N. Lau "Delay-Sensitive Cross-Layer Designs for OFDMA Systems with Outdated CSIT", IEEE WCNC'07 proceedings.
- [6] David H. Jacobson "Extensions of Linear-quadratic Control, Optimization and Matrix Theory", Academic Press Inc, 1977.

Determining Aircraft True Air Speed in Straight and Level Flight for Handicapped Air Racing

Sally Hume-Chignell¹, Guy Gratton¹, Cristinel Mares¹

1. School of Engineering and Design, Brunel University, Uxbridge, Middlesex, UK

me05sch@brunel.ac.uk

Keywords (3): Air Racing, Straight and Level Flight, Aircraft True Air Speed

Introduction

Handicapped Air Racing is a competition involving piston engine aircraft capable of at least 100mph in straight and level flight with a maximum weight of 5700kgs. The race is based purely on the ability of the pilot rather than the aircraft being flown^[2]. Each aircraft is given a handicap in the form of a take-off time based on the aircraft maximum TAS in straight and level flight. Thus, if all pilots fly a perfect race, all aircraft will fly over the finishing line simultaneously. The accurate determination of the aircraft TAS in straight and level flight forms the focus of this research; however, it is worth noting that whilst the method is developed primarily for this air race, it may be successfully applied to other applications including the calibration of onboard Pitot-Static Systems and aircraft performance evaluations.

The air race involves approximately twenty-five aircraft flying at maximum speed at an altitude of 700ft. During an actual race the aircraft fly over the finishing line within seconds of each other. Thus, the accuracy of the TAS determined is paramount to the success of the race. In addition, safety is a major player in the manner in which the TAS may be calculated. An additional factor to be considered is the time taken to determine the TAS of all aircraft as the race is weather permitting, thus, a short turnaround in results is desired to prevent the delay or cancelation of the event.

Methodology/Approach

In approaching the problem a full understanding of the issues associated with this type of air race was required. Despite numerous methods of determining an aircraft TAS existing already, they all came with significant disadvantages which hindered their application to this race. Thus, a new method^[1] based on the mathematics behind a current system was created.

The method developed is based on the known relationship between the Wind Vector (\vec{V}_w), the Groundspeed (\vec{V}_g) and the TAS (\vec{V}_a). The aircraft flies four legs along set headings, Figure 1. No two legs should be on the same heading and the first leg may be conducted on any heading. The

method assumes constant wind vector on all legs. The TAS is determined by superposing each leg on top of each other, Figure 2. The end points act as coordinates on the edge of the circle whereby the radius of the circle is the TAS and the offset of the circle to the centre point is the Wind Vector. The input variables are Groundspeed and Groundtrack. The method used requires only three legs be flown at equal spacings (120°). However, as this results in a triangular flight path which is an internationally recognized procedure by which an aircraft signals radio and navigational equipment failure, a fourth leg is added (leg 2). Testing has proved that three legs performed at intervals of between 90° to 120° produces an error identical to that of the GPS system used. Thus, the method permits room for pilot error.

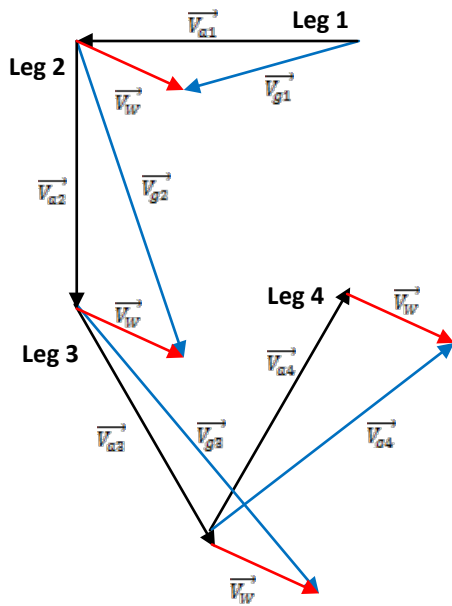


Figure 1. Flight path of the Aircraft

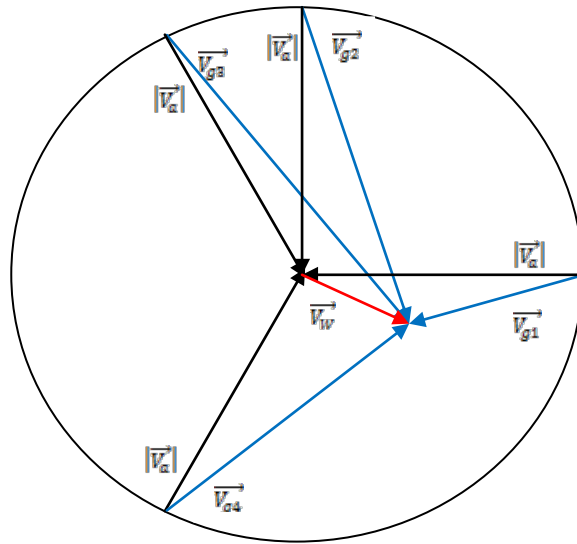


Figure 2. Circle created by superimposing each leg into one another

Results and discussion

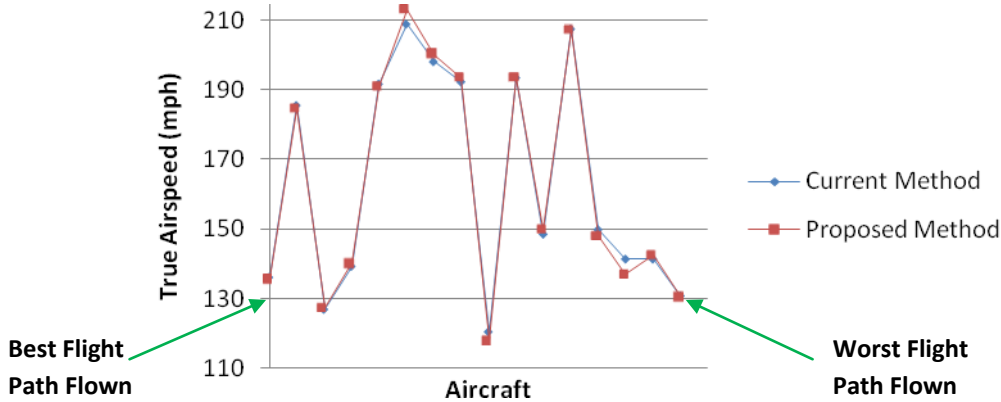


Figure 3. Graph comparing results from Current and Proposed Handicapping System

The graph shown in Figure 3 offers a simple view of the TAS calculated from both current and proposed handicapping systems. Each square on the line represents an aircraft. The aircraft are put in order from left to right in accordance with how well the aircraft flew the handicapping course. It can be seen that the proposed course produces results almost identical to that of the current system. There are a couple of larger differences between some aircraft however, there appears to be no apparent trend behind these occurrences. An important note to add to these results is that not a single aircraft flew the proposed system within the ideal range (90° to 120°). It may be assumed at this stage that as the results produced by the two methods are very similar despite the proposed method not been performed at its optimal, then the proposed method would offer an more accurate results than the current handicapping method if conducted as required.

When addressing the safety of the proposed system, the current method requires eight legs to be flown, each for a period of thirty seconds. Testing has shown that the pilots find the proposed method of four legs, each flown for a period of sixty seconds to be considerably more pilot friendly, thus, offering improved safety.

Conclusion

The proposed method of determining an aircraft TAS for the purpose of handicapping offers improved accuracy, thus, allowing for more precise handicaps to be applied to the aircraft. In addition, the method is considerably safer for the pilots to perform and maintain control.

Research is continuing on this project to consider the flight performance of the aircraft when in a straight turn, climbing flight and the final dive as the race course performed during Handicapped Air Racing also consists of these types of flight. It is anticipated that the final outcome from this further research will also be incorporated into the handicapping system offering even more accuracy.

References

- [1] Gray D, Using GPS to accurately establish True Air Speed (TAS), Dated *June 1998* – *privately published, no formal reference, available at http://www.ntps.edu/Files/tas_fnl3.pdf*
- [2] Gratton G B, Methods of handicapping the straight and level portion of handicapped air racing, *Draft under construction, no formal reference* [cited 17/09/07]



SED Research Student Conference

Brunel University

22-24th June 2009

Grain Refinement of Wrought Al Alloy by Intensive Melt Shearing

Hu-Tian Li¹, Y.Wang, M.Xia, S. Arumuganathar, Z, Fan

Brunel centre for advanced solidification technology, Brunel University,

Uxbridge, Middlesex, UK

Hu-tian.li@brunel.ac.uk

Key words: Nucleation; grain refinement; melt conditioning.

Introduction

For the ingots of wrought Al alloys, a fine and uniform as-cast microstructure is always desirable. To achieve this, grain refiners are usually employed in industrial practice. However, the refinement is markedly inefficient, where at best only 1% of added particles nucleate aluminium grains [1]. This inefficiency is undesirable not only for its cost implications, but also because refiner particles may be detrimental to mechanical performance. Recently, a novel solidification processing technology, MCAST (Melt Conditioning by Advanced Shear Technology) [2-3], has been developed in BCAST at Brunel University, for melt conditioning (MC) prior to solidification to produce fine and uniform as-cast microstructures with homogenous chemistry [3]. In this work, both standard TP-1 test and a deliberately designed experiment were used, to demonstrate the effects of intensive melt shearing on the nucleation behavior in an experimental wrought Al alloy, and pressurized filtration experiment and SEM investigation were conducted to understand the mechanism of enhanced nucleation. The influence of melt conditioning on the evolution of intermetallics will also be discussed in this paper.

Experimental

In this study, MC processing was carried out on an experimental wrought Al alloys and a model Al-Zn binary alloy with trace Ti addition. The alloy chemistry of the experimental alloy is as follows: Al-10.5Zn-2Mg-1.6Cu-0.35Fe-0.15Si-0.2Ti (all in wt.%). The melt temperature was set at 720°C; shearing temperature, 650°C; shearing time, 50sec; shearing speed, 500rpm. The standard TP-1 mould was used for producing samples with a cooling rate 3.5K/sec. The linear intercept technique was used to measure and assess the grain size using a Zeiss optical microscope with an Axio Vision 4.3 image analysis system. Identification of intermetallics and

oxides were conducted with a field emission gun Zeiss Supera 35 machine, equipped with an energy dispersive spectroscopy (EDS) facility and operated at an accelerating voltage of 3–20 kV.

Results and discussion

As shown in Fig.1, the average grain sizes of TP-1 samples cast at both 700°C and 650°C without melt conditioning were $180\pm 21.5\mu\text{m}$ and $123\pm 24\mu\text{m}$, respectively, while that of TP-1 sample cast at 650°C with melt conditioning was $48\pm 3.5\mu\text{m}$, indicating a significant grain refinement by melt conditioning. In order to eliminate the influence of pouring process on the nucleation and hence grain size evolution, a deliberately designed experiment was carried out. The quantification results of grain size in this work shows that the average grain size was decreased to around $270\pm 45\mu\text{m}$ with MC processing compared to $620\pm 118\mu\text{m}$ without MC processing.

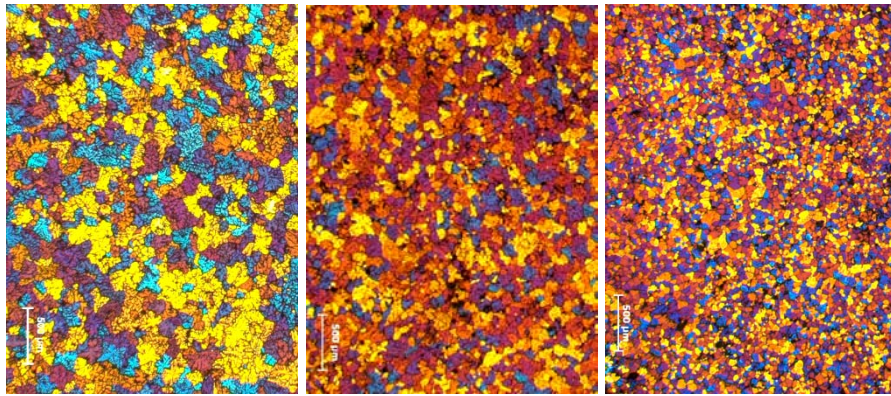


Fig1. Microstructures of experimental alloy produced with and without melt conditioning at different temperatures: (a) cast at 700°C Without MC; (b) cast at 650°C Without MC; (3) cast at 650°C With MC

After MC processing, TiAl_3 particles have a finer size, a narrow size distribution and a compact morphology, and are often found within the grain interior, as displayed in Fig.2.

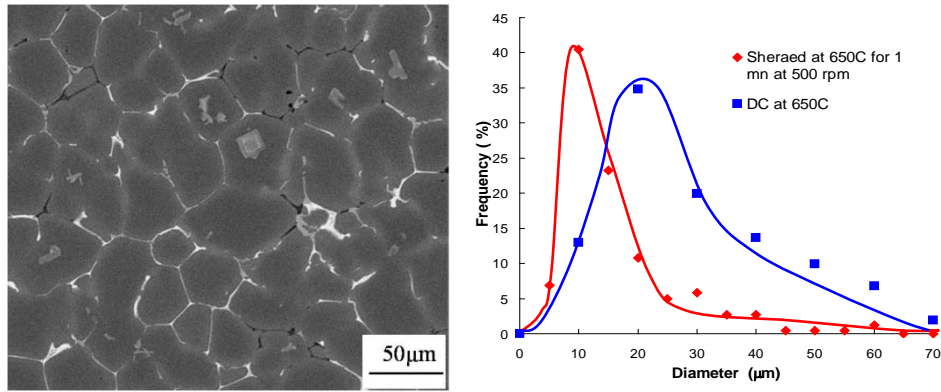


Fig.2 (a) morphology of $TiAl_3$ intermetallic particles in MC Processed samples, and (b) comparison of size distribution with and without MC processing

As displayed in Fig.3, the oxides inside α -Al grain display refined and dispersed particles in MC processed sample, which may act as nucleation sites for α -Al and intermetallic particles.

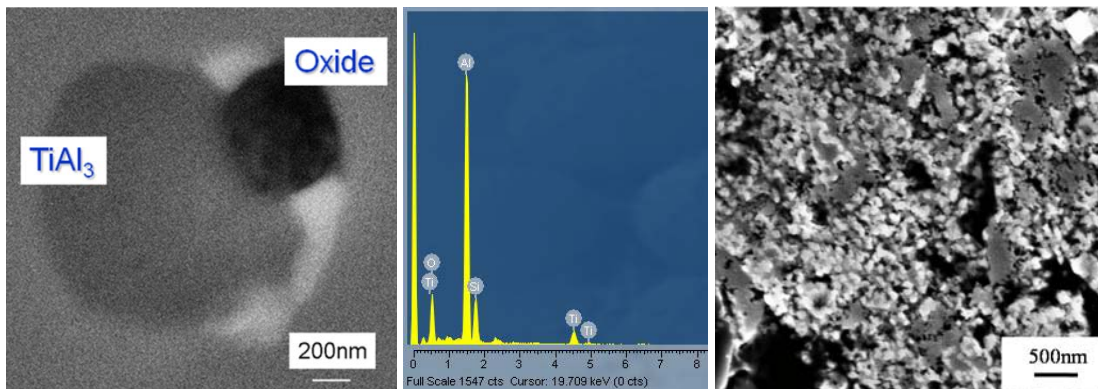


Fig.3 SEM image of oxides particles located within alpha Al associated with $TiAl_3$ intermetallics particles (a); its EDX spectrum (b), indicating its higher Ti content; and SEM images of oxides in MC Processed and Pressurization Filtered sample showing its dispersed particle feature.

As detailed in previous papers [2-3], the MC processed melt is extremely uniform in terms of compositional fields and thermal conditions. In order to understand the mechanism of this enhanced nucleation behavior, both the temperature field and composition field should be taken into account. However, after holding two samples with and without MC processing in the furnace for 3min, the temperature field should be the same. This argument is based on the fact that in the melt the thermal diffusion coefficient is four orders of magnitude greater than that of solute diffusion [4]. So the only difference is the compositional field which is much more homogeneous after MC processing. This suggests that Ti solute could segregate to the interface

between the potential nucleant particle, which may be oxide particle in the current study, and melt.

Conclusions

In summary, intensive melt shearing promotes nucleation through dispersed and refined oxide with narrow size distribution. Segregation of Ti to oxide surface improves the match or chemical affinity between oxide and α -Al /TiAl₃. Ti addition may be decreased to smaller amount through the intensive melt conditioning in an attempt to achieve refined grain structure in wrought Al alloys. MC processing promotes the formation of dispersed and compact intermetallics particle with narrow size distribution, which is less detrimental to mechanical properties of Al alloys. Further detailed investigations involving both high resolution transmission electron microscopy (HRTEM) observation and theoretical calculation on the crystallography relationship and interfacial features between oxide and α -Al are underway.

References

- [1] I.J. Polmear. Light alloys. Fourth Edition, Oxford: Butterworth-Heinemann Ltd, United Kingdom, 2006, p97.
- [2] Z. Fan and G. Liu. Acta Mater. 53 (2005), 4345-4357.
- [3] M. Hitchcock, Y. Wang, Z. Fan. Acta Mater. 55 (2007) 1589-1598.
- [4] A. L. Greer, A. M. Bunn, A. Tronche, P. V. Evans and D. J. Bristow. Acta Mater. 48 (2000) 2823-2835.



SED Research Student Conference

Brunel University

22-24th June 2009

HARDWARE IMPLEMENTATION AND POWER MODELLING OF 2D HAAR TRANSFORM FOR MEDICAL IMAGING

Abdul Naser Sazish and Abbes Amira

Electronic and Computer Engineering, School of Engineering and Design

Brunel University, West London, UB8 3PH, UK

Email: abdul.sazish@brunel.ac.uk

1. INTRODUCTION

In the past two decades, due to its capability to represent real life non-stationary signals the topic of wavelet transform has attracted a great deal of research. Consequently, the wavelet transform is gaining acceptance as an alternative contrivance to traditional time frequency representation techniques such as the discrete Fourier transform (DFT) and discrete cosine transforms (DCT) [1]. Due to its multi-resolution capability for signal representation, wavelet transform has also been utilized in many vital applications including medical image processing [2]. There is no doubt that there are great challenges to be explored in this area.

Reconfigurable hardware, especially field programmable gate arrays (FPGA) are widely used in digital signal processing and scientific applications [3]. FPGA offers an excellent performance for signal processing applications, due to its massive parallelism capabilities, multimillion gate counts, and special low power packages can reduce the amount of memory used, computational complexity and power consumption [4] that lead to significant contribution towards the large volumes medical modalities issues.

The idea of power estimation model for FPGAs is of growing significant importance as the issues of memory and computational complexity. Many embedded platforms, such as handheld devices, distributed sensors, and satellites demand low power in order to increase their functional lifetime. Power consumption for FPGAs can be modelled since some of the factors contributes are system variables. List of factors that requires consideration are as follows: clock frequency, number of interconnections, interconnect structure of the FPGA, power supply voltage levels, output loading, activity rates and logic block [5].

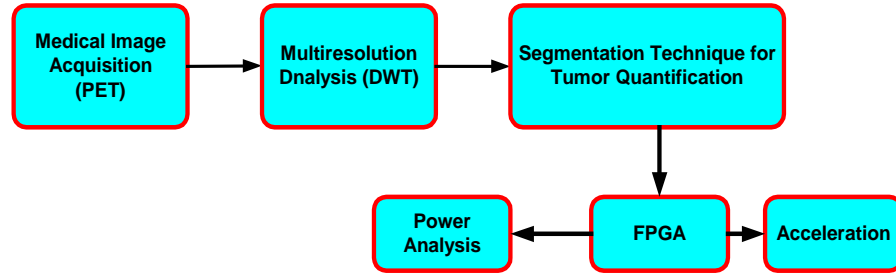


Fig.1. Proposed system for acceleration of medical image segmentation using FPGA

The aim of this paper is to develop an efficient hardware implementation of the 2D Haar wavelet transform (HWT) on different FPGAs platforms with the comparison of power estimation models using non-linear regression (NLREG) [6]. The HWT core can be integrated in the system presented in Fig.1 used in medical image segmentation.

2. FPGA IMPLEMENTATION RESULTS

In order to evaluate the performance of the proposed 2D HWT hardware implementation, the design has been implemented on the Celoxica RC1000 board equipped with the Virtex- 2000E F . The RC1000 has four memory banks that communicate with the host by means of DMA transfers. For evaluation purposes and to take advantage of the latest FPGA devices, the proposed design has been also synthesized using Virtex-4 (VLX200) and Virtex-5 (XC5VLX330) [7]. Various performance metrics such area occupied, LUTs, Inputs and Outputs (I/Os) pins and maximum frequency with $N = 16$ on different FPGA platforms and the comparison with other existing implementations are presented in Table 1. Concerning the slices and LUTs parameters, implementation on Virtex-E utilizes 295 slices and 314 LUTs, while on Virtex-5 occupies (44%) less area and more LUTs. It worth mentioning that with advanced FPGAs, the design occupies less area due to the number of available LUTs in the CLB. In Virtex- 4 each CLBs contains four slices (two LUTs and two FFs in each slice) and in Virtex-5 offers each CLB with two slices (four LUTs and four FFs in each slice). The proposed hardware implementation outperforms Virtex-E by (44%) in term of maximum frequency.

Platforms	N	Area (slices)	No. LUTs	I/Os	Max.frq.(MHz)
Proposed (HWT) Vietex-E	16	295	314	48	82
Virtex-E [8]	16	335	N/A	21	67
Proposed (HWT) Vietex-4	16	286	312	49	125
Virtex-4 [8]	16	358	N/A	21	121
Proposed (HWT) Vietex-5	16	186	332	49	154

Table1. Comparison of implementation results with different platforms and existing work

3. POWER ANALYSIS

Power consumption of components fabricated in CMOS technology, such as FPGA, comprises of static and dynamic parts. Static power is caused mainly by the leakage current between power supply and ground. The dynamic power is caused by signal transitions at the device transistors. Frequencies of signal transitions are obviously related to the clock frequency.

3.1 Modelling Results

The corresponding models are derived by performing nonlinear regression analysis on the power data obtained. Clock power (CP) in FPGAs depends on the distribution of the clock nets (which depends on the chip area over which the design is spread out). For the (CP) models, the power consumption associated with the total area (TA), frequency (f)

and voltage (v). Based on the graph illustrated in Fig. 2, the corresponding model is derived as follows:

$$CP = c_1 \cdot v^2 \cdot \frac{TA}{c_2} \cdot f + c_3 \cdot f + c_4$$

Where c_1 , c_2 , c_3 , and c_4 are scaling coefficients in the clock power model, the modelling results have been compared with Xilinx Xpower results. There is no significant difference for the power that has been modelled using NLREG with the data generated by XPower. The same procedure is applied for logic power (LP) model.

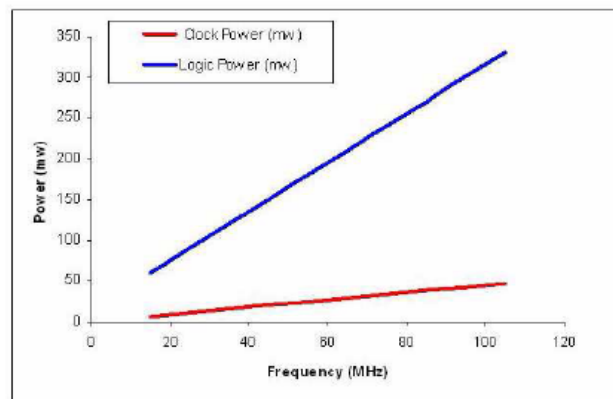


Fig.2. Clock and logic power modelling results using NLREG

4. CONCLUSION

In conclusion, the proposed hardware implementation of 2D HWT for medical image processing and the power estimation model for the clock and logic power are presented. The 2D Performance comparison with the existing work and other FPGA families has been conducted in terms of areas, number of slices, LUTs, I/Os and maximum frequency. Ongoing research will be focused on the development of different IP cores to accelerate the slowest part in the proposed medical image segmentation system and also enhance and develop the power modelling for it.

5. REFERENCES

- [1] S. Mallat, "A Theory for Multiresolution Signal Decomposition The Wavelet Representation", *IEEE Transaction on Pattern Analysis and Machine Intelligence*, 11, pp. 674-693, 1989.
- [2] M. Antonini, M. Barlaud, P. Mathieu and I. Daubechies, "Image Coding using Wavelet Transform", *IEEE Transactions on Image Processing*, vol. 1, no. 2, pp. 205-220, 1992.
- [3] L. Deng, K. Sobti, C. Chakrabarti, "Accurate Models for Estimating Area and Power of FPGA Implementations", in *Proc. of IEEE International Conference on Acoustic, Speech and Signal Processing*, Las Vegas, USA, pp. 1417-1420, 2008.
- [4] S. Chandrasekaran, A. Amira, S. Minghua, A. Bermak, "An Efficient VLSI Architecture and FPGA Implementation of the Finite Ridgelet Transform", *Journal of Real Time Image Processing*, vol. 3, pp. 183-193, 2008.
- [5] J. H. Anderson, F. N. Najm, "Active Leakage Power Optimization for FPGAs", *IEEE Transactions on CAD for Integrated Circuit and System*, vol. 25, no. 3, pp. 423- 437, 2006.
- [6] URL: www.nlreg.com.
- [7] Xilinx, San Jose, CA, XPower documentation, [Online]. Available: www.xilinx.com/support/library.htm.
- [8] A. Amira, S. Chandrasekaran, "Power Modelling and Efficient FPGA Implementation of FHT for Signal Processing", *IEEE Transactions on VLSI System*, vol. 15, no. 3, pp. 286-295, 2007.



SED Research Student Conference
Brunel University
22-24th June 2009

Non-Newtonian Behaviour in Molten Lead.

R. Ritwik¹, H.Men¹, Z.Fan¹

1. Brunel Centre for Advanced Solidification Technology (BCAST), Brunel University, Uxbridge, Middlesex, UK.

Ritwik.ritwik@brunel.ac.uk

Keywords (3): viscosity, metal, lead

Introduction:

Viscosity is a physical property which manifests itself when a relative motion between the different layers of liquid is set up. Viscosity plays an important role as a key to solve many quantitative problems in fluid flow as well as those related to the kinetics of reactions in metallurgical processes. Numerous experimental measurements of liquid metal viscosities have been made over the last hundred years or more. Even so, accurate and reliable data are still unavailable widely. Fairly large discrepancies exist between experimental viscosities obtained for some liquid metals. The reason for these discrepancies has been attributed to the high reactivity of these metallic liquids and the technical difficulty of taking precise measurements at elevated temperatures. Liquid metals have been believed to behave as Newtonian fluids [1]. But over the years cases have come up wherein the viscosity of the melt changed with the applied shear stress [2, 3]. This project work aims at establishing the viscosity behaviour of metals in their molten state at temperatures near their melting point. The studies are done to understand better the behaviour of molten lead when it is subjected to shearing procedures at high shear rates.

Methodology / Approach:

A rotating cylinder viscometer has been used to measure the viscosity of molten lead when the melt is subjected to high shear rates from zero shear rates. For the rotating cylinder technique the torque on a cylinder rotated in a liquid is related to the viscosity of the fluid. The viscosity is determined from measurements of the torque generated on the rotor arm of the rotating cylinder. When rotating the cylinder at a constant speed the viscosity can be obtained from the following equation:
$$\eta = \frac{\left(\frac{1}{r_1^2} - \frac{1}{r_0^2}\right)M}{8\pi^2 nh}$$
 [4], where M is the torque, n is the number of revolutions per second, r_1 is the radius of the bob, r_0 is the radius of the cup, h is the height of the bob and η is the viscosity of the liquid being tested.

The rotating cylinder viscometer used in the experiments is a cup and bob viscometer. The bob (47 mm dia, 33.1 mm height) and the cup (57.1 mm outer dia., 49.3 mm inner dia., 62.9mm

height) are made of stainless. Lead was melted in a furnace and poured into the cup. The bob was lowered till it was completely submerged inside the melt.

Nitrogen gas was used as an inert atmosphere to reduce the oxidation of the melt during the experiment. A steady flow of 2 bar Nitrogen gas was passed over the melt. Ramping experiments, where the bob was accelerated to a certain rotational speed in a fixed time, were conducted. The bob was rotated to various speeds to obtain different values of shear rate.

Results and Discussion:

The graph of viscosity vs. shear rate was studied and the slope of the curve and the intercept at zero shear rates was calculated. The intercept in the viscosity vs shear rate curve gives the viscosity of liquid metal when no shear forces are acting on the liquid. This value was compared to the viscosity values of the liquid from literature.

Temperature(°C)	Ramping time	Shear Rate (s ⁻¹)	Slope	Intercept(mPa.s)
387	10min	0 – 1476	16.3x10 ⁻³	3.11
387	10min	492 – 1476	17.71x10 ⁻³	2.90
387	10min	0 – 2460	16.56x10 ⁻³	3.01
437	10min	0 – 1476	14.56x10 ⁻³	2.06
437	10min	0 – 2460	14.64x10 ⁻³	1.90

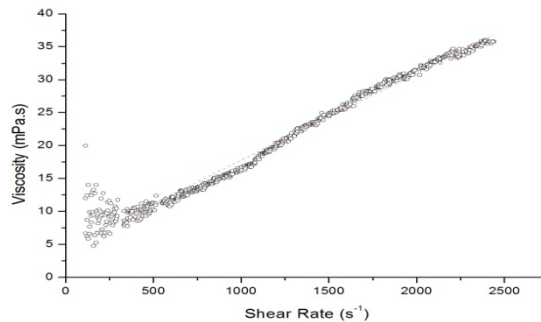


Fig.1. Viscosity vs Shear rate graph – Ramping Up to 1000rpm in 5 mins

The positive slope indicates a rise in viscosity during the ramping experiments. In other words, under the influence of shear forces, the viscosity of the liquid metal increases. Also, at higher temperature the viscosity of liquid metal at zero shear rate decreases, which is consistent with behaviour observed in literature [5].

Conclusions:

The increase in viscosity of Liquid lead with shear rate indicates that liquid metals show a shear thickening behaviour at high shear rates. Compared to the traditional belief that the viscosity of liquid metal remains constant under any shear rate (since they are believed to be Newtonian liquids), this experiment indicates that metals in the molten state are not Newtonian. This behaviour of molten metals suggests that further thought must be given to their viscosity.

References:

[1]Iida,T., Guthrie, Roderick I.L, The Physical Properties of Liquid Metals, *Clarendon Press – Oxford*, 1988.

[2]Wittenberg, L.J, Ofte, D., Curtiss, C.F., The Journal of Chemical Physics, Vol.48, No. 7 (1968), 3253-3260.

[3]Lashkari, O., Ghomaschi, R., Mat. Sc. Eng. A 486(2008), 333-340.

[4]Collyer, A.A., Clegg, D.W., Rheological Measurements, *2nd Edition, Chapman and Hall* (1998).

[5]Sobolev, V., Journal of Nuclear Materials 362 (2007) 235-247.

Grain Growth Simulation using Cellular Automata

F.M. Almohaisen^a and M.F. Abbod^b

School of Engineering and Design, Brunel University, Uxbridge, UK, UB8 3PH.

Fahad.Almohaisen@brunel.ac.uk, Maysam.Abbod@brunel.ac.uk

Keywords: Grain growth; Computer simulation; Cellular Automata.

Introduction

Physical and mechanical properties of materials and most of its engineering performance are found to be significantly related to their microstructures in addition to their compositions. Since it is difficult to monitor the microstructure coarsening during grain growth using physical experiments, computer simulation has been used as an effective alternative. In this study *cellular automata* (CA) model based on three transitions method will be investigated. Various models which were reviewed used probabilities based on energy change as transition conditions [1]. In some of those models the transition depends on energy difference of atoms during jumping and the activation energy, and the others make the energy of the grain boundary depend on the disorientation of the grains [2-4].

CA Model Procedure

In this model simulation matrix resolution (pixel) was chosen as 200×200. The number (q) of grains orientations was randomly selected for each grain where $1 \leq q \leq q_{max}$. According to Geiger et. al. [5] q_{max} must be more than 64, in this study the value 128 was chosen for q_{max} . The von Neumann neighbourhood has been used to apply the transition rules between the grain's boundaries. The timing in CA model is measured by CA step (CAS). In each step all the grains are investigated one by one and CA model checks all cells along the grain boundary and applies the transition rule if the conditions are satisfied.

The transition rules which have been used in this study are:

Rule 1: The total energies compared with the activation energy as:

$$E_A < E_T + E_B$$

(1)

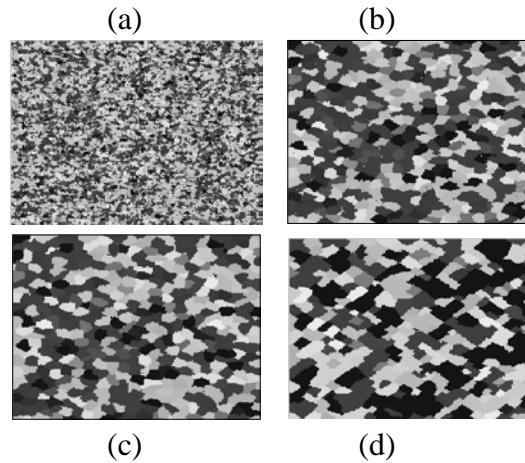
Rule 2: Only thermal energy is the driving force for the cells along grain boundary, in other word the grain will expand through the boundary of lowest thermal energy. The thermal energy is calculated every CA step.

Rule 3: A number of nucleuses with different orientations are randomly distributed in the simulation area. Then they start to grow at every CAS without effecting in the other grains, until all cells signed with an orientation number.

Results and Discussion

Morphology. Fig. 1 shows the final microstructure evolution during normal grain growth using different transition rules on a sample of Al-1%Mg at 200°C. It can be observed that most grains have polygonal shape, unless for rule 3 where a number of grains take the tetragonal shape.

Figure 1. 2D simulation of microstructure, (a) simulation space at CAS=0, (b, c and d) final simulation using the three rules respectively



The grain size was homogeneously distributed in the simulation area. Using the first and second transition rules most grains had in average 6 sides, which agree with the results of *Monte Carlo* (MC) model [3]. However, the first and second rules made the CA model more relevant to the actual processes of normal grain growth. Although, the third transition rule gave much rapid (short calculation time) and effective solution but it lacks physical meaning.

Growth Kinetics. Grain area was computed by the number of cells inside this grain. The average grain size was calculated by dividing the sum of all grains areas by the number of the grains in each CA step. Fig. 2 shows that for all transitions rules, the average grain size increases as the CA steps increase. Hence transition rule 2 used only the thermal energy as the driving force for migration boundary, the average area of grains increases very fast along the calculation time.

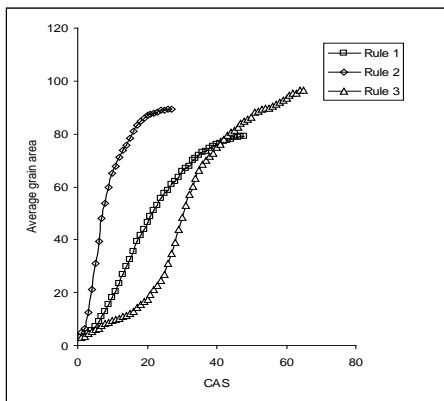


Figure 2. Average grain size (number of cells) as a function of CA steps.

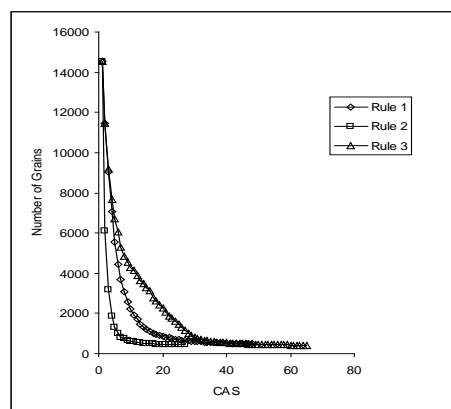


Figure 3. Number of grains in simulation region via CA steps.

In contrast, the first rule which combine all three kinds of energy (activation, thermal and boundary energy) the average grain area take longer time (CAS) to propagate. But it still increases almost linearly with CAS. The average grain area evolution using the third transition rule can be divided into three parts; the first part is at the beginning of simulation where the grains are small and the change of average size is small; then in the second part the grain size increments are very high, while at third part the change of average grain size decreases. The rate of change of the grain number within the simulation area throughout the calculation time is shown in Fig. 3. It clearly shows that for all transition rules the number of grains decreases rapidly at first stage and then the rate of change become very small. Fig. 3 shows that transition rule 1 gives the CA model more physical meaning, making the model much more stable than the other transition rules. Because transition rules 2 neglect many effective parameters, the rate of decreasing number of grains becomes very rapid compared with the other transition rules.

Conclusions

Cellular Automata model is more efficient and flexible to simulate physical phenomenon. Selecting more powerful transition rules which combines most of effective parameters makes the simulation more reliable. In this study three different transition rules were used to simulate normal grain growth. In the first rule, the thermal energy for each grain and the boundary energy were added and compared with activation energy in each calculation step. However, this made the CA model much closer to the processes in actual state. The second transition rule used only the thermal energy as the driving force during the grain growth. This rule made the calculation simple but it had neglected very important parameters. The last rule is based on theoretical process, which ended with much diverge from the physical state. Future work will include investigate the CA rules in 3D and validation of the results using experimental data.

References

- [1] D. Raabe, *Advanced Engineering Materials*, 2001, 3(100), 745.
- [2] N. Ono, K. Kimura, T. Watanabe, *Acta Mater.*, 1999, 47, 1007.
- [3] M.P. Anderson, G.S. Grest, *Acta Mater.*, 1984, 33, 509.
- [4] U. Kunaver, D. Kolar, *Acta Mater.*, 1998, 46, 4629.
- [5] J. Geiger, A. Roos, P. Barkoczy, *Acta Mater.*, 2001, 49, 623.



SED Research Student Conference

Brunel University

22-24th June 2009

Effects of Ultrasonic Vibrations on Processing Parameters of Polyethylene and Thermal and Mechanical Properties of Extrudate

Amir Khamsehnezhad, Robert Withnall, Peter Allan, Karnik Tarverdi, Jack Silverand Ali Ahmadnia

Wolfson Centre for Materials Processing, Brunel University, Uxbridge, Middlesex, UK

Amir.Khamsehnezhad@brunel.ac.uk

Keywords: Polyethylene, Extrusion, Ultrasonics

Introduction

The past decade has seen a dramatic rise in the applications of high-intensity ultrasound in chemistry, with a range of synthetic procedures and processing methods and subsequently polymer science also having benefited from sonication [1, 2]. Several studies have been done on different polymers with quite wide range of aims such as changing polymers chemical, structural, mechanical and processing properties. In area of polymer chemistry ultrasonic waves have been employed to control the molecular weight and its distribution through ultrasonic degradation and also synthesize novel polymers and copolymers [3-10]. Having a look at mechanical and rheological side of vibrations numerous studies have been done such as influence of longitudinal vibrations on Poiseuille flow of a non-Newtonian fluid [11-13] and, in detail, influence of transverse vibrations [14, 15]. It has been found that by superimposing longitudinal and transverse oscillations the effect of vibrations can increase the mechanical properties of extrudate as well as reduce die pressure and the die swell ratio [16]. As it mentioned in literature above, Ultrasonic Vibrations can affect polymers and their processing in different ways and the current study will focus on oscillations effect on polymer extrusion by investigating enhancement of processing conditions and extruded products properties. The aim of the current work is to improve production rate of polymer and save energy in the extrusion process as well as achieving positive effects on other properties of extrudate.

Experimental

Commercial grade of Polyethylene has been supplied by Polypipe in its granular form and used in this work. Betol Single screw extruder with three heating zones followed by a sonication mould and a strip die have been employed to carry out conventional and USV extrusion tests. The temperature setting which has been used for processing and preparation of polymer strips can be found in Table 1.

Table 1 .Processing conditions of Polyethylene Samples and Extrusion experiments

Barrel Temp.			Sonic Mould Temp.		Die Temp.
zone 1	zone 2	zone 3	Block 1	Block 2	
160	180	195	190	190	190

PE has been extruded using both conventional and USV methods in 5 different screw speeds and all the processing parameters have been recorded regularly. PE strips with thickness of ~1.2 mm have been used to prepare samples for DSC, DMA and Tensile Tests. DSC tests have been carried out at heating rate of 10°C/min and cooling rate of 5°C/min in heat/cool way between -80°C and 180°C to investigate materials thermal properties. DMA tests have been carried out at different frequencies in single cantilever mode with amplitude of 25 µm for temperature range of -140 up to 60°C with heating rate of 3°C/min. Tensile test specimen have been cut from the strips into type 5A dumbbell shape according to BS EN ISO 572-2:1996 and the tests have been carried out at 1mm/min speed for modulus determination and 5mm/min well up to post yield length.

Results and Discussion

A brief look at collected data from conventional extrusion of PE and a comparison of them with USV extrusion processing parameters shows that mostly affected parameters in extrusion process are barrel pressure, extruder motor current and melt temperature. It can be seen that barrel pressure in metering zone of the extruder decreases about 100 Psi after applying ultrasonics. Extruder motor current which can be used as a representative for power consumption of extruder motor has been reduced about 10% of its value for conventional extrusion and at the same time the melt temperature increased between 6-11°C depending on screw speed of the extruder and polymer's residence time in the sonic chamber. Reduction in barrel pressure can cause higher output rates which can be significantly clear in higher extrusion rates and also can save energy by creating less frictional heat in the barrel and also less power draw from the extruder motor. Temperature rise reduce the viscosity locally in die region and make the flow easier and reduce the resistance to flow. The change in flow behaviour can be seen from slight viscosity change of PE which has been measured by inline extrusion rheometer (strip die).

According to data obtained by DSC tests, melting and crystallisation temperatures of the materials didn't change and haven't been affected by applying ultrasonics but at the same time significant changes in melting enthalpy can be a reason for change in morphology and crystalline structure of PE. Irradiation or exposure of ultrasonics reduced the degree of crystallinity of PE but not definitely meaning that polymer chains could have been changed or may have been broken under USV exposure and could be investigated by taking a deeper look into its morphology.

Comparison of DMA results of both USV and conventionally processed extrudates around their glass transition temperature, T_g (-105°C), shows that for storage and loss modulus the extrudates which have been processed using ultrasonics have higher values than the ones which have been processed using normal extrusion process (~15% greater). In other words, polymer strips extruded using ultrasonics are stronger than the ones which have been processed conventionally.

Tensile test results as a proof for DMA tests showed that Young's Modulus and also strength at a known strain ($\epsilon=60\%$) of PE extrudates for USV extruded samples are greater than the other ones, meaning that strength and toughness of PE increased by applying ultrasonic vibrations on polymer melt.

Conclusion

It can be concluded that by adding Ultrasonic Vibration into conventional extrusion process, following benefits can be achieved:

- Extruder power consumption has been reduced.
- Melt temperature increased locally.
- Dynamic mechanical properties of the extrudate enhanced in lower temperatures.
- Mechanical properties; i.e. E-Modulus and Strength of the extrudates increased notably.

References

- [1] Price, G. J. (Ed.), 'Current Trends in Sonochemistry', Royal Society of Chemistry, Cambridge, 1992.
- [2] Mason, T. J. and Lorimer, J. P. 'Sonochemistry: Theory, Applications and Uses of Ultrasound in Chemistry', Ellis Horwood, Chichester, 1998.
- [3] Matyjaszewski K., Greszta D., Hrkach J.S., Kim H.K., *Macromolecules* 28 (1995) 59.
- [4] Price G.J., Norris D.J., West P.J., *Macromolecules* 25 (1992) 6447.
- [5] Yildiz G., Catalgil-Giz H., Giz A., *J. Appl. Polym. Sci.* 84 (2002) 83.
- [6] Chou H.C.J., Stoffer J.O., *J. Appl. Polym. Sci.* 72 (1999) 827.
- [7] Madras G., Chattopadhyay S., *Polym. Degradat. Stab.* 73 (2001) 33.
- [8] Price G.J., Lenz E.J., Ansell C.W.G. Ansell, *Eur. Polym. J.* 38 (2002) 1753.
- [9] Shen Y., Chen K., Wang Q., Li H., Xu H., Xu X., *J. Macromol. Sci. –Chem. A* 23 (1986) 1415.
- [10] Chen K., Chen S., Xu X., *J. Macromol. Sci.–Chem. A* 29 (1992) 55.
- [11] Manero O. and Mena B., *Rheol Acta* 16 (1977) 573–576.
- [12] Manero O., Mena B. and Valenzuela R., *Rheol. Acta* 17 (1978) 693.
- [13] Mena B., Manero O. and Binding D.M., *J. Non-Newt Fluid Mech.* 5 (1979) 427.
- [14] Kazakia J.Y. and Rivlin R.S., *Rheol. Acta* 17 (1978) 210–226.
- [15] Kazakia J.Y. and Rivlin R.S., *J. Non-Newt Fluid Mech.* 6 (1979) 145.
- [16] Casulli J., Clermont J.R., Von Ziegler A. and Mena B., *Polym. Eng. Sci* 30 (1990) 1551.

FPGA Implementation of Image and Signal Processing IP cores Using Dynamic Partial Reconfiguration

Benjamin Krill¹, Abbas Amira

Electronic and Computer Engineering, School of Engineering and Design, Brunel University, Uxbridge, Middlesex, UK

¹benjamin.krill@brunel.ac.uk

Keywords (3): FPGA, Partial Reconfiguration, IP Cores, Image and Signal Processing

Introduction

The complexity of the implementation of many image and signal processing techniques still remains as a heavy burden on standard microprocessors where large amounts of data have to be processed in real time. Therefore, either the design of high-performance dedicated circuits or parallel systems is strategic for applications that require real-time performances. This paper presents an overview about an approach for image and signal processing IP core implementation on field programmable gate arrays (FPGAs), exploring dynamic partial reconfiguration. It focuses on specifically on the dependency between the size of the reconfigurable area and the bitstream file generated. Furthermore, the environment provides a reduced power consumption by connecting the generated IP cores rather than integrating all the cores simultaneously as it is performed in existing approaches [1]. The proposed implementation approach has been carried out on the Virtex-5 FPGA [2].

Methodology/Approach

The environment consists of three main parts, i) the application and operating system part, ii) the FPGA static implementation and iii) FPGA partial reconfiguration area. Figure 1 shows how

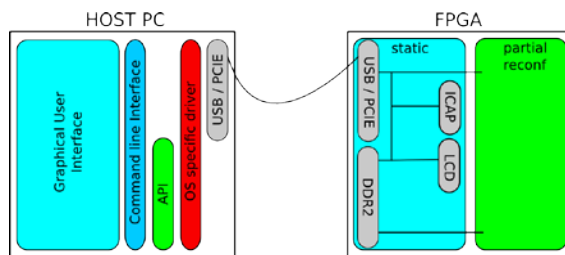


Figure 1: High level Design

these modules are connected together. The host application running on the PC is a graphical user interface (GUI) [3] which mainly provides the possibility to construct applications by drag and drop icons. It generates scripts which calls the command line tools to communicate with the FPGA over the API/operating system specific driver. The current prototype implementation uses a universal serial bus (USB) connection to the FPGA which could be exchanged by a peripheral component interconnect express bus (PCI-E). The Virtex-5 FPGA contains a static area and a partial

reconfiguration area. The static area provides all modules which must be operating during reconfiguration such as the memory controller, USB controller and ICAP [4]. All the other used components are Wishbone bus compliant and connected through shared bus interconnection [5].

Results and discussion

The environment provides a lightweight framework with enough room for IP cores. It can be used to chain up cores and run them on the FPGA by monitoring the acutely work and reprogram the partial area when the next stage of calculation could be done. Figure 2 shows the component (x-axis) to bit file (y-axis) utilisation. The bitstream size increases linearly with the components used. This study provides an assessment of how big the partial area should be selected to find a good balance between logic/functionality and the time to reprogram the partial reconfigurable area. Another important

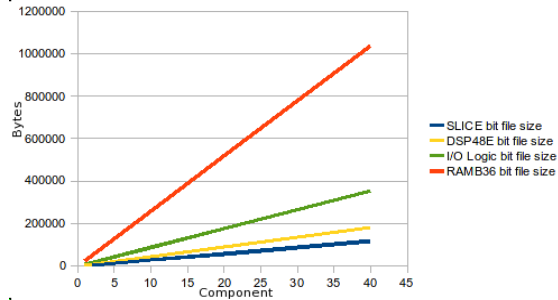


Figure 2: Comp. to Bitfile Size Utilisation

parameter is the power consumption as presented in [6], the power is the sum of two components: static and dynamic power. Static power results primarily from transistor leakage and dynamic power can be calculated by the equation $P_d = CV^2f$ (C: node capacitance, V: voltage, f: frequency). By shrinking the partial area to the minimum size of the biggest core the dynamic power consumption will be reduced because of the reduction in the logic used. This situation force PAR tool to deal with a given area.

Conclusions

This paper presents the current research state and implementation of the partial reconfigurable environment for IP cores used in image and signal processing. The implemented programs provide a toolchain to help users to integrate further IP Cores or to develop high level flow controlled applications. Further the partial reconfiguration design flow is fully integrated and hidden to the developer. Power consumption reduction is achieved by optimising the size of partial area and chaining more tasks in serial. Ongoing research is focusing on evaluation of more optimised IP cores and a mechanism to estimate the power consumption of all chained cores over the operation time.

References

- [1] Y. H. Cho, "Automatic target recognition systems on reconfigurable devices", Reconfigurable Computing: The Theory and Practice of FPGA-Based Computation, vol. 2, no. 1, pp. 591–612, 2008.
- [2] Xilinx INC. (ug190), "Virtex-5 FPGA user guide", 2009.

- [3] Benjamin Krill, “*A Reconfigurable System for IP Cores Generation based Image and Signal Processing Applications*”, SED Research Conference, 2008
- [4] Xilinx INC. (v2.1), “*Partial Reconfiguration Design with PlanAhead*”, 2008
- [5] Opencores (Rev B.3), “*Wishbone system-on-chip interconnection architecture for portable IP cores*”, 2002.
- [6] Derek Curd, “*Reduce Power with Virtex-5 FPGAs*”, Xcell Jo



SED Research Student Conference

Brunel University

22-24th June 2009

Use of Metallic Resonant Sensors in Torque Measurement

Transfer Standard

Jittakant Intiang

Brunel Design, School of Engineering and Design, Brunel University, Uxbridge, Middlesex, UK

Jittakant.Intiang@brunel.ac.

Keywords (3): Torque Measurement, Calibration, Resonant Sensor

Introduction

Quality of measurement in industry requires the measured value to be compared to reference standards, which are traceable to the base SI unit. This can be achieved by using transfer standards. The most common torque transfer standard, widely used in laboratories and in industry, is based on strain gauge sensors. Low sensor output signals require surface strain on the sensing elements to approach the elastic limit in order to obtain a measurable signal over a wide measuring range. As a result, the overload capability of strain gauge torque transducers is limited to about 20% of full range; this is too low for many applications. To overcome this problem, i.e. to increase overload capability whilst maintaining accuracy and resolution, work has been started to develop a new torque transfer standard using metallic resonant sensors [1]. Additionally, metallic resonant sensors give a frequency signal compatible with digital circuitry, so that analogue-to-digital conversion can be eliminated. Moreover, the resonant sensor provides better long-term stability, since the frequency signal is not dependent on the amplitude of the electrical signals and hence accuracy is not limited by signal-to-noise ratio.

Methodology/Approach

In 2005 Yan et. al [1] showed that the metallic resonant sensors based on a triple beam tuning fork (TBTF) design, activated by the PZT material, showed promise in the measurement of torque. However, the TBTFs with 40mm long (central tine 15.5mm, operating frequency 5-7kHz) expose some problems when assembled to the shaft for using as torque transducers. Finite Element Analysis (FEA) showed that the TBTFs not only measure the changes in tensile/compressive strain, which is the desired measured value, but experiencing shear strain and twist that effect the accuracy of torque transducer. The predominant cause was due to the length of the TBTFs which affects the measurement accuracy of the torque transducers used the

metallic resonant sensors. Reducing the overall size of the TBTFs will improve the accuracy whilst maintaining the stiffness of the resonant sensors. The first iteration was a TBTF device 20mm (9mm length tine) with the operating frequency 25kHz [2]. This sensor showed lots of improved realization and was calibrated at National Physical Laboratory (NPL) in UK against Torque Standard Machine (Deadweight Lever-beam) according to the British Standard (BS) 7882. From the calibration results, it is found that the class of accuracy of this torque transducer meets the requirements for class 1. The resolution of the indicator is the main parameter to limit the accuracy of this torque transducer so acquiring the indicating device with higher resolution would give benefit to improve the accuracy of this torque transducer.

Results and discussion

Since 2007, a new small version of the metallic resonant sensor has been produced. This resonant sensor has overall length 12mm (tine length 6mm, resonance frequency 40 kHz, $Q > 1000$). The sensor batches are currently being characterized and the torque measurement results used this miniaturized metallic resonant sensor as the torque transducers will be presented in the full publication submission later.

Conclusion

Quality of measurement in industry requires the measured value to be compared to reference standards, which are traceable to the base SI unit. This can be achieved by using transfer standards. The most common torque transfer standard, widely used in laboratories and in industry, is based on strain gauge sensors which the overload capability is too low for many applications. A new torque transfer standard using metallic TBTF resonant sensors was developed to overcome this problem whilst maintaining accuracy and resolution. The lateral force which degrades the accuracy of torque transducer using these sensors was solved by reduction in size. Presently, the miniaturization of the metallic TBTF resonant sensors was achieved by 70%. High stiffness of these metallic resonant sensors will additionally reduce the occurrence of wrong measurement values as a result of overload damage. Additionally, metallic resonant sensors give a frequency signal compatible with digital circuitry, so that analogue-to-digital conversion can be eliminated. Moreover, the resonant sensor provides better long-term stability, since the frequency signal is not dependent on the amplitude of the electrical signals and hence accuracy is not limited by signal-to-noise ratio. To support the use of these sensors in applications a transfer standard using this technology is recommended.

References

[1] Yan T, Jones B E, Rakowski R T, Tudor M J, Beeby S P and White N M, 2005. Stiff torque transducer with high overload capability and direct frequency output, IMEKO 19th Int. Conf. on Force, Mass, Torque and Density Measurements, February, Cairo, 5 pages

[2] J Intiang, J Weidenmuller, R T Rakowski, B E Jones, A Cheshmehdoost, 2007. Characteristics of 9mm Metallic Triple-Beam Tuning Fork Resonant Sensor. Sensors and their Applications XIV, Ed. S J Prosser and A Al-Shamma'a:Institute of Physics Publishing, 6 pages



SED Research Student Conference

Brunel University

22-24th June 2009

Materials from renewable resources for packaging applications:

Polylactic acid and starch

K. Manjula D. Silva¹, Karnik Tarverdi¹, Robert Withnall¹, Jack Silver¹

¹Wolfson centre for Materials, Brunel University, Uxbridge, Middlesex, UK.

Silva.Kodikara@brunel.ac.uk

Keywords : Extrusion, biodegradability, processing

Introduction

Human life has been extensively and inseparably associated with plastic materials due to the growing impact of plastics and its products. Utilization of plastic materials in packaging has increased exponentially over the last thirty years. However, the negative effect of these synthetic polymer based packaging has also increased exposing critical environment issues that has become a threat to human health and increased carbon foot print. Over the last few decades extensive efforts have been undertaken to use alternative materials from renewable resources but these polymers do not exhibit properties similar to commodity polymers.

Polylactic acid (PLA) is a versatile biodegradable polymer manufactured from fermentation of renewable agricultural feed-stocks into lactic acid followed by condensation polymerization to PLA. It has very good tensile strength but its impact properties and manufacturing cost have made its applications limited. However, wide production of PLA and its availability to the market is now expanding research on applications in different disciplines including packaging. Additives are also being developed today to improve properties of PLA. Starch is widely available natural material derived from renewable resources and easily biodegradable because of its nature. Research work has been carried out on these two materials [1-3] but as yet the results are inconclusive. This study is being undertaken as a part of the process of improving compatibility and also to ease the processability of starch and genetically modified organisms (GMO) free PLA blends under conventional polymer processing equipment to develop a packaging material.

Methodology

GMO free PLA and wheat starch blends were prepared and characterized in the presence of glycerol. Wheat starch and glycerol were premixed at 0, 2, 5, 8, 10, 15 wt% glycerol and then thoroughly mixed with PLA powder. Blend with 5% glycerol was also prepared in a similar manner with PLA pellets. Blends were extruded in a lab-scale co-rotating twin screw extruder, at a temperature profile of 130⁰ at feed inlet and 150⁰C for other zones. Pure PLA was extruded under similar conditions. Extruded strands were pelletized and injection moulded into tensile test bars and plaques. Degradation pattern was determined by Thermal Gravimetric Analysis (TGA) by heating to 600⁰C degrees at a rate of 10⁰C/min. Differential Scanning Calorimetry (DSC) test was carried out according to ASTM Method D 3417-83 and the thermal behavior was recorded. The tensile properties were determined according to BS EN ISO 527. Falling weight technique according to BS EN ISO 6603 was employed to measure impact properties. Microstructures of the blends were observed by a scanning electron microscopy (SEM). Fractured surface from a broken tensile test bar was gold coated before observation. Fourier Transform Infrared (FTIR) Spectroscopy was used to measure the spectra of the transparent thin films.

Results and Discussion

The thermal stabilities of PLA and blends were studied and maximum degradation temperatures T_{max} of the blends were determined by derivatized TGA. Weight losses by 5% ($T_{5\%}$) were also determined. The results demonstrate that the PLA degradation starts well above 300⁰C. Decomposition temperature of PLA is around 375⁰C but with the incorporation of starch and glycerol this temperature gradually decreased to 366⁰C. Temperatures of the blends at $T_{5\%}$ have decreased because of the starch as well as glycerol. Effect from starch towards T_{max} is higher than the effect from glycerol. At highest glycerol level $T_{5\%}$ has decreased almost by 130⁰ C compared to that of pure PLA. Apparently T_{max} of starch has increased in the blends. High enthalpy relaxation is observed in raw PLA as well as in the blends. However enthalpy relaxation diminishes in the second heating cycle. Broad crystallization peak is observed in the blends above 5% glycerol and it is very prominent above 8% glycerol in the second heating cycle. Glass transition temperature (T_g) decreased with increasing glycerol level in the blend.

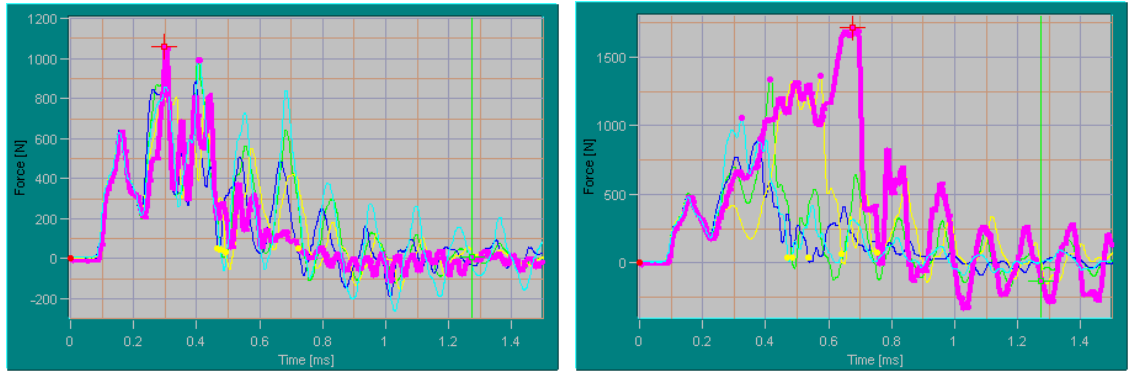


Figure 1. Impact behaviour of 85P15S and 85P15S15G blends on the left and right hand side, respectively

Tensile strength of the blends decreased with starch as well as glycerol. Upon addition of glycerol, strength is reduced but there is no significant difference in the percentage of decrease upon glycerol level. Glycerol was capable of increasing elongation and at most it has increased elongation of the blends by 10% compared to neat PLA. Moreover, there is an increasing trend in elongation and decreasing trend in modulus with glycerol levels. Impact behaviour demonstrates that there is no effect from starch towards energy absorption of the blend and resistance to deformation is considerably reduced. Figure 1 shows variation in force with time for Starch and PLA blends without and with glycerol. With the incorporation of glycerol, force as well as energy absorption is increased. At 15% glycerol level, very high energy absorption is observed and it was almost 43% greater than raw PLA.

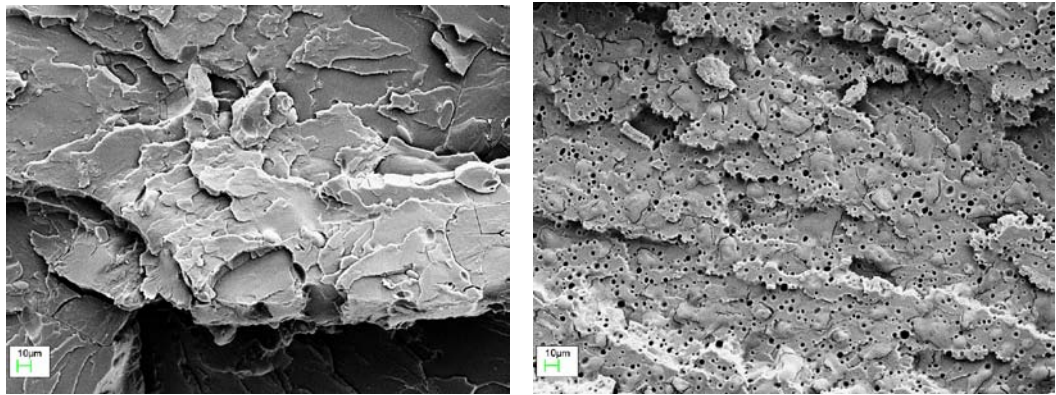


Figure 2 SEM micrographs of 85P15S and 85P15S15G blends on the left and right hand side, respectively

SEM micrographs of starch and PLA blends without and with 15% glycerol are shown in Figure 2. Better dispersion in the presence of higher glycerol is clearly seen in the micrographs. FTIR analysis show better plasticization and some interaction between PLA and starch in the presence of glycerol.

Conclusion

With the use of small particle sized PLA, better mixing has been achieved between PLA and starch. Results also suggest that the Tg of the PLA/starch blend can be reduced with increasing glycerol facilitating the processing of the blends under conventional polymer processing equipments. It is also observed that the ductility of PLA/ starch blends can also be enhanced with addition of glycerol to the blend. It is noticeable that the blends with glycerol have high energy absorption. Morphology shows better dispersion between PLA and starch in the presence of glycerol. Plasticization effect of glycerol is better and its coupling effect up to the technological requirements could be better depending on the mixing techniques, time and processing conditions. It is early days yet, but at this stage the experimental results demonstrate that enhanced material properties are achievable with controlled blending of PLA and starch.

Reference

- [1] H. Wang, X. Sun and P. Seib, Strengthening blends of poly(lactic acid) and starch with methylenediphenyl diisocyanate, *J Appl Polym Sci.* 2001, **82**, 1761–1767.
- [2] H. Wang, X. Sun and P. Seib, Mechanical properties of poly(lactic acid) and wheat starch blends with methylenediphenyl diisocyanate, *J Appl Polym Sci.* 2002, **84**, 1257–1262.
- [3] J.F. Zhang and X. Sun, Mechanical and thermal properties of poly(lactic acid)/starch blends with dioctyl maleate, *J Appl Polym Sci.* 2004, **94**, 1697–1704.



SED Research Student Conference

Brunel University

22-24th June 2009

A Novel Design for a Reconfigurable Micro-processing Cell

Rakan Alsharif¹, Harris Makatsoris¹

1. School of Engineering and Design, Brunel University, Uxbridge, Middlesex, UK

im06rra@brunel.ac.uk, Harris.Makatsoris@brunel.ac.uk

Keywords (3): Microfactory, Reconfigurable Manufacturing systems, Flexible manufacturing system.

Introduction

A new concept of machine tool design has been introduced during the last decade, aiming at satisfying the market demand and achieving better competitive position [1-4]. Reconfigurable Manufacturing Systems (RMSs) represent a new direction in designing and operating manufacturing processes by focusing on several aspects including; increase efficiency, achieve better market response and increase in process and production quality. Also, this concept provides the capability of performing a wider range of manufacturing processes and switching quickly between these processes based on current market demands [5].

This paper presents a new type of reconfigurable manufacturing system. The description of the system's design, its main components and architecture as well as performance is included.

Methodology/Approach

The approach followed in developing the system is highly iterative with several feedback loops. It was deemed necessary to adopt such an approach to ensure that not only the design is relevant but also it does progress the state of the art and takes into account the many considerations in machine design. The key design feature of the proposed architecture is the concurrent processing using multiple machining centres on the same frame. Perform several machining processes concurrently is quite a challenge and several considerations in the operation of the machine as well as the design of the machine itself have to be taken into account. Such considerations include safety as well as precision and repeatability that may be reduced as results of the proposed design. In addition, such as architecture requires an advanced control system to ensure coordination of machining and material handling processes.

Results and discussion

Validating such a novel architecture is a crucial step in the design process. Static and dynamic analyses have been performed to assess this design using finite element analysis (FEA) [6].

First, a static analysis has been done to study the reaction of the granite base while all three processing heads attached to it. Even that contact areas between the base and processing heads are under stress, the base is considered in a stable condition. The second step was to calculate the maximum dynamic displacement during each mode. This is a key step to estimate the stability and precision of each machining process. Therefore, damping level can be increased in order to have more precise processes.

Conclusion

In this paper, a novel design of a reconfigurable micro machining cell is presented and assessed using both static and dynamic FEA analysis. A comparison with an earlier design is also provided. The aim of this work is to progress the state of the art in the design of machine tools for micro manufacturing. This is achieved by a new architecture of a composite micro manufacturing system aiming at point of use manufacturing applications. Such systems are aimed at settings where highly customised precision components are required such as hospitals. The design presented in this paper has taken into account flexibility and reconfigurability and also tries to address issues such as reduction in energy usage, factory space and production time. Computational results have demonstrated that such a design can provide high levels of precision for the target application regardless of allowing several processes taking place concurrently while sharing a common base and obtaining services from the base. Further work includes a design that is detailed enough to allow construction of a real life prototype.

References

- [1] Okazaki, Y., Mishima, N., Ashida, K., (2004) “Microfactory – Concept, history and developments”, *Journal of Manufacturing Science and Engineering*, Vol. 126, No. 4, pp 837-844
- [2] Ashida, K., Mishima, N., Maekawa, H., Tanikawa, T., Kaneko, K., and Tanaka, M., 2000, Development of desktop machining Microfactory, Proc. J-USA Symposium on Flexible Automation, pp. 175–178.
- [3] Mehrabi, M. G., Ulsoy, A.G. and Koren, Y., 2000, Reconfigurable manufacturing systems: key to future manufacturing. *Journal of Intelligent Manufacturing*, 11, 413–419.
- [4] Lee, G. H., 1998, Design of components and manufacturing systems for agile manufacturing. *International Journal of Production Research*, 36(4), 1023–1043.

- [5] Fujii S, Morita H, Kakino Y, Ihara Y, Takata Y, Murakami D, Miki T, Tatsuta Y (2000). Highly productive and reconfigurable manufacturing system. *Proceeding Pacific Conference Manufacturing 2*:970–980.
- [6] Alsharif, R., Makatsoris, C., Sadik, S., (2008) “A novel Architecture for a Re-configurable Micro Machining Cell”, *The 6th International Conference on Manufacturing Research Proceedings*, Brunel university, UK, September 9-11, 2008, pp. 437-445.



SED Research Student Conference

Brunel University

22-24th June 2009

A Comprehensive Bandwidth Requesting Method for IEEE 802.16 WiMax Networks using Piggyback Requests

Usman Ahmed Ali¹, Dr. Qiang Ni².

1. Electronic and Computer Engineering, School of Engineering and Design, Brunel University, Uxbridge, Middlesex, UK

usman.ali@brunel.ac.uk

2. Electronic and Computer Engineering, School of Engineering and Design Brunel University, Uxbridge, Middlesex, UK

Keywords: QoS, Contention, Resource Request, WiMax.

Introduction

The IEEE 802.16 is a Broadband Wireless Access standard (BWA), which promises to provide Quality of Service support to applications having end-to-end delay, jitter and maximum loss rate [1]. In this standard, the Base Station (BS) is given responsibility to allocate bandwidths which are required by the Subscriber Stations (SSs). The Base station (BS) acts like a central server [4]. The Subscriber Stations (SSs) just have to send a bandwidth request to Base Station (BS) in order to give BS the knowledge of each SSs requirement. The SS can send this bandwidth request by participating in a competition during a contention resolution procedure. The parameters that are considered by this contention resolution are backoff start/end values and the number of transmission opportunities [3]. The IEEE 802.16 MAC protocol classifies five service classes, the unsolicited grant service (UGS) which is used for constant bit rate services, the extended real-time polling service (ertPS) used for real-time traffic having variable data rate, the real-time polling service, the non real-time polling service and the best-effort service. For the best effort class there are principally three different ways of how a SS can send a bandwidth request to BS i.e. during the bandwidth request contention phase, by means of unicast bandwidth requests, or piggybacked requests [5].

The IEEE 802.16 standard explains a method to ask for bandwidth in which a request is only granted for the amount of desired bandwidth by the HOL-packet which is present in a traffic queue, though, some packets can turn up between the arrival of the first packet thus generating the requesting process and the real time in which this request will be honored [2].

Methodology/Approach

In order to solve the bandwidth allocation problem, we have proposed a new aggregate approach for bandwidth request, in which a piggybacked request is generated previously and then the traffic queue is checked again. It then updates the bandwidth requested to the BS, so that the BS can get a more updated request and like wise a small number of requests will be used for the same quantity of bandwidth. We conducted a comprehensive simulation study using the OPNET Modeler 11.5 [6]. This simulation models accounts for both Physical and MAC layer and each WiMax cell has a frame size of 10 ms and it used TDD with an uplink subframe whose duration will be approximately 50% of the frame.

Results and discussion

We are able to get some results from our proposed model but these results show quite big delay for bandwidth allocation. In order to reduce this delay we are going to split the different types on traffic. By doing so the base station will know the total amount of bandwidth it requires for each type of traffic using piggyback requests. We are working on this model and as soon as the results become available, we shall update them in our paper.

Conclusion

The standard did not provide fairness to the important applications like video and voice. Their performance is degraded further in favor of applications which have lower priority. Our proposal is more stable as it provides fairness to those critical applications. All the bandwidth requests are piggybacked on previous packets for different application types.

References

- [1] IEEE, IEEE 802.16 Standard—Local and Metropolitan Area Networks— Part 16: Air Interface for Fixed Broadband Wireless Access Systems (IEEE Std 802.16–2004), IEEE Std., October 1 2004, revision of IEEE Std 802.16–2001.
- [2] J. Delicado, Qiang Ni, F. M. Delicado, and L. Orozco-Barbosa, “A Novel Aggregate Bandwidth Requesting Mechanism for IEEE 802.16” in press.
- [3] J. Delicado, F. M. Delicado, and L. Orozco-Barbosa, “Request Mechanisms to Reduce the Contention Period in 802.16: A Comparison,” in Proceedings of the 10th IFIP International Conference on Mobile and Wireless Communications Networks (MWCN 2008), 2008.
- [4] A. Vinel, Y. Zhang, Q. Ni, and A. Lyakhov, “Efficient Request Mechanism Usage in IEEE 802.16,” in Proceedings of the 49th IEEE Global Telecommunications Conference (GLOBECOM 2006), San Francisco, California, USA, November 27–December 1 2006.

- [5] Q. Ni, A. Vinel, Y. Xiao, A. Turlikov, and T. Jiang, “Investigation of Bandwidth Request Mechanisms under Point-to-Multipoint Mode of WiMAX Networks,” *IEEE Communications Magazine*, vol. 45, no. 5, pp. 132–138, May 2007.
- [6] OPNET Technologies, “OPNET Modeler 11.5,” 2005.

Monoclonal antibody purification using robotic phase system selection coupled with counter current chromatography (CCC)

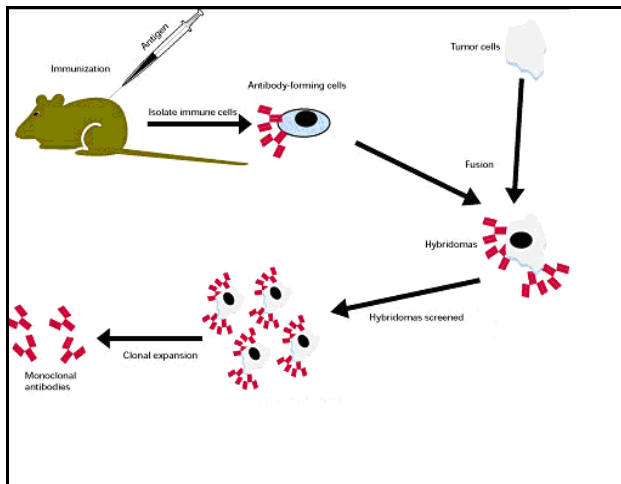
Samantha Fernando, Derek Fisher and Ian Garrard

*Advanced Bioprocessing Centre,, Brunel Institute for Bioengineering, Brunel University
Uxbridge, Middlesex, UK*

Samantha.fernando@brunel.ac.uk

Introduction

Figure 1: Monoclonal antibody production



Background 1: Monoclonal Antibodies

Antibodies are widely acknowledged as the initial defence mechanism of the body’s immune system. Monoclonal antibodies were developed by Kohler and Milstein. By fusing antibody producing cells with (immortal) tumour cells to produce cell lines that secreted specific antibody continuously. (Figure 1). This has led to a multi million pound industry for biopharmaceuticals and establishment of monoclonal antibodies as market dominators both for analytical uses and therapeutically (e.g. as specific targeting agents coupled with drugs).

Background 2: Current problems in the bioprocessing of monoclonal antibodies

Purification of pharmaceutical antibodies is required for the removal of impurities. High dosage requirements of specific antibodies warrant the importance of an economically large scale purification process. As demand for increased quantities of monoclonal antibodies has developed, intensification of cell culture productivity (from 1g/l to 10g/l) has spectacularly improved upstream productivity (figure 2). This to the extent that downstream processing which accounts for about 50-80% of total production costs has now been seen as the bottleneck in production. The necessity to produce a downstream purification technique that can complement the dramatic improvements in upstream processing has never been so important (figure 3).

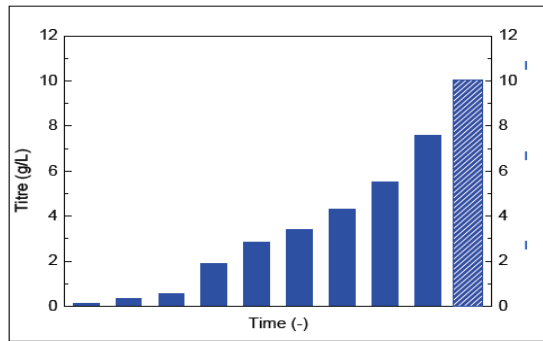


Figure 2: Increasing fermentation titres

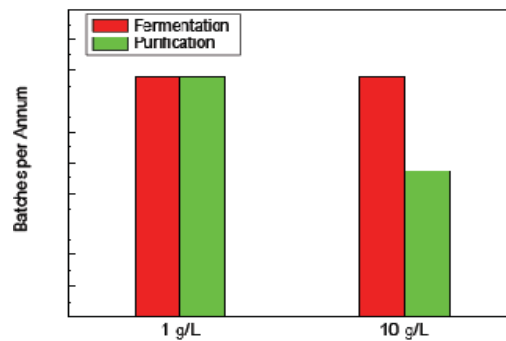


Figure 3: Process bottleneck

Methodology/Approach

Objective of Current Research: Counter current chromatography as step change in the purification of monoclonal antibodies

At the Brunel Institute for Bioengineering (BIB) monoclonal antibody purification has been proposed by the investigation of CCC. CCC is a form of continuous liquid chromatography, which the BIB team have developed up to process scale. Key to this technique is phase selection. The selection of phases for CCC can be laborious and requires considerable insight into the effects of particular solvents on the distribution ratio of compounds, which can cover a wide range of hydrophobicities. A robotic selection method for small molecules in aqueous-organic two-phase systems has previously been developed [1] and is applied routinely as part of the facilities of the Brunel Advanced Bioprocessing Centre (ABC).

In current work on the use of Brunel's countercurrent centrifuges for the purification of monoclonal antibodies [2,3] there has been a need to select phase systems to provide appropriate distribution ratios of monoclonal antibodies and contaminating proteins in aqueous two-phase systems (ATPS), which preserve protein structure and function, allowing purifications to be achieved without loss of biological function of the antibodies.



Phase systems (4ml) were prepared on a w/w basis from concentrated aqueous stocks of PEGs and salts using a Perkin Elmer Multiprobe Liquid handling robot (Fig 4). Samples were incorporated into the phase system as part of the make-up of the phases. Mixing was achieved by inversions of tubes several times. Phases were then permitted to settle until a sharp interface was observed. The volume ratio was estimated by measuring the height of both phases. The robot was used to samples both the top and bottom phases and dispense the samples into vials or a 96-well plate for analysis.

Figure 4: Perkin Elmer Multiprobe Liquid handling robot

Results and discussion

We have extended our experience of the liquid handling robot and aqueous-organic system to prepare PEG-salt phase systems; to perform partitions, take samples for analysis, and perform analyses[4-5]. Systems have included PEG 400, 1000, 3350 and 8000 (molecular weight 400-8000) with sodium, potassium or ammonium phosphate, sulphate or citrate. In this work we have gained considerable insight and encountered many problems which have lead to extensive troubleshooting. This includes the issues with viscosity of the PEG solutions, precipitation of salts (ultimately affecting system volume) and difficulty in sampling. All these issues have been overcome by familiarization of robotic programming.

Conclusion

This work has shown the coupling of robotic screening of ATPSs has a definite commercial value. This is compounded by poor protein partition predictably being the major cause of the limited use of ATPSs in industry.

References

The help and advice of Lukasz Grudzien is gratefully acknowledged.

[1] Garrard, I. (2005) *J. Liq. Chrom. & Rel. Technol.* **28**, 1923-1935

[2] Sutherland, I.A. Audo, G. Bourton, E. Couillard, Fisher, D. Garrard, I. Hewitson, P. & Intes O. (2008) *J. Chromatogr. A.*, **1190**, 57-62

[3] Guan, H., Bourton, E. Hewitson, P. Sutherland, I.A. & Fisher, D (2009) *Separation and Purification Technology* **65**, 79-85

[4] Bensch M, Selbach B & Hubbuch J. (2007) *Chemical Engineering science.* **67** 2011-2021.

[5] Susanto A, Treier K, Knieps-Grunhagen E, Von Lires E & Hubbuch J. (2009) *Chem. Eng. Technol.* **32** 140-154.



SED Research Student Conference

Brunel University

22-24th June 2009

Load Flow Analysis with Voltage and Reactive Power Optimization in Distribution Networks using NEOS Solvers

Jan Veleba^{1,2}, Malcolm Irving²

1. Department of Electric Power Engineering and Ecology, Faculty of Electrical Engineering, University of West Bohemia, Pilsen, Czech Republic
2. Brunel Institute of Power Systems, School of Engineering and Design, Brunel University, Uxbridge, Middlesex, UK

jveleba@students.zcu.cz, jan.veleba@brunel.ac.uk

Keywords: Load Flow, NEOS Server, Nonlinearly Constrained Optimization.

Introduction

For decades, the conventional load flow calculation is used for understanding the basic behaviour of electric power systems. The main aim is to compute all the unknown variables such as voltage magnitudes, angles, injected active and reactive powers in all buses and by obtaining power flows and total power losses of the network. The most widely-used numerical methods, historically employed for the load flow analysis, are the Gauss-Seidel (G-S), Newton-Raphson (N-R) and Fast-Decoupled (F-D) method, respectively. Nowadays, the conventional load flow calculation has also been used as a first step to perform many other power system analysis tasks, such as optimal power flow calculation (OPF), security constrained economic dispatch (SCED), contingency analysis, network planning, etc. However, the complexity of the load flow analysis, combined with many other optimization tasks, can pose an increased burden for the commonly-used programming tools and numerous commercial programs. Therefore, some of the new software packages can be broadly employed among others also for the load flow analysis and eventually they could represent more straightforward and flexible approach.

This research paper is focused on the NEOS (Network Enabled Optimization System) project. NEOS currently contains 65 solvers, which can be used for solving the variety of optimization problems. For each problem, user needs to choose the appropriate solver and for this solver, the problem must be formulated in the input data file using specific text format (e.g., GAMS, AMPL, MPS). After that, such an input data file is submitted to the server through the e-mail/web interface or by using a specialized program on the client's computer. The problem is

delivered to the NEOS Server, where the calculation is performed. Results can be seen on the NEOS Server by entering the job number and password. Additionally they can be sent to the user's e-mail address.

The major task of this paper is to prove the suitability of the NEOS Optimization Server for the load flow analysis of large power systems and for the voltage and reactive power optimization in distribution networks. According to the authors' opinion, the affirmative answer can be expected in this paper.

Methodology/Approach

In the general form, the load flow calculation is a nonlinearly constrained, large-scale, static optimization problem with both continuous and binary variables. Such a problem, similarly as in [2], can be formulated as

$$\text{minimize } f(x)$$

subject to

$$g(x) = 0;$$

$$h_l \leq h(x) \leq h_u;$$

$$x_l \leq x \leq x_u.$$

Function $f(x)$ is an objective function, mostly a generation cost function for the slack bus of the solved power system. However, when the PV buses are situated in the network, another objective function has been developed and tested. Function $g(x)$ represents the power balance equations and function $h(x)$ comprises the equations for power flows, total power losses and reactive power generations by shunt compensators. Unknown vector x includes voltage magnitudes, angles, transformer tap ratios and another ancillary variables.

The input data file, created with the above described structure, can be tested in NEOS environment and results can be obtained for further studies.

Results and discussion

The AMPL language, fully introduced in [1], has been used for the description of electric power systems. Due to a relatively extensive volume of input data, a special program has been created for converting input data from Matlab into the AMPL format. In a comprehensive simulation using different NEOS solvers on networks between 57 and 734 buses, only four solvers were found suitable for solving the above described problem. Sequentially, the voltage and reactive power optimization has been accomplished and tested in case of synchronous compensators and generators with AVR, shunt capacitors/reactors, static series capacitors and tap changing transformers.

Conclusion

In this research paper, the NEOS project proved its robustness and suitability for the load flow analysis and for the voltage and reactive power optimization in distribution networks. It is expected, that a progressive study and use of this optimization tool will be broadly performed and tested in the area of power system analysis.

References

[1] R. Fourer, D.M. Gay, and B.W. Kernighan, *AMPL: a modeling language for mathematical programming - 2nd edition*, Brooks Cole, December 2002.

[2] Y.H. Song, *Modern Optimisation Techniques in Power Systems*, Springer, 1999.

RESCON '09

DAY TWO: SESSIONS



SED Research Student Conference

Brunel University

22-24th June 2009

Various Delay Channel Access Algorithms for the IEEE 802.11n

Dionysios Skordoulis¹, Qiang Ni¹

1. Electronic & Computer Engineering, School of Engineering and Design, Brunel University, Uxbridge, Middlesex, UK

Dionysios.Skordoulis@brunel.ac.uk

Keywords: IEEE 802.11n, MAC, scheduling

Introduction

In this abstract we investigate the potential benefits of a delayed channel access algorithm for the next-generation high-throughput wireless networks. The IEEE 802.11n latest draft [1] attains rates of 100+ Mbps by introducing innovative enhancements at the physical layer (PHY) and Media Access Control sublayer (MAC), e.g. MIMO and frame aggregation, respectively. However, frame aggregation's operation adheres due to the EDCA's (Enhanced Distributed Channel Access) scheduler priority mechanism from IEEE 802.11e [2], resulting in the network's poor overall performance. As high priority flows have low channel utilization because of their traffic characteristics, the low priority flows throughputs can be amerced even further. This abominable performance was first described in [3] and a delayed channel access (DCA) algorithm was initially proposed that it impels stations (STAs) into further deferring in a way that it allows throughout more packets to arrive and it results to the end aggregated frame size to increase further. Although, the proposal was interesting, TCP flows with various TCP window sizes wasn't considered during the evaluation and as we explain in this work, these could result in aggravate and negative behaviour, mainly because of a functioning halt (short deadlock) occurring in both TCP and DCA's algorithm. The scope of the research is to derive alternative methods, based on the initial DCA, which will overcome this problem.

Methodology/Approach

We propose two separate algorithms, known as ADCA and SDCA. They both differ over their methods and design but the simulation results derived from each show significant improvements over the original IEEE 802.11n specification and the initial DCA. The first enhancement has a dynamic nature, where the algorithm's conditional triggers will be regularly adapted over the progressive traffic status, thus it is called Adaptive DCA (ADCA) [4]. Our proposal introduces an adaptive aggregate size threshold that gradually increases or decreases until the flight size (number of segments in the sender's buffer size) of the TCP flow is reached. The second proposal, named as Selective DCA (SDCA) [5] is a flow discriminative function that will allow DCA to countermand its operation over the TCP segments. The algorithm is based on the recording and analysis of the time arrival intervals between consequent packets arriving from higher layers. Both of our approaches are MAC-exclusive solutions without the need of a cross-layer design.

Results and discussion

The models for both proposals are implemented and simulated in OPNET Modeler 10.5. For our main scenario, we consider an overloaded 802.11n WLAN that includes three STAs and an Access Point (AP) with operational PHY rate at 117 Mbps. We set two types of HDTV flows over User Datagram Protocol (UDP) between the AP and two of the STAs (one type each) and an internet file transfer from the third STA to the AP transmitted over TCP. All MSDUs are 1500 bytes in size and the offered loads are 19.2 Mbps, 24 Mbps and 120 Mbps for the HDTVs and FTP, respectively. From Figure 1, it is perceptible the importance of the various DCA algorithms as the throughput of the internet file transfer flow increases greatly compared with the standard TGN (No DCA). However, in Figure 2 we can derive the consequences of initial DCA over lower TCP CWND as the throughput reduces but the alternative solutions that we propose overcome this problem and at the same time retain first-class outcomes. On the other hand, the high priority flows do not get hindered and they maintain their maximum goodputs.

Conclusion

In conclusion, although we know that DCA increases the network's performance, when it comes down to TCP traffic with small window buffers there is an issue which needs to be resolved. Both of our proposals, ADCA and SDCA, where are adequate in their own manner, can extensively improve the channel efficiency and the data throughput. These resolutions may be implemented on any future high-throughput next-generation network that adapts frame aggregation with the EDCA based scheduler.

References

- [1] IEEE P802.11n, Draft 2.5, "Part 11: Wireless LAN Medium Access Control (MAC) and Physical Layer (PHY) Specifications: Enhancements for Higher Throughput", IEEE-802.11 WG, July 2007.
- [2] IEEE Std. 802.11e WG, "Part 11: Wireless LAN Medium Access Control (MAC) and Physical Layer (PHY) Amendment 8: Medium Access Control (MAC) Quality of Service Enhancements", IEEE-SA Standards Board, November 2005.
- [3] L. Changwen, A.P. Stephens, "Delayed Channel Access for IEEE 802.11e Based WLAN", IEEE ICC '06, June 2006, vol.10, pp.4811-4817.
- [4] D. Skordoulis, Q. Ni, K. Borg, G. Min, "Adaptive Delayed Channel Access for IEEE 802.11n WLANs", IEEE ICCSC '08, May 2008, pp. 167-171
- [5] D. Skordoulis, Q. Ni, C. Zarakovitis, "A Selective Delayed Channel Access (SDCA) for the high-throughput IEEE 802.11n", IEEE WCNC '09, April 2009

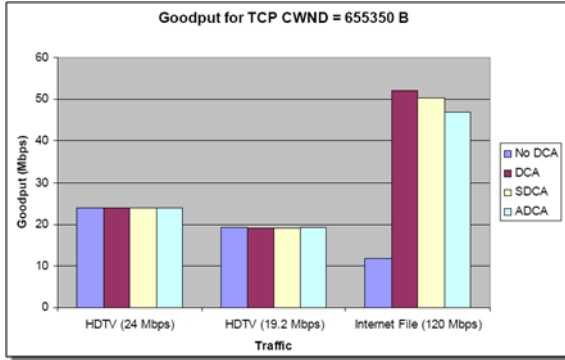


Fig. 1 – High TCP CWND

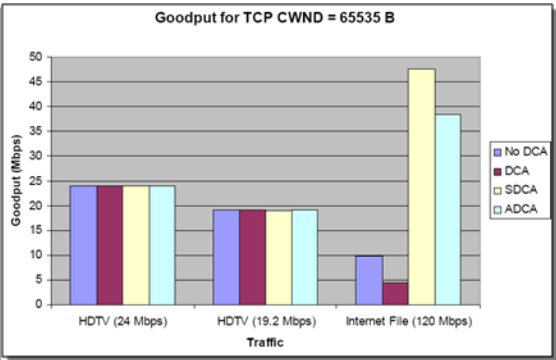


Fig. 2 – Low TCP CWND



SED Research Student Conference

Brunel University

22-24th June 2009

Effects of the Interaction between Physical and Mental Workload on Human Performance

Abdulrahman Basahel , Mark S. Young

Human-Centred Design Institute, School of Engineering and Design
Brunel University, Uxbridge, Middlesex, UK

lged003@Brunel.ac.uk

Keywords: Physical workload, Mental workload, Human Performance.

Introduction

Workload is an important factor that affects human performance in an operating system. Many tasks in the workplace impose a physical workload (PWL), which in turn places loads on mental tasks and cognitive resources [4]. The human response to both mental and physical workload as well as their interactions lead to increase in level of arousal, which can be measured by a rise in both heart rate (HR) and blood pressure [3]. Workload measurement is capable of solving many problems related to system design, increasing demands, and unacceptable performance. This study will investigate the effect of the relationship between physical and mental workload and level of arousal on operators' performance.

Physical and mental workload interaction and performance

In fact, a number of studies have investigated the impact of physical and mental workload on performance, though the two types of workload have been investigated separately without consideration of their interactions [1]. In addition, the results of many previous experiments on the effects of physical workload on mental task performance are not homogeneous [1]. However, some researchers argue that increasing the level of physical effort leads to a decrease in performance level similar to increasing the difficulty of a task [2]. Regarding the effects of combinations of PWL and mental workload (MWL), some research has reported that a short period of physical activity caused a decline in performance accuracy in mental tasks, such as map understanding, whereas other experiments have concluded that a physical load has no effect on complex mathematical tasks [4]. In contrast, other studies have demonstrated an inverted 'U'-shaped relationship between physical workload and an arithmetic mental task performance [4]; however, Perry et al. (2008) pointed out that physical activities in a soldier scenario (e.g., standing, walking, jogging) have no clear influence on cognitive tasks (e.g., planning loads in a helicopter).

The study motivation and hypotheses

This experimental study generally aims to investigate the impact of interactions of physical load, using a bicycle-ergometer, and mental workload, using arithmetic tasks, as multi-task demands on individual performance under various combinations of each workload type (low, medium and high). It will also measure the level of arousal in each condition in order to match the variables to determine how these factors affect task performance. A review of the literature found a gap in investigation of the influence of concurrent physical and mental workloads on performance [1,4]. In particular, little research has been conducted on the influence of physical workload on performance of highly difficult arithmetic tasks [4]. Furthermore, some research demonstrated an inverted 'U'- shaped relationship between physical demands and responses [4]. Moreover, acceptable individual performance occurs at an intermediate level of arousal, as suggested by some researchers [5]. As a result, we will design a factorial laboratory experiment under nine conditions as showed in figure 1 to evaluate the impact of physical load and mental load interactions on operator response as related to their level of arousal while performing a task. This is a summary of the experiment that will be developed more deeply in future work.

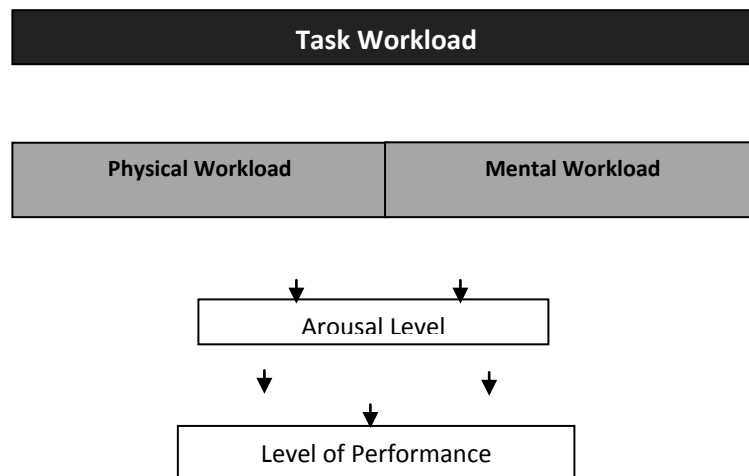


Figure 1- Design of Experiment

This experiment will hypothesise that performance will decrease with high levels of physical demand and mental workload because of overloading of workload and arousal levels. In addition, unacceptable performance will occur under low physical workload while doing a main task and with low mental task workload conditions as a result of underload of workload and arousal level. In contrast, in the interactions between physical and mental workload, it is expected that acceptable task performance will occur at the intermediate level of factor interaction and medium level of arousal variable. As previously reported [2, 4], a relationship has

been found between PWL, MWL, and operator performance; however, this relationship depends on the level of each factor.

Conclusion

Task workload measurement is a necessary tool in the process of operating system design and diagnosis. This research study will examine the effect of combination of physical and mental demands in dual occupations on human performance. Furthermore, this experimental study will consider various levels of load of each factor in order to identify the level of interaction of these factors and arousal variables that leads to optimum level of performance. This will be validated by the results of the experiment which are in progress.

References

- [1] Astin A. and Nussbaum M. A, "Interactive effects of physical and mental workload on subjective workload assessment". *Proceedings of the Human Factors and Ergonomics Society 46th Annual Meeting*, 2002.
- [2] Didomenico A. and Nussbaum M. A, "Interactive effects of physical and mental workload on subjective workload assessment". *International Journal of Industrial Ergonomics*, Vol. 38, No.11-12, pp. 977-983, 2008.
- [3] Fredericks T. K., Choi S. D., Hart J., Butt S. E. and Mital A, "An investigation of myocardial aerobic capacity as a measure of both physical and cognitive workloads". *International Journal of Industrial Ergonomics*, Vol. 35, No.12, pp.1097-1107, 2005.
- [4] Perry C. M., Sheik-Nainar M. A., Segall N., Ma R. and Kaber D. B, "Effects of physical workload on cognitive task performance and situation awareness". *Theoretical Issues in Ergonomics Science*, Vol. 9, No.2 , pp. 95-113, 2008.
- [5] Young M. S. and Stanton N. A, "Attention and automation: new perspectives on mental underload and performance". *Theoretical Issues in Ergonomics Science*, Vol. 3, No.2 , pp.178-194, 2002.

Smart implants for measurement of strain during fracture healing

Jaya. L. Nemchand¹, Anthony.W.Anon¹, Benjamin.J.Jones¹, Darren.J.Wilson²

¹Experimental Techniques Centre, Brunel University, Uxbridge, UB8 3PH UK

Smith and Nephew Research Centre, York, YO10 5DF

Jaya.Nemchand2@brunel.ac.uk,

Keywords: Intramedullary nailing, fracture healing, bone callus

Abstract

The object of this study is to determine strain distribution in an intramedullary nail during fracture healing. Loads carried by the nail during simulated fracture healing were monitored *in-vitro* by the use of embedded strain gauges. Measured strain was higher on the medial side of each of the fractures in various positions. Simulated bone composite material was applied to the fracture incrementally, to approximate fracture healing. Strain was measured after each step of callus bridging and a gradual decrease was observed.

Introduction

Intramedullary (IM) nailing is the method of choice for stabilising diaphyseal long-bone fractures to facilitate healing. Continuous monitoring of changes of the *in-situ* load distribution between the implant and bone is conventionally carried out using X-Rays, MRI and micro CT imaging. During fracture healing, load sharing between the implant and the bone changes; a telemetry system can be used to measure these load changes. Bergmann *et al.* has developed and demonstrated the use of telemetry measurements with strain gauges [1]. A later study by Schneider *et al.* [2] concluded that “an implant equipped with a multi channel telemetry system is a powerful tool to investigate loading *in-vivo*.” However, the fracture healing process consists of early stage bone tissue which progressively develops to mature osteogenic bone. This process is not adequately expressed in the proposed test methodology. Therefore consideration was given to the development of a material whose properties could be varied, approximating early to mature bone callus material [3] and incorporating these variable property materials in simulated fractures and subsequent mechanical testing regimes. However, there has been no published study to measure the load supported by a cannulated IM nail during the healing process [2].

Methodology

A tibial nail was instrumented with 12 strain gauges, wired to a data logger, mounted on machined flats at three strategic positions with 4 gauges at each of these of positions. The instrumented tibial nail was implanted in an anatomically correct bone mimic. Three segmental transverse fracture patterns were investigated in the proximal, midshaft and distal third of each sawbone. A polymer interface was attached at the top and the bottom of the construct to interface with a calibrated test machine. The nail construct was loaded in compression axially, beginning at 0 Newton, and increased to 500 N at 50 N increments. The expected resultant force on the tibia during peak loading in single leg stance phase of gait was approximated by a single load line aligned 9mm medial to the centre of the tibia at the ankle and 23mm medial to the centre of the tibia at the knee [4]. An experiment was initiated to achieve a composite with mechanical properties approximating bone callus material. Sample mixtures of resin and particulates or fibrous materials were cast. Under compression testing, stress-strain data was compared to the load bearing properties of human bone.

Results and Discussion

It was observed that for each construct, the highest strain value was medially positioned. The lowest value was found on the posterior side. The highest strain observed ranged from 400 $\mu\epsilon$ to 550 $\mu\epsilon$ at a peak load of 500 N. The hysteresis for each curve was virtually zero. Considering the above observations, the strain measured showed consistency in the results. The hypothesis proposed in the orthopaedic industry is that forces measured from an intramedullary nail, normalised by the ground reaction force, will progressively decrease in a sigmoidal manner as a midshaft fracture heals. However, a reduction in nail load will depend on the fracture mechanics and the patient activity. Schneider *et al.* reported a 50% drop in the load transmitted in the nail for a midshaft comminuted fracture [2]. The modulus of elasticity for human bone in compression is 18.2 GPa typically [5]. The values of the composites designed range from 68 - 111 MPa. At 111 MPa, the composite used was 0.6% of the actual modulus of elasticity of bone, but is used as a proxy model to approximate early-stage healing. The composite was applied to the fracture on the proximally fractured sawbone construct. The composite was applied in 8 steps for the callus bridging. Strain measurement was taken after each step and a drop in strain was observed.

Conclusion

Loading the bone during healing has been previously investigated in the animal model; this indicates a decrease in strain as healing progresses. In this study, the decrease is significant for some strain gauges and appears to be dependent upon gauge position relative to the callus. This study utilises a composite material to approximate early callus to show the response of mechanical loading on the nail when initial callus bridging occurs. The decrease in strain measurement is consistent with the study conducted by Schneider *et al.*, which demonstrated that fracture healing results in a large reduction of implant loads [2]. This study simulated early fracture healing and did not consider the influence of connective and muscular tissue activity

which plays a significant role in fracture healing. However, this study highlights that bone healing processes play an important role in the loading regime of the intramedullary nails and proposes an experimental methodology to replace animal models in the development of novel implants.

References

- [1]. G. Bergmann , F. Graichen , J. Siraky , H. Jendrzynski and A. Rohlmann; *J Biomech.*, **21** (1988) 169-176
- [2]. E.Schneider, M.C. Michel, M.Genge, K. Zuber, R. Ganz and S. M. Perren; *J Biomech.*, **34** (2001) 849-857
- [3]. GB Patent: GB0907766.1
- [4]. Hutson, Zych, Cole, Johnson, Ostermann, Milne, Latta; *Clin Orthop Relat R.*, **315**, (1995)129-137
- [5]. *Bones Structure and Mechanics* – J.D.Currey, Princeton University Press,2002

Fingerprint Sensing: Issues and Solutions

Shahzad Memon¹, Wamadeva Balachandran ²

Centre for Electronics Systems Research, School of Engineering and Design, Brunel University,
Uxbridge, Middlesex, UK
Shahzad.memon@brunel.ac.uk

Keywords: Fingerprint sensor, Levels of fingerprint, Nanotechnology

1.0 Introduction

The use of automatic recognition and identification systems for maintaining security levels has increased globally in the last decade. These systems are practically implemented at various places such as airport security, border and immigration services, cash machines and mobile devices. Using physical and psychological traits of an individual (is known as biometrics) for positive identification has become increasingly popular [1]. Figure. 1 shows the market share of Biometric Technologies during the period 2009 – 2014 [4]. According to the report published by the International Biometric Group, in the coming years the fingerprint technology will contribute more revenues. The use of fingerprints as a biometric is both the oldest mode of personal identification and the most prevalent in use today. Fingerprint has been used by law enforcement agencies since the late 1800s, and machine based fingerprint systems has been commonplace since the 1960s [2]. In the recent past, the Automated Fingerprint Identification

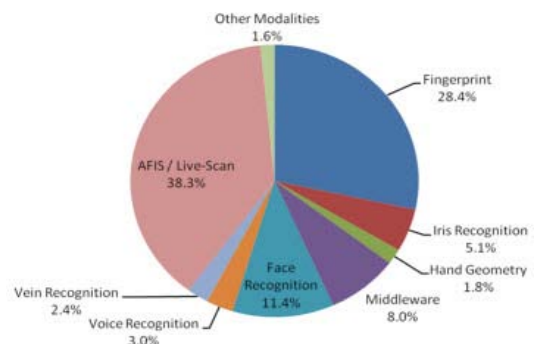


Figure 1. Market Share for Biometric

Technologies
Systems (AFIS) (See Fig. 2) has become an essential tool in the above mentioned applications as well as in access control [3]. The performance of many of the existing fingerprint sensors is subject to spoofing (fake & dummy), and identification and authentication is limited to about 85%. It is therefore necessary to develop new fingerprint sensors to improve False Acceptance Rate (FAR) and False Rejection Rate (FRR) in order to provide better biometric identification systems.

1.1 Automatic Fingerprint Identification Systems (AFIS)

In every AFIS the fingerprint sensor is a main module that obtains the unique features up to three levels (see Fig. 3). The level-1 refers to the overall pattern formed by the flow of ridges, classification, ridge count, focal areas and orientation on the surface of the finger [6]. Level-2 refers to major ridge path variations, also known as minutiae, the location of the major changes in individual ridges such as ending, bifurcations, islands, dots combinations, and their relationships [7]. Finally, Level-3 includes all dimensional attributes of a ridge such as

ridge path deviation, width, shape pores, edge counter, incipient ridges, breaks, creases, scars and other details [8]. The rapid developments in device fabrication technology facilitate to design and develop finger print capture devices with various technologies such as optical, thermal, capacitive, pressure, acoustic and radio frequency (RF). Although most of the fingerprint sensors using these technologies are small in size, has adequate

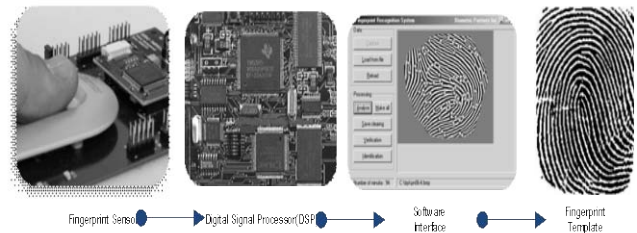


Figure.2 Automatic Fingerprint Identification

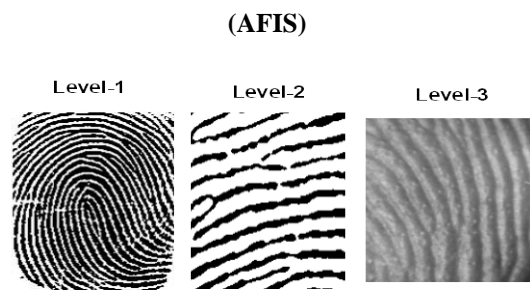


Figure.3 Levels of Fingerprint Features

resolution and has fast image processing capabilities, but they are vulnerable to liveness detection and have high values of FAR and FRR [5].

Currently the rapidly advancing interest in the use of nanotechnology for sensing applications has created the possibility to design novel sensing techniques for many applications. The mechanical, electrical and thermal properties of nanostructures such as nanowires and carbon nanotubes (CNT) (see Fig. 4) have demonstrated their future usage for electronics, biotechnology and aerospace applications [9]. By using the arrays, it is possible to design a fingerprint array sensor that may alleviate the shortcomings of the existing fingerprint sensors.

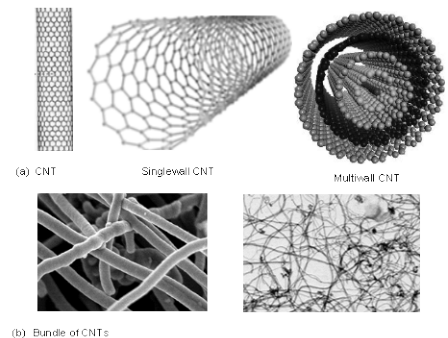


Figure.4 Carbon Nanotubes Nanostructures

1.2 Methodology/Approach

The methodology of this research is represented in Figure.5. The research commenced by critically literature reviewing on fingerprint sensor technologies that are available at present. In the second stage practical testing of fingerprint sensors were accomplished to understand the functionalities and the limitations associated with them. In the third stage (current stage) some simulations studies with respect to sweat pore activities are being undertaken to evaluate the inherent low currents.

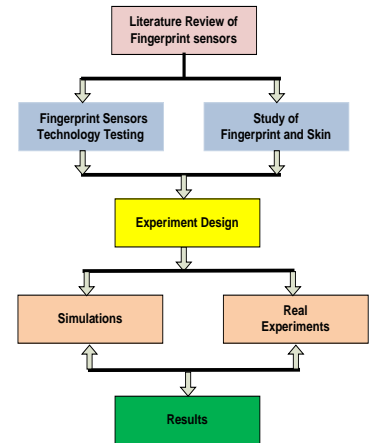


Figure.5 Research Methodology

1.3 Conclusion

The research is being pursued to design and develop a nanotechnology based novel fingerprint sensor that will eliminate spoofing and improve both FAR and FRR. In addition the sensor will have an inherent feature of liveness detection.

References

- [1] John D. Woodward, Nicholas M. Orlans and Peter T. Higgins, Biometrics. McGraw-Hill Professional, 2003
- [2] David R. Johnson. (2002, Suspect identities: A history of fingerprinting and criminal investigation. Journal of Interdisciplinary History 33(2), pp. 281-282.
- [3] Nalini Kanta Ratha, Ruud Bolle. (2004, Automatic Fingerprint Recognition System.
- [4] Anonymous (2008, October 2008). Biometrics revenues by technology 2009. 2009/(0315), pp. 1.
- [5] Fernando Alonso-Fernandez, Fabio Roli, Gian Luca Marcialis, Julian Fierrez, Javier Ortega-Garcia and Joaquin Gonzalez-Rodriguez. (2008, Performance of fingerprint quality measures depending on sensor technology. Journal of Electronic Imaging 17(1), pp. 11.
- [6] D. Maltoni, D. Maio, A. K. Jain and S. Prabhakar, Handbook of Fingerprint Recognition. New York: Springer Verlag, 2003
- [7] Neil Yager and Adnan Amin, "Fingerprint verification based on minutiae features: a review " Pattern Analysis & Applications, vol. 7, pp. 94-113, 2004.

[8] Anil Jain, Yi Chen and Meltem Demirikus. Pores and ridges: Fingerprint matching using level 3 features.

[9] Prithu Sharma and Perit Ahuja, "Recent Advances in Carbon nanotube-based electronics," Materials Research Bulletin, 2007.



SED Research Student Conference

Brunel University

22-24th June 2009

Simulating of graphene's epitaxial growth on SiC surface

Nikolai Issakov

Supervisor – Dr. Harris Makatsoris

Advanced Manufacturing & Enterprise Engineering

Key words: graphene; epitaxy; interface; truncated bulk; bilayer; dangling bond; SPML

Introduction

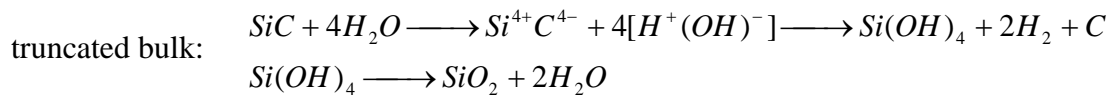
Epitaxial growth on the differently terminated SiC surfaces is simulated with a view to interpretation of interface processes leading to graphene's synthesis and development of the all-carbon nano-electronics paradigm based on the planar 2D structure. The unique properties of graphene comprise the ballistic transport, giant charge carrier mobility, large electron free path, ability to overcome thousands of inter-atomic distances without scattering, the superior conductivity and quantum conductance. The exclusive electronic structure of graphene determining the unique properties is arisen from symmetry of crystalline lattice [1-4]. The periodicity in honeycomb lattice is expressed in terms of two sub-lattices in view of equivalent and interpenetrating triangles. As a result of quantum-mechanical hopping between these sub-lattices 4-valence electrons of each carbon atom conventionally expressed as $2s^2 2p_x^1 2p_y^1$ is modified into $2sp^3$, *i.e.* the valence level has one *s*-orbital and three *p*-orbitals (promotion). Three atomic orbitals $2s$, $2p_x$ and $2p_y$ are tied up by strong covalent bonding, *i.e.* sp^2 hybridised, and form three new molecular orbitals. Their wave functions while forming the π state in the *XY* plane with the appropriate π and π^* bands join carbon atom to three neighbors. The $2p_z$ orbital is corresponding to nonbonding π state formed valence π and conduction π^* bands responsible for the conductivity. The π bands separate the occupied and empty states in some energy range including the Fermi level and intersect in the Dirac's points near the edges of the Brillouin zone (BZ). As a result graphene is a semiconductor with zero-gap. The low energies of charge carriers depending on wave vectors around the BZ obey the linear dispersion relation not characteristic of the other condensed matters. It implies the existence of quasi-particles like to relativistic fermions described by different components of the same wave function in the Dirac's equation rather than the Schrodinger equation. The graphene's behavior should be different and unpredictable as opposed to conventional metals and semiconductors. First of all it concerns the problems of synthesis and interaction with the other condensed matters.

Methodology

The updated approaches to graphene's synthesis include mechanical splitting, chemical exfoliation, organic synthesis by CVD, epitaxial growth on the solids. The latter carried out on the SiC surfaces involving decomposition of substrate, Si sublimation and graphitization on the surfaces owing to excess of carbon is the most advanced one [5, 6]. However, whichever mechanism and control on these processes in interface area are not clear. Therefore the work was intended for simulating of graphene's epitaxial growth on the differently terminated SiC surfaces. Our work was undertaken on the basis of relevant experiments. Computational model and electronic structure were studied by using the CASTEP code based on the first principles of DFT within the generalized gradient approximation [7]. Ultrasoft pseudopotentials were used with a plane wave basis cutoff equal to 240 eV. Integration over the BZ was performed by special 8 k-points on a 3x3x1 MP grid. By using this program a truncated bulk with 100 atoms forming two slabs, each by identically oriented Si-C bilayers were compiled for the both polar Si-rich and C-rich surfaces [8]. Useful information about the total energies, final change of enthalpy, electronic band structure was obtained by relevant calculations.

Results & Discussion

The system theoretically studied was made of single carbon layer on top either the (0001) or (000 $\bar{1}$) surfaces of *4H-SiC* polytype. At first a substrate of this geometry including four bilayers arranged into 2 slabs with the H saturated dangling bonds on the upper and the lower edges was constructed. The (0001) and (000 $\bar{1}$) surfaces taken into account while removal of Si atoms from the top-level of the upper Si-C slabs were changed by the first (buffer) graphene's monolayer (MG). Reactivation on the both Si-rich and C-rich surfaces and removal of Si atoms from two bilayers result in graphene's monolayer of 25 C atoms covering the third Si-C bilayer of



Optimization and calculation of final enthalpy for both terminated surfaces revealed endothermic character of this reaction. The great value and positive sign of ΔH is attributed to high energy required for breaking the old bonds in SiC substrate. The reaction can only be realized in term of $\Delta G = \Delta H - T\Delta S < 0, i.e. T\Delta S > \Delta H$. It means the reaction can proceed spontaneously only under extremely high temperature defined of order $\geq 1000^\circ C$.

The electronic structure of system *4H-SiC/MG* studied for different polar termination shows the band structures are strongly depending on type of substrate. The band gap of 2.368398 eV including the Fermi level of 1.384010 eV was found for the (0001) surface. It corresponds to the first MG experimentally formed on Si-rich surface when the Fermi level falls around the Dirac

points [9]. The closer band gap of 1.323900 eV with the Fermi energy of 1.551510 eV was characteristic of the (000 $\bar{1}$) surface. This system with graphene's buffer succeeds to feature of substrate band structure that proved, however, to be displaced into the lower energy area. Also, in area of negative energies one more band gap succeeds to band structure of 4H-SiC truncated bulk and requires special interpretation.

This computational model may be compared with the model calculated *Ab Initio* by the VASP code. The unit cell consists therein of three atoms, two C atoms and one Si atom. At the XY plane two of atoms are located just below the C atoms of the first graphene layer. The third atom has no C atom above. Significant distinction of interaction between the first graphene's layer and substrate is explained by different bonds on top-level termination. On the Si-faced surface every Si atom forms three dangling bonds directed toward the interface plane. It provides the stronger interaction with the buffer layer of graphene. For the C-faced surface every C atom provides one dangling bond and the weaker links [9, 10]. The metallic properties are characteristic of the Si-faced surface. The semi-conducting or semi-metallic properties were generated on the C-faced surface [10]. Epitaxy on the SiC C-faced results in structurally homogeneous graphene of high quality. The roughness and disorder inherent from substrate are reduced. On the Si-rich face a charge transfer from substrate to graphene and electronic mobility proved to be lower. [11, 12].

Conclusion

Epitaxial growth owing to thermal oxidation of carbon under elevated temperatures form the first MG layers on the top of both polar surfaces 4H-SiC. These overlayers kept on right graphene geometry are devoid the characteristic properties of freestanding graphene. Strongly bound to substrate this buffer has the different electronic properties succeeding the Si-face and C-face structures. Properties of SiC/MG system are depending on interface geometries of differently terminated truncated bulk. Interface intrinsic defects induce special states in the vicinity of the Fermi levels. Further experiments are needed to understand the nature of these states, influence by interface quality and stacking order in SiC/MG system. Technologies of the SPML and local oxidation methods providing ionization of water from the ambient interface and the oxidant for electrochemical reaction enable the real time study of all these synchronous processes [13].

References

- [1] Novoselov K S, Geim A K, Morozov S V, Jiang D, Katsnelson M I, Grigorieva I V, Dubonos S V and Firsov A A 2005 *Nature* **438** 10 197-200
- [2] Geim A K and Novoselov K S 2007 *Nature Materials* **6** 183-91
- [3] Katsnelson M I 2007 *Materialstoday* **10** 20-27

- [4] Geim A K and MacDonald A H 2007 *Physics Today* **60** 8 35-41
- [5] Feng X, Chen Z, Ma J, Zan X, Pu H and Lu G 2003 *Opt. Mater.* **23** 39-42
- [6] Berger C et al 2004 *J. Phys. Chem. B* **108**, 19912
- [7] Segall M D, Lindan P J D, Probert M J, Pickard c J, Hasnip P J. Clark S J, Payne M C
2002 *J. Phys.: Condens. Matter* **14** 2717-44
- [8] Starke U. 1997 *Phys. Stat. Sol.* **202** 475
- [9] Varchon F et al 2007 *Phys. Rev.Lett.* **99** 126805
- [10] Mattausch A and Pankratov O 2007 *Phys. Rev. Lett.* **99** 076802
- [11] Hass J, Feng T, Li X, Li Z, Zong W A, de Heer P N F, Conrad E H, Jeffrey C A and
Berger C. 2006 *Appl. Phys. Lett.* **89**, 143106
- [12] Hiebel F. Mallet P, Varchon F, Magaud L and Veuillen J-Y 2008 *Phys. Rev. B* **78** 153412
- [13] Tseng A A, Notargiacomo A and Chen T P 2005 *J. Vac. Sci. Technol. B* **23** 877-94



SED Research Student Conference

Brunel University

22-24th June 2009

Content based Image Retrieval with Semantic Annotations: A Review and Evaluation

Nasullah Khalid Alham, Maozhen Li

Electronic and Computer Engineering, School of Engineering and Design, Brunel University,
Uxbridge, Middlesex, UK

Nasullah.KhalidAlham@brunel.ac.uk

Maozhen.Li@brunel.ac.uk

Keywords: Image Annotation, Machine Learning, Evaluation

Introduction

The past decade has seen a rapid development in Content Based Image Retrieval (CBIR). CBIR is the retrieval of images based on their low level features such as color [1], texture [2], shape [3] etc. However there is a widely held view that the performance of CBIR is limited due to the existence of the “semantic gap”. Smeulders et al [4] describes the *semantic gap* as “the lack of coincidence between the information that one can extract from the visual data and the interpretation that the same data has for a user in a given situation.” How to narrow down the semantic gap still remains an open issue. Automatic annotation of images is regarded as one of the main solutions for reducing the semantic gap. Automatic image annotation is the method of automatically generating label or labels to describe the content of an image. Automatic image annotation is commonly regarded as a multi-class image classification. Typically, images are annotated with one or more labels, based on extracted low level features. Although a number of machine learning techniques are available for image annotation. The techniques are usually evaluated under different environments using different low level features of images. To facilitate the selection of best machine learning techniques to be used in image annotation. There is a need for evaluating some representative techniques under the same environment using the same set of low level features. We have evaluated seven representative machine learning classifiers for image annotation from the aspect of accuracy and efficiency. To facilitate performance evaluation, an image annotation prototype has been implemented which builds training models on low level features extracted from sample images.

Methodology/Approach

We have implemented a prototype system using Java programming language and the WEKA package version 3.5[5]. The system learns the correspondence between low level visual features and image labels. Low-level MPEG-7 descriptors [6] such as scalable color and edge histogram are used. First the low-level features are extracted from the images. Next stage is to assign the

low-level feature vectors to pre-defined categories. After a model is trained, it is able to classify an unknown instance, into one of the learned class labels in the training set. Figure 1 shows the user interface of the prototype system which supports automatic annotation of images using 7 classifiers.



Figure 1: A snapshot of the system.

Results and discussion

The 7 classifiers were evaluated from the aspects of accuracy in annotating images and efficiency in training the models. Figure 2 shows the accuracy of the 7 classifiers increase when the numbers of sample images are increased in the training process. Among the 7 classifiers, SVM performs the best producing most accurate results in annotating images. SVM achieves a level of accuracy over 90% when 5000 images are used in the training. The decision tree C4.5 algorithm performs the worst with a level of accuracy of just 70%. However, from the results presented in Figure 3 we observe that SVM incurs one of the highest overhead in training the model. Training a SVM is equivalent to solve a quadratic programming problem with linear and constraints in a number of variables equal to the number of data points [7]. The training time of SVM can increase to almost 100 seconds even though the sequential minimal optimization (SMO) [8] is used, a fast algorithm for training SVM models.

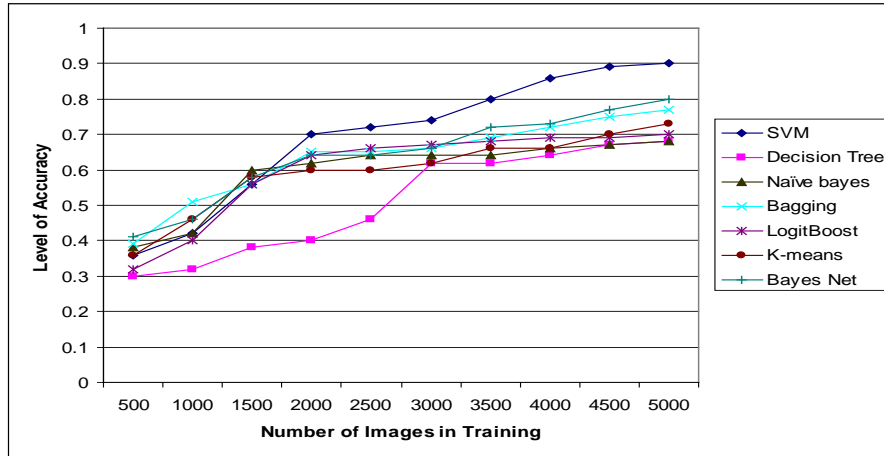


Figure 2: Accuracy in image annotations.

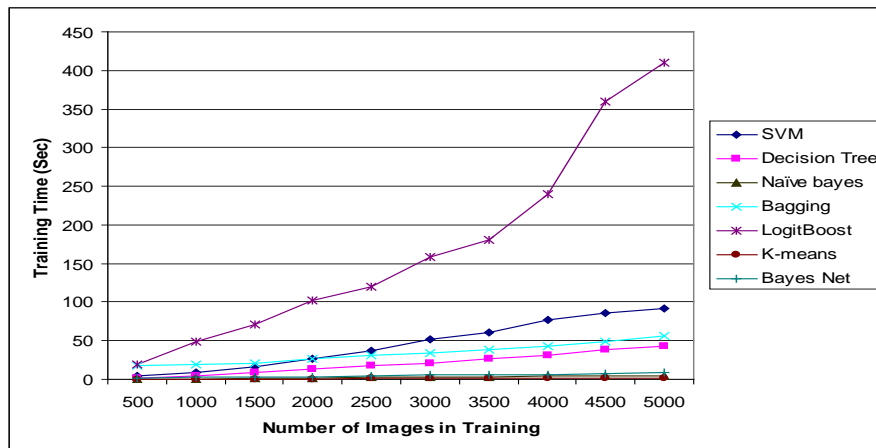


Figure 3: Overheads in training models.

Conclusion

The evaluation of the representative classifiers for image annotation shows that in order to achieve high level of accuracy in image annotation; we need to have a sufficiently large number sample images in the training stage. Support Vector Machine performs better than other classifiers in term of accuracy. However the training time of the classifier is longer than other classifier especially with larger dataset. The evaluation results confirm that SVM models are too large to be used in a practical hence the speed of annotation is lower. The challenge is to speed up the training process of SVM while maintaining the high accuracy level. There is a need of further research to speed up the training process of SVM in order to be used in real life application. One of the solutions to the problem is using SVM in a distributed environment using a number of computers where different computers can potentially exchange only a small number of training vectors.

References

[1] T. Kim, S. Kim, K. Lee (2005) "Content-Based Image Retrieval Using Color and Pattern

Histogram Adaptive to Block Classification Characteristics”, CAIP 2005: 120-127

[2] N. Vasconcelos (2007) “From Pixels to Semantic Space: Advances in Content-Based Image Retrieval” Published by the IEEE Computer Society, 0018-9162/07.

[3] V. Chitkara, M. Nascimento, and C. Mastaller: (2000) “Content based image retrieval using binary signatures” In Technical Report TR0018, Department of Computing Science, University of Alberta, Edmonton, Alberta, Canada.

[4] A.W. M. Smeulders, M. Worring, S. Santini, A. Gupta, R. Jain: (2000) “Content-Based Image Retrieval at the End of the Early Years”, IEEE Trans. Pattern Analysis. Mach. Intell. 22(12): 1349-1380

[5] Weka 3 - Data Mining with Open Source Machine Learning Software in Java. Available at: <http://www.cs.waikato.ac.nz/ml/weka/> [Accessed February 27, 2009].

[6] T. Sikora (2001) “The MPEG-7 visual standards for content description-an overview”, IEEE Trans. Circuits Syst. Video Techn 11(6): p. 696-702

[7] D. Pavlov, J. Mao, B. Dom (2000) “Scaling-Up Support Vector Machines Using Boosting Algorithm”. ICPR p: 2219-2222

[8] J. Platt (1998) “A Fast Algorithm for Training Support Vector Machines” Microsoft Research Tech Rep MSR-TR-98-14



SED Research Student Conference

Brunel University

22-24th June 2009

The Collection, Communication and Inclusion of End User Data in Design Development

Chris McGinley

Inclusive Design Research Group, School of Engineering and Design, Brunel University,
Uxbridge, Middlesex, UK

chris.mcginley@brunel.ac.uk

Keywords: inclusive design, data communication, ergonomics

Introduction

Data useful for 'inclusive' design projects (e.g. ergonomics) is often underused in design development at a professional level. This study investigates forms of user data adopted in design development projects, the barriers that exist, and how useful information might be communicated through designer-friendly data tools. This study will report on the development of tool concepts, co-design workshops, and design case studies that the researcher engaged in. These studies revealed how designers prefer to engage with user data, and which tool concepts might more effectively communicate end user data, in more human, engaging and inspirational ways.

Gathering user data with inclusive considerations

Where inclusive design is concerned, the underlying philosophy considers the needs of those that are often overlooked in the design process; an effective means of doing this is to include 'extreme users' [1] in the design process. This often produces notable results, and challenges designers to include the requirements of underrepresented end users. However, this process can be difficult and time consuming to set up without established access to specific user groups, and increasing user participation typically adds to project expenses [2].

Designing data for designers

To explore anthropometric data use in industry, eleven UK based design consultancies were interviewed by a member of Brunel University's Inclusive Design Research Group [3]. A collection of eight concept tools were then developed and illustrated based on the feedback received, such as 'People Universe', a user database of individual video profiles, images and measurements, using a highly visual browsing approach as well as conventional keyword search, and 'tagging'.

Workshops

The tools were presented during two workshops involving students, academics and professional designers, for discussion, assessment, and co-design tasks. This allowed individual comments, followed by group discussion, rating and co-design. The co-design task (figure 1a) resulted in the creation of new tool concepts (figure 1b), borrowing and combining features from the tools presented and developing new ideas to create a completely new concept, these tools were presented by the teams, allowing them to explain the features they had included and the benefits they predicted they might have for the design process. The goal of the workshops was to identify the data tool features that were considered useful by those intimately involved in the design process.

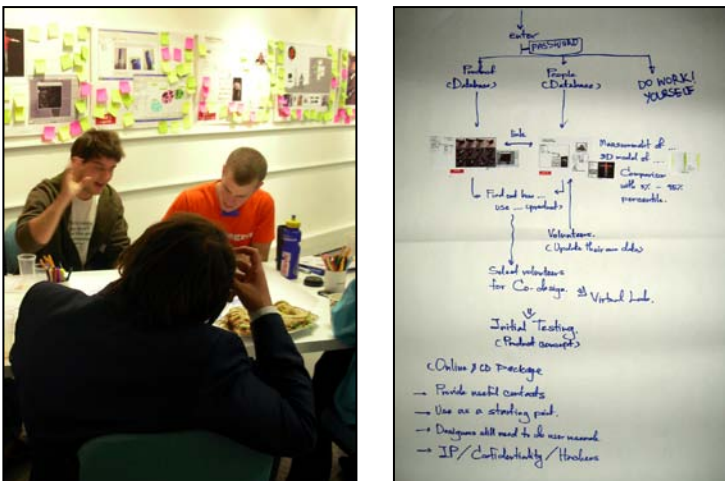


Fig 1a, 1b - Workshop and sample of co-designed tool

Live case studies

In order to observe the data needs of live design projects and consider how tools might be incorporated, the researcher joined research teams engaged in two design development projects being coordinated by the Design Council. The two live product briefs were in new realms of investigation for the design companies involved, hence there was a genuine lack of data. This influenced the large quantity and front-end focused user data requested by the design groups. Having little prior experience highlighted that when a project is familiar there is more confidence in intuition and prior knowledge, whereas if the brief is substantially different from previous projects there is less confidence in applying prior knowledge. Data collection was expected to be holistic and communication of this information was expected to be heavily summarised, easily digested and engaging.

Discussion

There is a prevalence of designers utilising prior knowledge, unless the project is unique enough that they must engage with new scenarios, users and data. However, a tool that could collate appropriate information and make it accessible to the less experienced designer, or act as a point of reference, both a tangible and updatable data source for the more experienced designer could have great value.

Conclusion

Designers desire end user insights, but even when appropriate to a design project the ergonomic data currently available to designers is largely in an inappropriate and unappealing format. There is great potential to make use of user data by communicating it in more engaging ways. However, data on its own is not enough, the way data is presented should make understanding implicit, and naturally build on the knowledge a designer already possesses. A major step will be talking the designers' data language to allow them to add to their design development in a natural way. The criteria of an 'appropriate' and 'usable' tool need to be further explored. The features of a tool also require further development considering more specific criteria as indicated by designers, particular consideration being given to the stage of the design process in which such tools should be employed.

References

- [1] Dong, H, Cassim, J, Clarkson, J. 2007. Best Practice of Critical User Forums. Paper presented at the Include Conference, Royal College of Art, London, UK (April 2007) .
- [2] Damodaran, L. 1996. User Involvement in the Systems Design Process - a practical guide for users. *Behaviour & Information Technology*, 15, pp. 363-377.
- [3] Nickpour, F., Dong, H., 2008. Designing Anthropometrics: Insights Into Designers Use of People Size Data. Technical Report, School of Engineering and Design, Brunel University.



SED Research Student Conference

Brunel University

22-24th June 2009

Grid Connection Oriented Modelling of Full Converter wind turbines: Provision of frequency response

D. D. Banham-Hall^(1,2) (dominic.banham-hall@brunel.ac.uk), G.A. Taylor⁽¹⁾ (gareth.taylor@brunel.ac.uk), C. Smith⁽²⁾ (christopher.smith@convertteam.com), M.R. Irving⁽¹⁾ (malcolm.irving@brunel.ac.uk)

(1): Brunel University; (2): Convertteam Ltd. (UK)

Abstract

Prospective and historic growth in the offshore wind industry in the UK is driving attempts to take advantage of economies of scale through development of larger turbines and larger power parks. Individual wind farms, consisting of hundreds of wind turbines and providing a combined output of several hundred megawatts, are imminent. As the penetration of wind power in UK electricity generation increases, adequate provision of ancillary services in support of grid stability and security has become increasingly important to transmission system operators, including the Great Britain's National Grid. Many present and future generations of offshore wind turbines are likely to continue to deploy full converter technology in order to allow maximum power capture and provide greater flexibility when providing ancillary services to the grid. The first objective of this paper is to present a grid connection oriented model of a fully fed induction generator wind turbine such as is commonly used for UK offshore installations. The second objective is to present Matlab-Simulink simulations that demonstrate that this type of wind turbine can provide frequency response to the grid.

Key words: wind turbine, frequency response, full converter

1. Introduction

Early utility scale wind turbines consisted of induction generators directly coupled to the grid and blades that entered the stall region at rated wind speed. Such wind turbines could not control active power or participate in voltage control. Consequently, as wind installations came to represent a larger share of the generator mix, variable speed concepts were introduced that allowed power regulation. This includes the full converter wind turbine.

There are three prominent generator technologies within the class of full converter wind turbines; The longest standing uses a synchronous generator, whereas much research has been drawn to the potential benefits of permanent magnet machinesⁱ. Meanwhile, many of the UK's offshore

wind farm installations have used the full converter induction generator technology, in order to take advantage of the relatively large 3.6MW wind turbine available in that classⁱⁱ.

With the prospect of offshore wind farms having capacities of hundreds of Megawatts, there is a requirement for these farms to participate in the active balancing of demand and generation through frequency response. Participation in this market requires that wind turbines can rapidly respond to frequency deviations on the grid by being capable of providing 10% response in 10 seconds.

2. Modelling Full Converter Wind Turbines

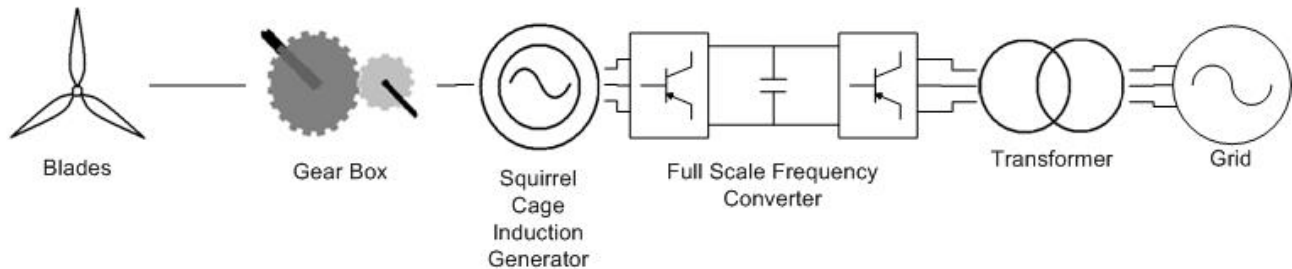


Figure 4: Fully Fed Induction Generator Wind Turbine

Figure 4 shows the principle components of a full-converter wind turbine model; this includes a C_p characteristic of the wind turbine blade energy capture, two-mass drive train, induction machine, a simplified full scale frequency converter and the turbine transformer. Blade pitch control acts to reduce aerodynamic power capture when the turbine reaches rated speed.

Full scale frequency converters typically consist of back to back Insulated Gate Bipolar Transistor (IGBT) bridges, connected with a common d.c. link with capacitor storage. Modelling the dynamics of bridge switching typically leads to slow simulations due to time constants in the order of microseconds which are associated with switching dynamics. Consequently, the converter model presented has been optimised for the investigation of frequency response, where timescales of interest are typically of the order of seconds and minutes.

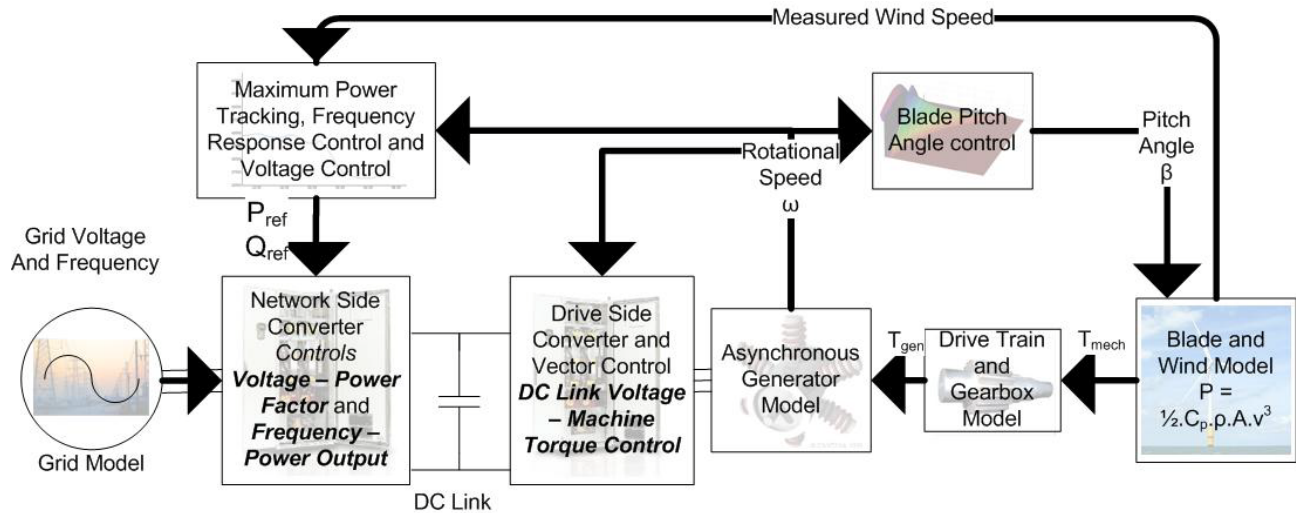


Figure 5: Full Converter Wind Turbine Control Strategy

A Matlab-Simulink model has been implemented, incorporating the control strategy outlined in Figure 5. Conventionally, active power is controlled on the machine side, through a speed controller. However, under the control strategy of Figure 5, the converter's control of active power is on the grid side and allows for an external wind farm controller to take responsibility for the power tracking of the turbine. Consequently, the machine side converter controls the d.c. link voltage and the pitch controller has to act to limit rotor speed. This strategy means that de-loading for frequency response can affect either the turbine's speed or the pitch angle; depending on the prevailing wind speed. When below rated wind speed, controlling a turbine in this manner allows a degree of energy storage due to the rotor's inertia speed and consequently a near instantaneous response to low frequency grid event. At rated wind speed, the wind turbine's response to the frequency deviation is shown to be limited by the blade pitch angle adjustment.

The simulation work conducted is applicable to utility scale wind turbines, such as would be used in offshore wind farms. The simulations demonstrate that rapid response to grid frequency deviations can be achieved using wind turbines. The turbines can both de-load rapidly in the event of a rising frequency and be operated de-loaded and ready to respond to sudden falls in grid frequency with an increase in output. The flexibility of full converter wind turbines allows the grid code requirements for frequency response to be met.

Acknowledgement

The authors would like to thank Helge Urdal and Jonathan Horne of National Grid for their valuable guidance and input to this project in a steering capacity concerning GB grid connection codes.

References

- [1] “2GW of wind and rising fast – Grid compliance of large wind farms in the Great Britain transmission system” – Helge Urdal and Jonathan Horne – Proceedings of the Nordic Wind Power Conference, NWPC’ 2007 – 1-2November 2007
- [2] “Frequency Response Capability of Full Converter Wind Turbine Generators in Comparison to Conventional Generation” – Conroy, J.F.; Watson, R. – IEEE Transactions on Power Systems – May 2008 -vol. 23 iss. 2 – pp649-656
- [3] “SWT-3.6-107 Technical Specification” – Siemens Wind Power, 2009, <http://www.powergeneration.siemens.com/products-solutions-services/products-packages/wind-turbines/products/swt-3-6-107/techspecification/techspecification.htm>



SED Research Student Conference

Brunel University

22-24th June 2009

Investigating Factors affecting Loss of Control of General Aviation Aircraft

M.A. Bromfield

Brunel Flight Safety Laboratory,

School of Engineering and Design,

Brunel University,

Uxbridge,

Middlesex, UK

Keywords: aviation, safety, control

Introduction

A quarter of all fatal General Aviation accidents in the UK during the period 1980 to 2006 involved Loss of Control (LoC) in Visual Meteorological Conditions (VMC) [1]. LoC – which effectively is a stall/spin event, has consistently appeared in accident statistics over this period, but at very different rates for different aircraft types. This raises two important questions - why do these LoC events happen and why is there a difference between aircraft types?. A noticeable difference exists between the Cessna 150 and Cessna 152, two aircraft similar in appearance and highly popular in the pilot training environment. The Cessna 150 falls approximately on the average for stall/spin related fatal accidents in the UK GA fleet, whereas the Cessna 152 exhibits an extremely low accident rate. Brunel Flight Safety Laboratory, in conjunction with the UK General Aviation Safety Council, undertook to try and understand why this is so, using this as a case study to provide insight into possible causal factors.

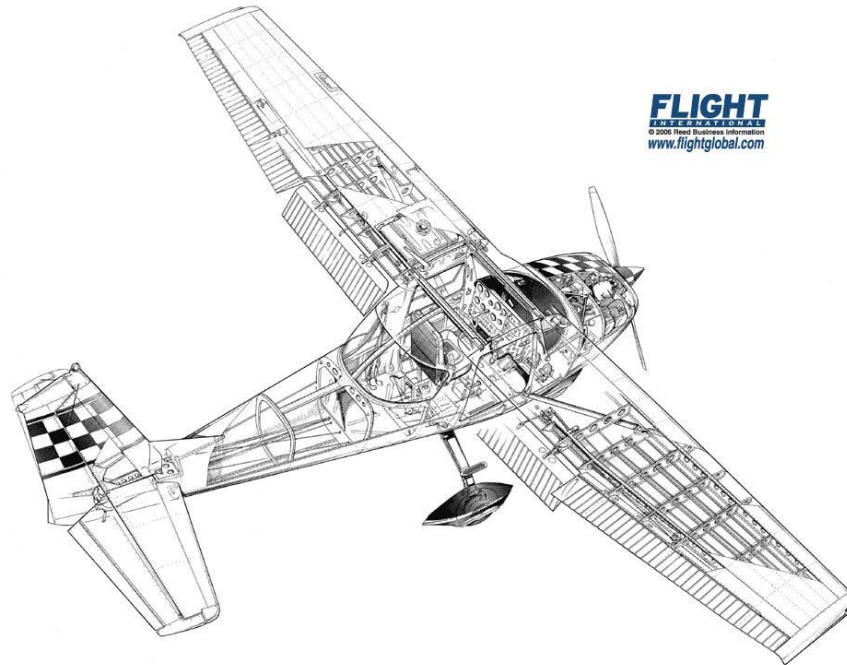


Figure 1, Cessna Model 150 [2]

Methodology/Approach

The key design differences affecting performance and handling qualities were thoroughly researched using available published material and informal interviews with type-experienced students, pilots and flying instructors.

A flight test programme was then commenced using examples of both aircraft types to gather additional research data in order to assess and compare the apparent performance and handling qualities (both qualitatively and quantitatively). The flight tests were performed at different centre of gravity conditions relevant to the key design differences, concentrating upon apparent longitudinal (static and dynamic) stability and control characteristics, stalling and low-speed handling characteristics, and cockpit ergonomics / pilot workload [3].

In all tests, normal (unmodified) flying club aircraft were used, in most cases with a 2-man (Test Pilot + Flight Test Engineer) crew. Data was recorded manually on test cards and automatically using a low-cost, portable Flight Data Recorder (FDR).

Results and discussion

Flight test results so far, show differences in the Apparent Longitudinal Static Stability of the aircraft models. In the low speed area, the C152 has a much steeper slope than the than C150 model. Stick force cues form a major part of the 'pilot in the loop' control feedback to the pilot. Steep stick force gradients provide positive cues to the pilot of airspeed changes allowing good

quality airspeed (point) tracking. Shallow or neutral stick force gradients provide little or no cue to the pilot of airspeed changes and increase the possibility of the pilot exceeding safety-critical critical boundaries such as the critical angle of attack (at the stall) at the low speed end of operations or the flap limiting airspeed at higher speed end of operations during takeoff, approach, landing and go-around.

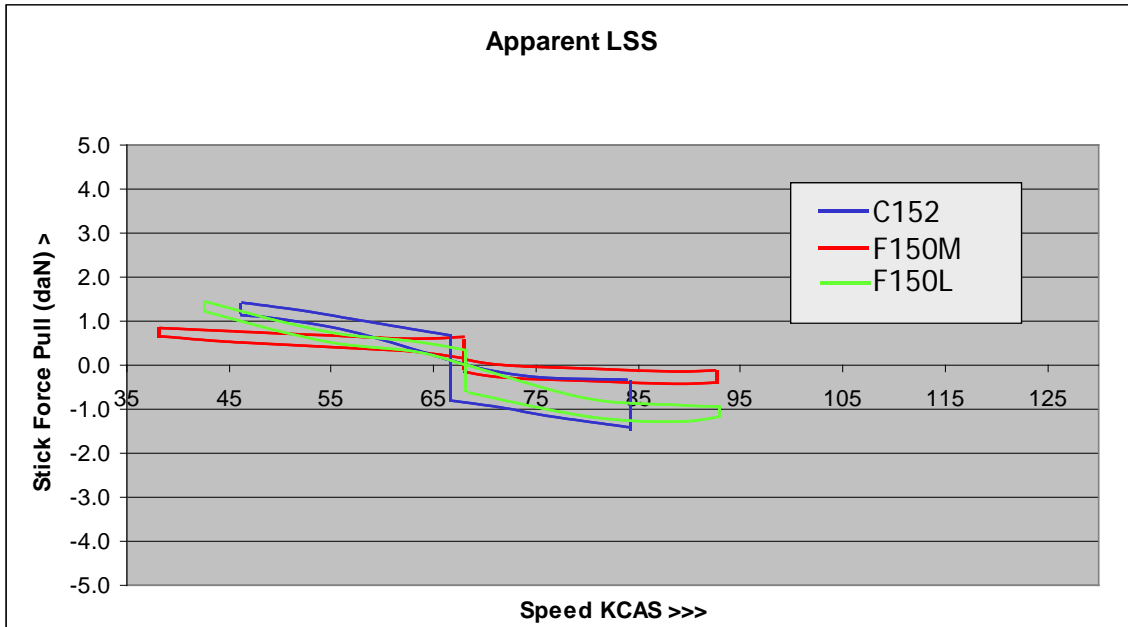


Figure 2, Apparent Longitudinal Static Stability – Landing Configuration 30° Flap

In the landing configuration, the C150 is near neutral, indicating a CG dependency with a possible cliff-edge change. Trim change with flap test showed a large out of trim force on retraction, the C150 Flap indicator widens scan with readability issues. In the stall, with power on and flaps deployed, only attitude warnings provide cues for the onset of stall and there is risk of an undemanded spin occurring.

Conclusions

The results so far highlight differences in stick force gradients and pilot cues during safety critical phases of flight low, slow and near to the ground. These apparent differences in stick force gradient are most probably due to CG & flap variations between aircraft models tested.

Further Work

The next step in the research programme, is to cycle volunteer pilots of different experience levels, through safety-critical conditions in the safe environment of Brunel’s flight simulator to simulate variations of stick force gradient due to CG and aerodynamic effects. Pilot workload will also be measured together with pilot assessment of the tasks undertaken.

Acknowledgements

Thanks to both Dr Guy Gratton and Dr Mark Young for their support and encouragement during the course of the research to date. I also gratefully acknowledge the financial support of The

Thomas Gerald Gray Charitable Trust. The General Aviation Safety Council's 'Stall/Spin Working Group' provided initial accident data. The Civil Aviation Authority (UK) who provided accidents reports, on which statistical analysis was based.

References

[1] Jackson M., Stall/Spin Accidents, Flight Safety, General Aviation Safety Council, November 2007.

[2] Flight International, <http://www.flightglobal.com>, 2006.

[3] Bromfield M.A & Gratton G.B., "Investigation of Factors Affecting Loss of Control of GA Aircraft", presentation to the Society of Experimental Test Pilots, La Jolla, San Diego, March 20~21, 2009.



SED Research Student Conference
Brunel University
22-24th June 2009

Dynamic Metadata Synchronisation for Multimedia Retrieval

Mohammad Rafiq Swash, Member of IEEE & IET and Prof. Abdul H. Sadka
Electronic and Computer Engineering, School of Engineering and Design,
Brunel University, Uxbridge, Middlesex, United Kingdom
{Rafiq.swash, Abdul.sadka} @brunel.ac.uk

Keyword: WordNET, Multimedia Synchronisation and Metadata

1.0 Introduction

Multimedia synchronisation is performed widely using SMIL (Synchronised Multimedia Integration Language) which integrates streaming audio and video (images, text or any other type) [1]. SMIL allows the authors to use a text editor to write script codes for multimedia synchronisation and presentation e.g. <par> command synchronises audio and video by playing them at the common time line [2][3]. In addition, time-alignment method is used for synchronisation of multimedia files. In [4], time alignment method is used to synchronise the closed-caption with voice in a video clip. However, our interest is to synchronise outputs of classifiers in common timelines in a XML file as this will improve retrievability of multimedia that corresponds with users demand. In this paper, we propose new methods to synchronise outputs of classifiers in common time-lines.

2.0 Methodology

Figure 6 shows the Dynamic metadata synchronisation scheme that is designed to synchronise MEX file(s) produced by low/mid-level classifiers in order to improve searchability and search accuracy in the RUSHES system 0. During synchronisation, the system calculates and generates statistical reports (availability of faces, vegetation, etc.) in percentage format as well as the number of shots in the video clip. This report is used for a video content visualisation, search result categorisation and presentation of video content in a very comprehensive way by grouping the availability of items.

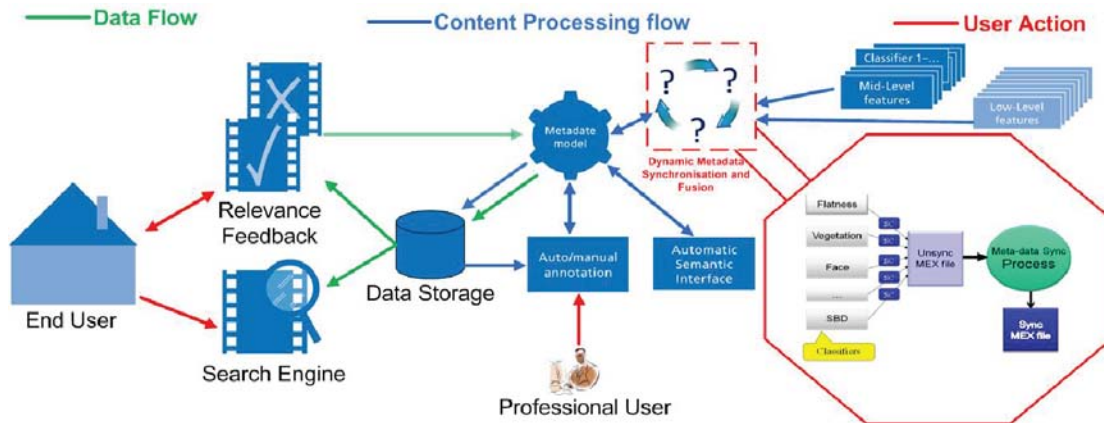


Figure 6 - Dynamic metadata synchronisation in the RUSHES system

As seen in Figure 6, classifiers analyse a video clip independently. Metadata synchronisation module retrieves classifiers results and synchronises the results by generating segment(s) based on the classifiers output. In fact the metadata is synchronised based on (2.1) static temporal segment, (2.2) textual keyword and (2.3) shot boundary detection

2.1 Metadata synchronisation based on static temporal segment

Metadata synchronisation based on static temporal segment synchronises a MEX file produced by classifiers by generating temporal segment(s) and grouping all operators output which is within the temporal segment time line. This scheme is good when there is no need to consider any classifiers including shot boundary detection while MEX file(s) needs to be synchronised based on their common time lines.

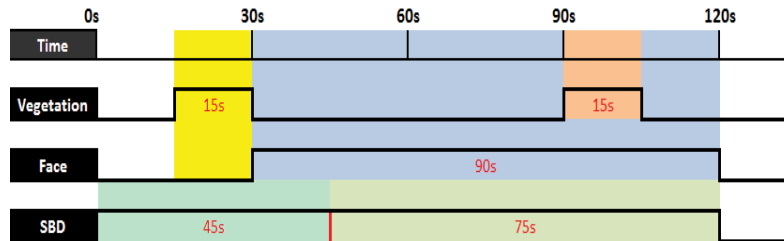
2.2 Metadata synchronisation based on textual keyword

Metadata synchronisation based on textual keyword synchronises a MEX file by prioritising one classifier at the time. This prioritisation is defined by the keyword and the prioritised classifier time line(s) (StartTimeStamp and EndTimeStamp) is used to generate temporal segment(s) for the synchronisation. Minimum temporal segment threshold is introduced to avoid very small video shots. The prioritised classifier time line is used if it is greater than the threshold time line otherwise threshold time line is used to generate temporal segment(s). This method plays a key role when search is carried out on a particular object e.g. face, vegetation, etc in which case this method can produce an optimum synchronisation. This method uses supervised keyword library and uses WordNET to expand the query.

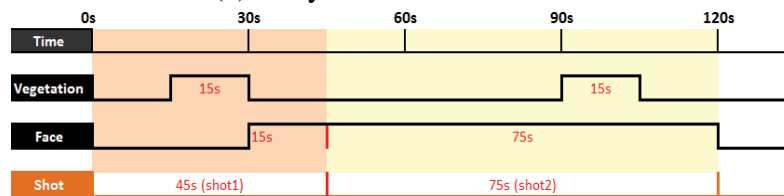
2.3 Metadata synchronisation Based Shot Boundary Detection

Metadata synchronisation based on shot boundary detection synchronises a MEX file produced by classifiers by generating temporal segment(s) from shot boundary detection time line information dynamically. Maximum threshold is introduced to avoid lengthy shots in order to

improve on the search performance. Figure 7.(a) shows a graphical representation of the MEX file of a video clip which contains annotations of vegetation, face and shot boundary detection and Figure 7.(b) shows the synchronised version of the MEX file that has 2 shots generated from shot boundary detection time-lines and the annotations are fitted into these two shots.



(a) Unsynchronised MEX file



(b) Synchronised MEX file

Figure 7 - Graphical representation of MEX files

2.0 Result

Metadata synchronisation based on SBD (proposed system) is tested on the RUSHES video database. The system is running stable and superior on any number of complex annotations and video shots. Figure 8 shows the results indicating that as number of annotations and video length increases, the frame rate decreases. This is due to the lengthy shots with annotations; the system processes all shots and annotations for synchronisation purposes as well as calculating statistical reports.

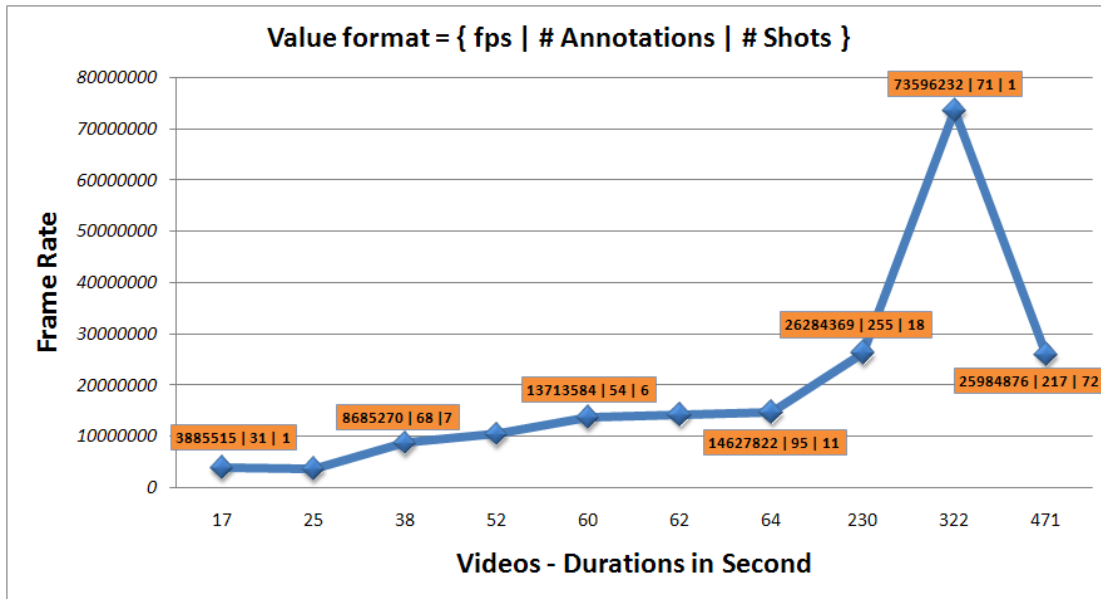


Figure 8 – Dynamic Metadata Synchronisation Experiments

3.0 Conclusions

Three different metadata synchronisation algorithms have been developed that synchronises classifiers output dynamically by generating temporal segment(s). Minimum/Maximum threshold is introduced to avoid a very long/short shot. The experiments conducted on the RUSHES video database shown in Figure 8 that the system is running superior on any number of complex annotations and video shots.

4.0 Acknowledgement

This work is supported by UE “RUSHES” project under Grant FP6-045189.

5.0 References

- [1]. Rutledge L., Hardman L., and. Ossenbruggen J., “The use of smil: Multimedia research currently applied on a global scale”, in *Modeling Multimedia Information and Systems Conference*, pp. 1-17, 1999.
- [2]. Synchronized Multimedia Integration Language (SMIL), Specification, W3C Recommendation, Jan, 2009, <http://www.w3.org/TR/REC-smil/>
- [3]. Hoschka P., “An introduction to the Synchronized Multimedia Integration Language“, Oct-Dec. 1998, pp.84-88
- [4]. Cho J., Jeong S. and Choi B., “Automatic classification and skimming of articles in a news video using korean closed-caption”, *Computational Linguistics and Intelligent Text Processing*, 2004, pp. 694-703.

RUSHES Project, March, 2009, <http://www.rushes-project.eu>



SED Research Student Conference

Brunel University

22-24th June 2009

3D Video Transmission over Wireless Networks

Umar Abubakar¹, A. H. Sadka²

Electronic & Computer Engineering, School of Engineering and Design, Brunel
University, Uxbridge, Middlesex, UK

eepgasu@brunel.ac.uk

Keywords: Scalable video coding, 3D Multiple Description Coding, Error resilience, FGS

Introduction

Mobile communications has gained a growing interest from both customers and service providers alike in the last 1-2 decades. Visual information is used in many application domains such as remote health care, video –on demand, broadcasting, video surveillance etc. In order to enhance the visual effects of digital video content, the depth perception needs to be provided with the actual visual content. 3D video has earned a significant interest from the research community in recent years, due to the tremendous impact it leaves on viewers and its enhancement of the user's quality of experience (QoE) [1]. In the near future, 3D video is likely to be used in most video applications, as it offers a greater sense of immersion and perceptual experience [2]. When 3D video is compressed and transmitted over error prone channels, the associated packet loss leads to poor visual quality [1][4]. Hence, error resilience techniques for 3D video are needed [1][3][4].

The motivation behind this research work is that, existing schemes for 2D colour video compression such as MPEG, JPEG and H.263 cannot be applied to 3D video content. 3D video signal contain depth as well as colour information and are bandwidth demanding. On the other hand, the capacity of wireless channels is limited and wireless links are prone to various types of errors such as noise, interference, fading, handoff, error burst and network congestion [1][4]. To mitigate the effect of errors, on the perceptual video quality, error resilience and scalability need to be investigated for optimization of quality of service (QoS). Figure 1 shows 3D video over heterogeneous networks while figure 2 shows the block diagram of the 3D Video Coding Techniques.

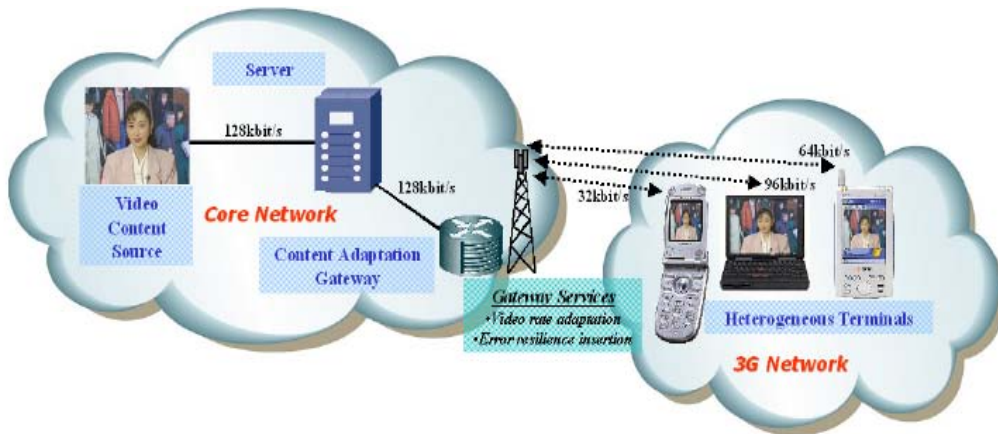


Figure 1: 3D Video Communication over 3 G Networks [2]

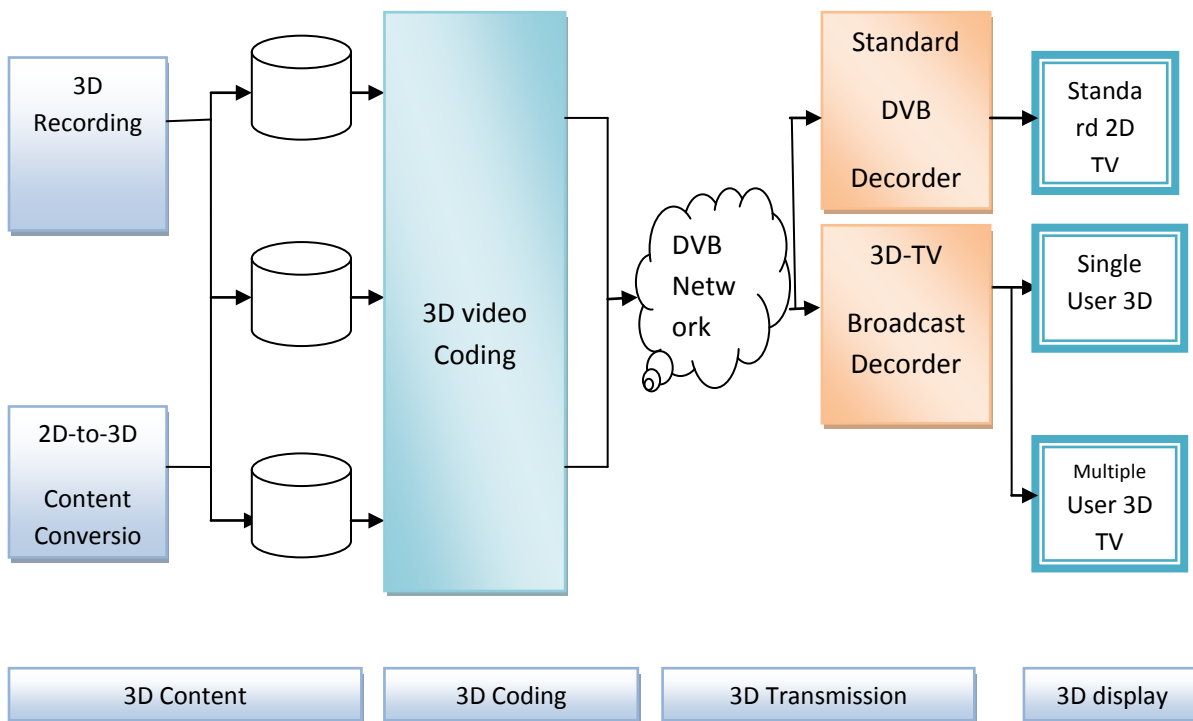


Figure 2: 3D Video Coding Techniques

Aim/Objective of my research

This research work aims at developing an end-to-end QoS control scheme for providing optimal user's quality of experience (QoE) in 3D video transmission over 3G mobile networks and improving the error robustness of the compressed 3D video under error-prone conditions [1][2].

Methodology/Approach

The work programme will be divided into a number of work packages each addressing a specific element of the research programme with specific milestones, target and time projections. The skeleton of the work programme is as follows:

- Collection and analysis of user’s requirements, needs, preferences, perceptions etc. of 3D video communications.
- Adaptive compression schemes for 3D video content such as Scalability, Texture/Depth compression, etc.
- Network-aware adaptive error resilience techniques for compressed 3D video.

Results and discussion

A simple efficient multiple description coding (MDC) algorithms is to be developed. The algorithm uses a coding technique which fragments a single media stream into n independent sub streams called descriptions. According to Sadka and Karim, H.264/SVC decoder then uses post processing to combine the descriptions to provide better image quality. Scalable MPEG-4 FGS and H.264/SVC typically generate one lowest quality base layer and several high quality reference frames in the enhancement layers which improves coding efficiency. The base layer is necessary for the reconstruction of 3D video, while enhancement layers are applied for quality improvement. The decoded video from the base layer and several enhancement layers can be combined to generate a higher quality video. Comprehensive literature review of several MDC video codecs was given by [3][5].

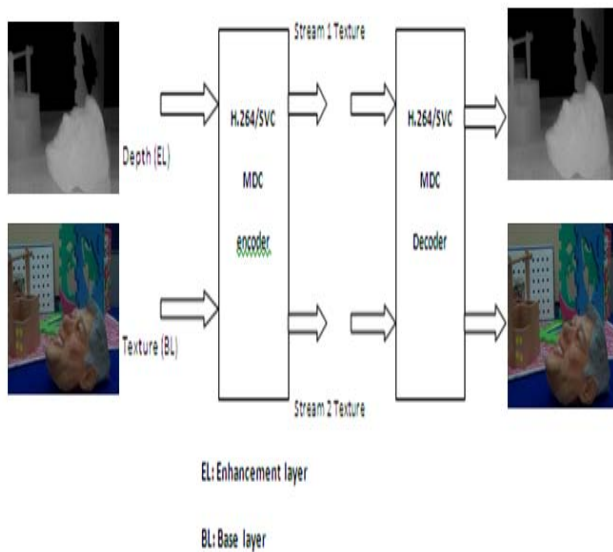


Figure 3: Proposed MDC Algorithm

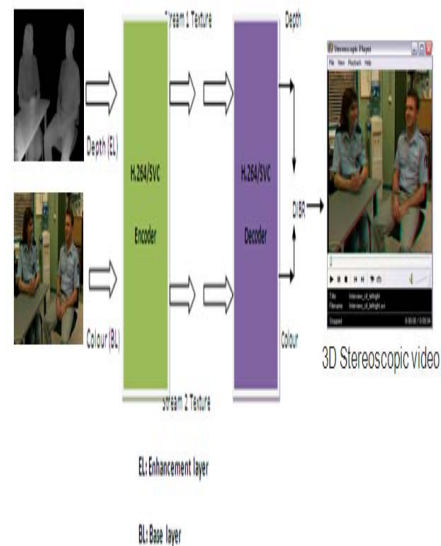


Figure 4: SVC 2D video plus depth

Conclusion

Finally, the combination of Scalable Video Coding (SVC) and MDC (scalable MDC) for 3D video is investigated for error robustness and scalability. A scalable MDC scheme based on even and odd frames is proposed for H.264 based SVC. The proposed algorithms provide better 3D

video performance than the original SVC in error prone environments such as the 3G mobile networks.

References

- [1] A. H. Sadka, "Compressed Video Communication" John Wiley and Co, March 2002.
- [2] S. Dogan, S. Eminsoy, A. H. Sadka, A. Kondo, " Video content adaptation using transcoding for enabling UMA over UMTS", 5th International workshop on WIAMIS, April 21-23, 2004, Lisbon Portugal.
- [3] H. A. Karim, C.T.E.R. Hewage, S. Worrall, S. Dogan, A. Kondo, " Scalable Multiple Description 3D Video Coding based on Even and Odd Frame", Proceedings of the 26th picture coding symposium (PCS) 2007, 4pp, Lisbon, Nov. 2007.
- [4] O. Schreer, P. Kauff, T. Sikora, "3D video communication" John Wiley & Sons, Ltd. 2005.
- [5] H. Karim, A. H. Sadka, A. M. Kondo, " Reduced Resolution Depth Comparison for 3D Video over Wireless Networks", IEE 2nd int. workshop on signal processing for wireless comm.. (SPWC2004), London, UK, June 2004, pp.96-99.



SED Research Student Conference

Brunel University

22-24th June 2009

Coordinated Active Voltage Control for Distribution Networks with Distributed Generation

Maciej Fila^{1,2}, Gareth A. Taylor², David Reid¹, Malcolm Irving²

1. EDF Energy Networks, Crawley, West Sussex, UK

2. Electronic and Computer Engineering, BIPS, School of Engineering and Design, Brunel University, Uxbridge, Middlesex, UK

maciej.fila@brunel.ac.uk

Keywords: active network management, active voltage control, distributed generation

Introduction

Existing approaches to the design, control and operation of 11 kV distribution networks often restrict optimal utilization. When confronting the increasing demand and growing amount of distributed generation being connected to the networks, it is essential for distribution system operators to employ new and more active network management practices. This paper presents and discusses a range of active voltage management schemes based on coordinated voltage control. These schemes can be used to improve the voltage profile in 11kV distribution networks and increase their ability to accommodate distributed generation. Technical limitations and commercial barriers are discussed.

Coordinated active voltage control principles

Active control of the network comprises of continuous (real-time) monitoring and management of the system in order to be able to undertake proactive actions to ensure the regulatory status of the system. The coordinated control of distributed generation, load flow, fault level, voltage profile etc. is performed in order to optimize operation of the network for both consumer and generator benefit.

Voltage control issues were identified as the main factor preventing the DG integration at 11 kV networks [1]. An unacceptable voltage rise at the point of common coupling (PCC) is very often the limiting factor of the generator output. Active voltage management can be the simplest and most cost effective solution in order to ease the constraints applied to the generator export capacity due to voltage regulation.

A range of coordinated voltage control schemes have been proposed with various levels of complexity, effectiveness, communications requirements and investment costs. Solution choice will depend on cost, topology of the network and the amount of DG. The Three main categories of coordinated voltage management for 11 kV networks have been identified. These are:

1. Centralized distribution management system (DMS) control [1]
2. Local Voltage Controller [2]
3. Advanced AVC relay [3]

Results and discussion

Software tools have been used to investigate the performance of active voltage control schemes and their ability to provide network capacity to accommodate DG on the two network case studies. Both cases are based on EDF Energy networks. Network models, historical load data for the substation, feeder currents and existing generation outputs have been used to analyze the performance of both the GenAVC and SuperTAPP n+ schemes.

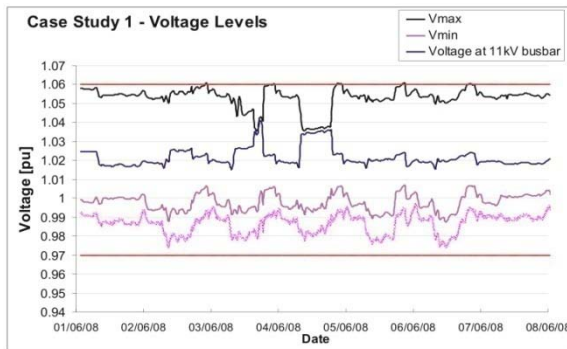


Fig.1. Performance of the SuperTAPP n+ scheme for case study 1

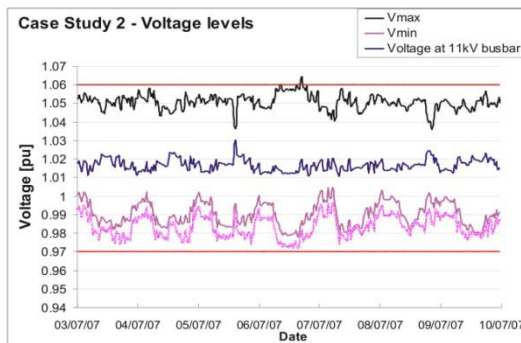


Fig. 2. Performance of the SuperTAPP n+ scheme for case study 2 with 6 MW of DG

Conclusion

Either conventional network reinforcement techniques or active network management schemes for voltage control can be used to overcome issues associated with the connection of DG. Before deciding which method is going to be used, it is essential to consider a number of factors such as cost, efficiency, network characteristics, communications availability, existing and future amounts of DG export. When considering active network management techniques, suitable and accurate assessment software is essential.

It has been shown that the GenAVC scheme is a very effective solution in order to increase network capacity for the DG and maintain the network voltage profiles within the specified limits. With a single remote measurement at the PCC, performance of the scheme is effective and it can be further improved by the installation of additional RTUs at strategic nodes within the network.

The SuperTAPP n+ scheme can significantly improve the voltage profiles of heavily loaded networks with significant penetration of DG as well as resolving the issues associated with the voltage rise effect at DG point of connection. The scheme is a very cost effective solution that provides adequate voltage control in distribution networks.

References

- [1] "Network management systems for active distribution networks – a feasibility study," DTI Technical Report, K/EL/00310/REP, 2004.
- [2] C.M. Hird, H. Leite, N. Jenkins, H.Li, "Network voltage controller for distributed generation", *IEE Proc., Gener. Transm. Distrib.*, vol. 151, pp 150-156, March 2004.
- [3] J. Hiscock, N. Hiscock, A. Kennedy, 2007, "Advanced Voltage Control for Network with Distributed Generation", *Proceedings CIRED 2007 conference*.

Sketch-Based Clothing 3D Virtual Humans

Hui Yu, Shengfeng Qin, David Wright

Design, School of Engineering and Design, Brunel University, Uxbridge, Middlesex, UK

hui.yu@brunel.ac.uk

Keywords: sketch-based, virtual clothing, virtual humans

1. Introduction

The traditional method for dressing humans is to sew up 2D garment patterns [1]. This can make it tedious for users to create, modify and try various styles of garments. We have developed a virtual dressing system based on a sketching interface allowing users to draw 2D garment profile strokes on screen, and a more elaborate 3D geometric garment surface is generated and dressed on the body (Fig. 1).

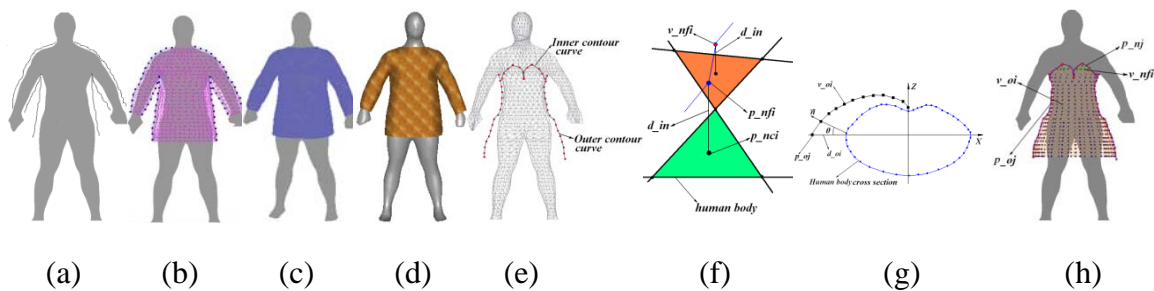


Figure 1: Examples of a 3D garment generation (a) Sketch the profile of a sweater. (b) Mesh construction. (c) Mesh refinement. (d) Rendering result. (e) Spline curve fitting. (f) Vertices from inner curves. (g) Vertices from outer curves. (h) Garment vertices.

2. Methodology

2.1 Garment Generation

The generation of a garment’s vertices is based on the distances between the body and garment contour curves including inner and outer contour curves (Fig. 1 (e)). Different algorithms are developed to generate 3D garments’ vertices for these two kinds of curves (Fig. 1 (f), (g)).

Garment vertices from outer contour curves: We calculate the distance d_{oi} from the outer contour curve denoted by $s_{oc} = \{p_{o_1}, p_{o_2}, \dots, p_{o_j}, \dots\}$, to the human body. The point depth of an outer contour curve is set to the z-value of the nearest point of the human body. Then, we use

the following equation to specify the distance between the body curve and the interior garment's vertices (Fig. 1 (g)): $dr_i = d_{o_i} * \cos(\theta) * \lambda + \delta$.

Garment vertices from inner contour curves: Through the use of ray tracing techniques, a set of points denoted by $s_{nc} = \{p_{nc_1}, p_{nc_2}, \dots, p_{nc_i}, \dots\}$ are obtained by intersection between an inner contour curve and the body. Then s_{nc} is offset to s_{ncf} by a distance d_{in} from the human body along each triangular face that each point of s_{nc} is projected onto (Fig. 1 (f)). Interior garment vertices, v_{nfi} , within the boundaries are interpolated using the distance field of the body (green points in Fig. 1 (h)).

2.2 Garment Surface Optimisation

Two kinds of constraints are used during the generation of a 3D garment position. One constraint is from human body features, the other is the distance between the projected 3D curve and the body surface. The level set method devised by Osher [2] is used to optimise garment shapes and mimic cloth tension (Fig. 2 (a)-(c)). Improved Laplacian and Loop mesh processing schemes are used to optimise mesh surface (Fig. 2 (d)-(h)).

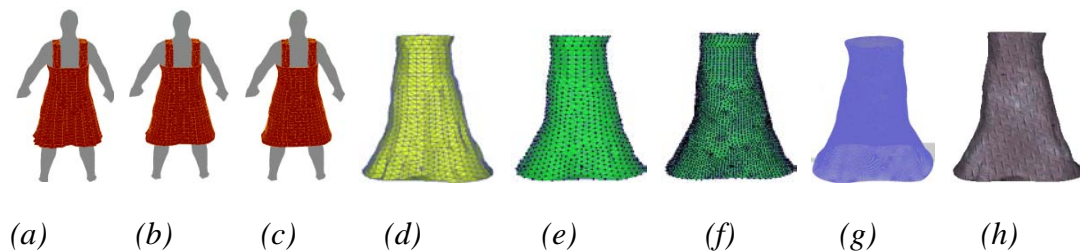


Figure 2: (a) Full tension. (b) 50% tension. (c) 10% tension. (d) The original mesh. (e) Smooth using the improved Laplacian method. (f) Loop subdivision 1 iteration. (g) Loop subdivision 3 iteration. (h) The rendered result.

2.3 Penetration Detection

We developed a layer-distance-based algorithm to perform penetration detection. We compute signed distances denoted by d_c from vertices of a body to the garment surface represented by S_g along the normal direction of body vertices. If $d_c \geq 0$, there is no penetration else there is penetration. If penetration occurs, related vertices of the garment are moved outwards by Δd in the direction of the face normal. The value of Δd is determined by the following equation $\Delta d = |d_c| + \sigma$. The variable σ is a small tolerance. Fig. 3 (a) shows detection of penetration and (b) is the result of penetration response.

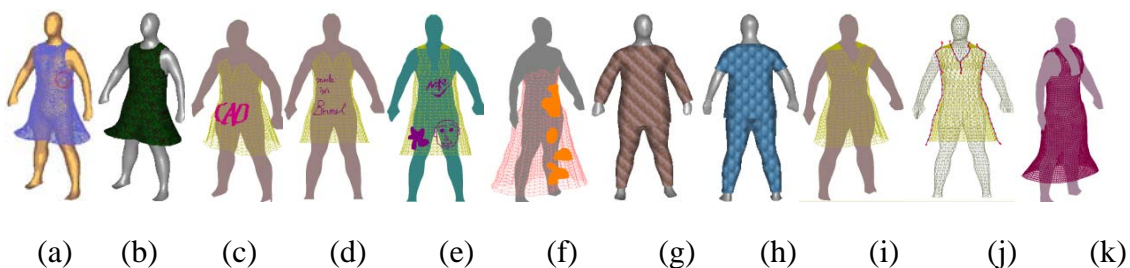


Figure 3: Examples of penetration detection and more results

3. Results and discussion

Our system can generate various styles of garments based on users' sketches (Fig. 3 (g) - (k)). Three decoration tools are developed allowing users to add detail to garment surfaces such as brand names, pockets and some other decorations (Fig. 3 (c)-(e)). We are aware that the system can be improved to allow users to edit and deform the garment surface directly in the future.

4. Conclusion

We have presented a novel approach for dressing virtual humans based on a sketch interface. The system has been developed using C++, OpenGL and GPU programming. Our system generates refined garment mesh surface, which make it possible to deform or change garments arbitrarily by applying mesh editing algorithms. However, this system does not take garment material into account, so algorithms can be applied to demonstrate material properties.

Acknowledgements

This work is supported by UK EPSRC Grant EP/p501245.

5. References

- [1] Vassilev, T: Dressing Virtual People, *SCI'2000 conf*, Orlando, July 23-26, 2000.
- [2] S. Osher, Fronts propagating with curvature-dependent speed: algorithms based on Hamilton-Jacobi formulations. *J. Comput. Phys.*, 79(1):12.49, 1988.



SED Research Student Conference

Brunel University

22-24th June 2009

Neuro-Fuzzy System and Particle Swarm for Optimising Metals Heat Treatment Process

Tawfeeq Al-Kanhal and M.F. Abbod

School of Engineering and Design, Tawfeeq.Al-kanhal@Brunel.ac.uk

Keywords: Particle Swarm Optimisation, Neuro-Fuzzy system, Heating Treatment

Introduction

Heat treatment is a process used to alter the physical and mechanical properties of materials without changing the product shape by controlling heating and cooling rates. In the steel industry, determining the optimal heat treatment regime that is required to obtain the desired mechanical properties of the steel is considered as one of the hard and complex processes in the industry. This is because the search space is large and complicated. Therefore, it is important to develop a system that is capable of selecting the optimal heat treatment regime so the required metal properties can be achieved with the least energy consumption and the shortest time.

In this research experimental heat treatment data is used to develop a neuro-fuzzy (NF) system that models the materials properties such as the hardness and its depth. Based on this model, Particle Swarm Optimisation (PSO) is used to optimise the heat treatment process by selecting different heat treatment conditions. The selected conditions are evaluated so the best selection can be identified.

This work addresses the issues involved in developing a suitable methodology for developing an NF system and PSO for mechanical properties of the steel.

Methodology

In the field of artificial intelligence, neuro-fuzzy refers to combinations of artificial neural networks and fuzzy logic. An NF system is defined as fuzzy system which employs a self learning algorithm derived and inspired by neural network concept to achieve its fuzzy sets and fuzzy rules using processing data samples **Error! Reference source not found.** . The next step is to integrate the NF systems with PSO methodology [1] so that the system can predict the optimum heat treatment regime.

PSO is utilised to find the optimal heat treatment conditions which will provide the desired mechanical properties such as hardness and depth of hardness with the aid of the NF as the model used to predict the metal properties (Figure 1). The heat treatment data that is used to train the NF model is organised as input parameters (diameter, austenitic temperature, tempering temperature, induction speed, pressure, and sub-zero treatment) which the outputs

are the hardness and its depth. The model was trained and tested using NF model which gave very good prediction accuracy. Accordingly, there are two objectives that need to be achieved, the hardness and its depth which lead to the need of a multi-objective optimisation algorithm. Two methods were used to evaluate both objectives: the first using Pareto Front function while the second method is based on a mean value of the normalised objectives.

The PSO algorithm was set to a population size of 100, while the inertial cognitive and social constants are as follows: $W_{min} = 0.4$, $W_{max} = 0.9$, $c1 = 1.4$, $c2 = 1.4$.

Results

The NF system was tested using experimental data which proved to be able to give accurate predictions. Simulation results shown in Tables 1 and 2 based on the mean normalised objectives and the Pareto Front methods respectively show that the system was able to fine the desired properties by adjusting the heat treatment conditions.

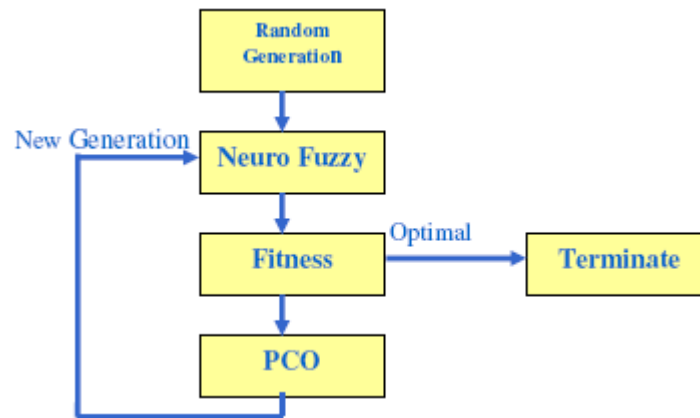


Figure 1. Block diagram of the system.

Table 1. Optimisation results of the NF and PSO using normalised objectives.

Diameter (mm)	Austenitic Temperature (°C)	Induction Speed (m/s)	Pressure (Bar)	Sub-zero treatment (°C)	Tempering Temperature (°C)	Hardness (MPa)	Depth of Hardness (mm)	Desired Hardness (MPa)	Desired Depth of Hardness (mm)
385	1012	0.52	26	-105	100	855.98	44.03	856	44
455	1002	0.54	30	0	102	876	24.81	876	25
455	1004	0.54	31	0	107	862	23.98	862	24
385	1020	0.49	26	-139	105	851.99	47.99	852	48
546	953	0.74	15	0	150	849	41.76	849	42
546	937	0.68	34	-5	107	875	28.98	875	29

380	1008	0.51	28	-3	105	932	30.58	932	34
455	1013	0.51	28	-5	103	883	28.39	883	34
455	1008	0.53	29	0	105	856	25.50	856	28

Table 2. Optimisation results of the NF and PSO using Pareto-Front.

Diameter (mm)	Austenitic Temperature (°C)	Induction Speed (m/s)	Pressure (Bar)	Sub-zero treatment (°C)	Tempering Temperature (°C)	Hardness (MPa)	Depth of Hardness (mm)	Desired Hardness (MPa)	Desired Depth of Hardness (mm)
385	1025	0.45	19	0	100	855.84	44.47	856	44
455	976	0.53	30	-10	100	875.99	25.01	876	25
455	930	0.4	28	-18	100	862.01	24.01	862	24
385	1025	0.4	15	0	100	851.57	48.05	852	48
546	930	0.650	15	0	150	849.15	41.99	849	42
546	940	0.8	27	0	108	875.39	29.06	875	29
380	991	0.4	25	0	100	930.65	35.03	932	34
455	1009	0.4	25	0	100	885.00	33.45	883	34
455	978	0.42	26	0	100	855.91	28.07	856	28

Conclusion

The NF system and PSO have been developed successfully and working effectively. This system has been able to determine the heat treatment regime and the required to obtain the desired mechanical properties of the steel which considered as helpful tool in industry.

References

- [1] J.-S. Roger Jang, "ANFIS: Adaptive-Network-Based Fuzzy Inference Systems", IEEE Transactions on Systems, Man, and Cybernetics, Vol. 23, No. 03, pp 665-685, May 1993.
- [2] J. Kennedy, and R. Eberhart, "Particle Swarm Optimization", Proc. IEEE Int'l. Conf. on Neural Networks, Perth, Australia, pp.1942-1948, November 1995.

Efficient Implementation of Wavelet Packet for Medical Image Segmentation and Analysis

Shadi AL-Zu'bi¹, and Abbes Amira²

Department of Electronic & Computer Engineering, School of Engineering and Design,

Brunel University, Uxbridge, Middlesex, UK

shadi.alzubi@brunel.ac.uk

Abstract. This paper presents an efficient implementation and evaluation of wavelet packet for 3D medical image segmentation and analysis. Promising results have shown that region of interest can be accurately detected and segmented using wavelet packet.

Key words: Medical images Segmentation, Wavelet Packet, Thresholding.

1 Introduction

Segmentation refers to the process of partitioning a digital image into multiple regions. The result of image segmentation is a set of regions that collectively cover the entire image, or a set of contours extracted from the image [1]. The goal of segmentation is to simplify or change the representation of an image into something that is more meaningful and easier to analyze and usable in future applications [2]. The research invested in this paper concentrates on a multiresolution analysis with discrete wavelet transform (DWT) and wavelet packet (WP).

2 Proposed System

Fig. 1 discusses the proposed medical image segmentation system using multiresolution analysis and thresholding. System input is a three-dimensional volume acquisition. Thresholding and multiresolution analysis can be applied to the medical image to obtain a segmented or transformed slice respectively.

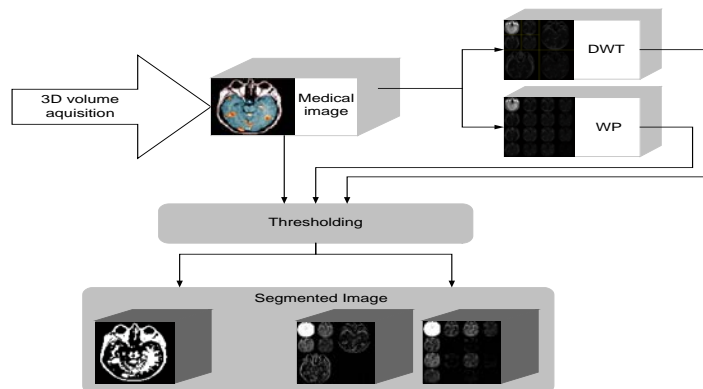


Fig. 1. Medical image segmentation system.

Fig.2 illustrates the differences between DWT and WP at different levels of decomposition for a phantom image [3]. The differences between DWT and WP are just in the details coefficients where the next decomposition of DWT is applied on average coefficient from the previous decomposition, unlike WP where next decomposition is applied on all previous decomposition coefficients. The average coefficient in both DWT and WP is the same, but the details coefficients are transformed in WP unlike DWT [4].

3 Results and Analysis

Due to the noise located around ROI as illustrated in Fig. 2, the best level of decomposition could not be identified and ROI could not be detected. Therefore, a thresholding technique is used to remove this noise.

3.1 Problem Formulation

A typical diagnostic problem in the abdominal region is to detect the lesions which located in the liver and compare the spheres volume with the measured volumes using thresholding and multiresolution analysis.

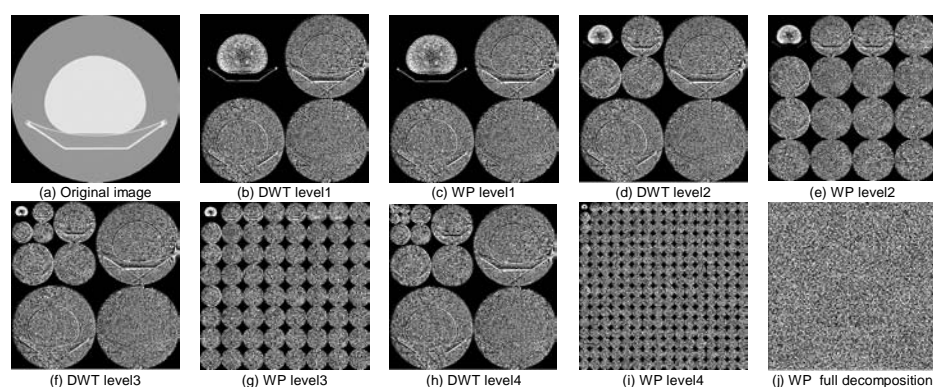


Fig. 2. (a) Original image [3] (b–i) DWT and WP at levels 1, 2, 3, 4 (j) WP at full decomposition.

Table.1 shows that the difference between errors using the spatial domain and the wavelet domain is too big because lesions volumes in this case are very small. But in different situations the wavelet domain may detect the objects with better efficiency and smaller errors.

Groups		G1 area/ G2 area	G1 pixels /G2 pixels spatial domain	Percentage of error (spatial domain) %	G1 pixels /G2 pixels wavelet domain	Percentage of error (wavelet domain) %
G1	G2					
2	12	0.0280	0.0228	+ 18.57	0.0387	+ 27.65
3	8	0.1406	0.1463	- 4.05	0.2152	+ 34.67
4	12	0.1111	0.1139	- 2.52	0.1677	+ 33.75
5	12	0.1736	0.1714	+ 1.27	0.1355	-28.12
6	8	0.5625	0.5780	- 2.76	0.7342	+ 23.39
6	10	0.3600	0.3657	- 1.58	0.4603	+ 21.79
8	10	0.6400	0.6327	+ 1.14	0.6270	-2.07

8	12	0.4444	0.4447	+ 0.07	0.5097	+ 12.81
10	12	0.6940	0.7028	- 1.27	0.8129	+ 14.63

Table 2. Error percentages for diameter measurements.

3.2 Hard Thresholding and Soft Thresholding

Hard thresholding is less complex than soft thresholding, Soft thresholding replaces each pixel which has greater value than threshold value by the difference between threshold value and pixel value, unlike hard thresholding which replaces it by zero (no change). This leads to make the process more complicated and increase the algorithm processing time.

4 Conclusions

Segmentation is very important for medical image processing and object detection.

Thresholding solves many problems in multiresolution analysis by removing the noise from the images and find the best level of decomposition to detect the mentioned objects.

Measurements are taken in this paper to compare the used technique result with the real values. Ongoing work is to focus on the implementation of novel image segmentation approaches using multiresolutional and statistical models.

References

- [1] Fardin Akhlaghian Tab, Golshah Naghdy1, and Alfred Mertins, "Multiresolution Image Segmentation with Border Smoothness for Scalable Object-Based Wavelet Coding. (2003)
- [2] David W. G. Montgomery, Multiscale Compression and Segmentation of Volumetric Oncological PET Imagery. (2006)
- [3] BIN laboratory, Geneva University Hospital, (2007)
- [4] Zhongchao Shi, Ryosuke Shibasaki, An approach to image segmentation using multiresolution analysis of Wavelets. Center for Spatial Information Science, The University of Tokyo, Japan, IEEE. (1999)



SED Research Student Conference

Brunel University

22nd-24th June 2009

Anthropometrics without Numbers!

An Investigation of Designers' Use and Preference of People Data

Farnaz Nickpour 1, Hua Dong 2

1. Inclusive Design Research Group, School of Engineering and Design,

Brunel University, Uxbridge, Middlesex, UK

2. Human Centred Design Institute, School of Engineering and Design,

Brunel University, Uxbridge, Middlesex, UK

farnaz.nickpour@brunel.ac.uk

Keywords: Inclusive design, anthropometric data, data tool

1. Introduction

Inclusive design is an approach to design that not only ensures that products, services, interfaces and environments are easier to use for those with special needs or limitations, but in doing so also makes them better for everyone [1]. However, there is still missing knowledge to encourage and support designers in adoption and implementation of inclusive design [2]. Anthropometric data is piece of this missing knowledge which provides accessible information on users' capabilities and limitations [3]. Support and resources for designers on this type of data seems to be limited and exclusive. Integrating such data into inclusive design tools is yet to be considered. This study aims at understanding and evaluating the existing use of anthropometric data by professional designers in order to explore means of presenting such data more effectively.

2. Methodology

Three fundamental aspects of designers' general data behavior in relation to the use of anthropometric data were investigated, including:

A. Data use

B. Data preferences

C. Data suggestions

Interview and ranking questionnaires were adopted as the complementary methods:

2.1 Interview

Structured but open-ended interviews were adopted. Design consultancies were targeted and experienced designers with medium/high management roles from ten UK-based design consultancies were interviewed. Eleven designers were interviewed.

2.2 Questionnaire

Five anthropometric data tools from a wide platform of sources, presentation formats and data types were presented to the designers which they then graded through use of a ranking questionnaire. The questionnaire formulated based on existing five anthropometric data tools is demonstrated in Figure 1.

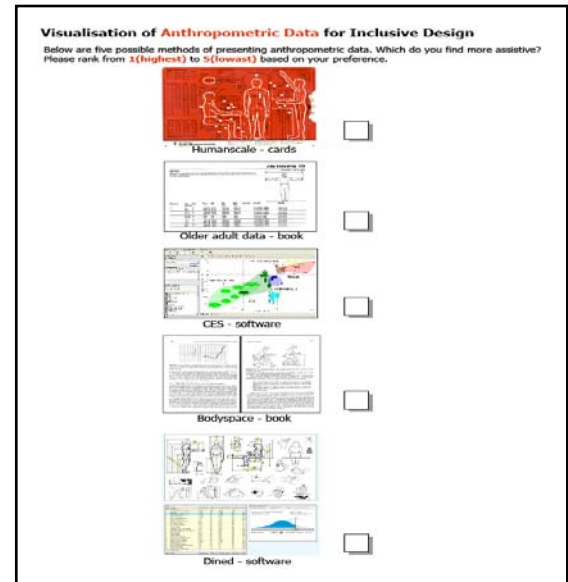


Figure 1: Questionnaire conducted with designers.

3. Results and discussion

3.1 Designers' current use & perceptions on anthropometric data

When asked about their current sources of anthropometric data, designers hardly mentioned any existing data tools. Many interviewees reported they had not used such data tools for a considerable time. Instead, the designer's main stated methods of data collection were practical, pragmatic and included prototyping (model making & mock ups) and working with people (both measuring & asking for user feedback).

3.2 Designers' suggestions on means of data presentation





3D data representation was preferred against 2D data and designers expressed enthusiasm for simulations of people taking into consideration variants such as age, gender as well as user physical and mental. Most designers stated they would prefer a simple, intuitive, highly visual tool which is fast, easy to learn and easy to work with.

3.3 Designers' preferences on anthropometric data tools

Table 2 summarises the designers' preferences of the five data presentation tools. The numbers in the 'highest' cell shows how many designers ranked the tool the highest (i.e. most

preferred) and the numbers in the ‘lowest’ cells show how many designers ranked the tool the lowest (i.e. least preferred).

Table 2: Summary of the designers’ preferences on existing data tools

Anthropometric data tool	Highest	Lowest	Comments
	t	t	
 <p>Tool 1 [4] Interactive card with a rotating wheel to enable selection of age and gender</p>	2	3	Holistic, interesting presentation of data, out-dated, irrelevant, too much information
<p>Tool 2 [5] Handbook with many data tables and simple illustrations</p>	2	1	Simple, easy to use, boring, unexplained, separated data
 <p>Tool 3 Software enabling 2D data visualisation and comparison of data</p>	5	0	Complex, good features, unprofessional graphics, too analytic, time-taking to work with
 <p>Tool 4 [3] Book incorporating data and guidelines</p>	0	6	Comprehensive, too much text, academic, student-oriented, lacking colour, too scientific
 <p>Tool 5 [6] Web-based resource enabling selection of data and visualisation of percentages</p>	1	0	Interactive, accessible, visually unprofessional, irrelevant data, useful features

4. Conclusion & further work

4.1 Conclusion

This study shows that the use of anthropometric data sources by designers in consultancies is very limited and minimal; experienced designers tend to rely mainly on experimental methods such as physical prototyping and engagement with people. Experienced designers

perceive and evaluate such methods as more effective and useful compared to referring to anthropometric data sources.

This study highlights the need for development of a highly visual, simple and intuitive data tool based on the interviewed designers' preferences and suggestions. This has to be done by carefully adopting the designers' existing approaches to data collection and use and by adapting existing data into that.

4.2 Further work

After the investigation stage, based on the raised issues regarding designers' data use, evaluations, preferences and suggestions, a number of tool concepts were formulated and further developed into mock-up data tools.

In order to communicate the findings of the study, get the designers' feedback on the formulated tool concepts and involve designers as users to co-design the tools, a series of workshops with designers were planned and feedback was received from two early workshops. Based on the careful qualitative and quantitative analysis of workshop findings, some of the tool concepts will be selected to be further developed and prototyped. The prototyped tools will then be made available for trial and test by the designers as users again.

References

- [1] **Coleman, R, Clarkson, J, Dong, H and Cassim, J** (2007) Design for inclusivity: A Practical Guide to Accessible, Innovative and User-Centred Design, Gower, London
- [2] **Dong, H and Clarkson, J** (2007) Barriers and drivers for inclusive design: designers' perspective. Paper presented at the Include 2007 Conference, Royal College of Art, London, UK, 1-4 April 2007
- [3] **Pheasant, S and Haslegrave, C** (2006) Bodyspace: anthropometry, ergonomics and the design of work, Taylor & Francis, London



SED Research Student Conference

Brunel University

22-24th June 2009

Quality of Service Management for Real-Time Rich-Media Applications and Development of Related Software

Sivanantharasa Panchadcharam, Dr G.A. Taylor, Dr. Q. Ni

School of Engineering and Design, Brunel University, Uxbridge, UB8 3PH, UK

s.panchadcharam@brunel.ac.uk

Keywords : Network monitoring tool, Real-Time Rich-Media (RTRM) applications, Quality of Service (QoS)

Aim of Study

The development of network monitoring tools for Real-Time Rich-Media (RTRM) applications remains a significant challenge for both academic and industry researchers. The availability of efficient tools for specifically monitoring RTRM applications is scarce and most do not fully satisfy all the requirements of the users. For this reason many academic and industry researchers are investigating this topic.

Development of such tools requires considerable knowledge concerning the current market and existing technology in order to establish the specific requirements. This involves a detailed study and investigation of the deployment of new and existing RTRM applications with considerable emphasis on customer-related case studies, research papers, journals and surveys from different users, combined with the usage of existing RTRM application monitoring tools. Analysing the shortcomings and determining the scope for improvement is essential when developing a novel tool in a competitive market place.

Methodology

In this research an experimental test bed has been designed and developed that can provide a network laboratory facility for monitoring packet loss and jitter parameters for RTRM applications, such as a video streaming application where the client and server programs can be run in the same computer or different computers in a LAN. The basic architecture of this proposed method is shown in Figure 4. The gateway emulator can detect the video application packets (such as RTP packets [1]) and analyse the data inside them to display the time stamp, packet length, payload type, sequence number, etc. as shown in Figures 1,2 and 3.

Delay $D(i,j)$ and jitter J is calculated using the following Equations (1) and (2), respectively:

$$D(i,j)=(R_j-R_i)-(S_j-S_i)=(R_j-S_j)-(R_i-S_i) \tag{1}$$

$$J = J + (| D (i-1, I) | - J) / 16 \tag{2}$$

R_i & R_j in Equation (1) are the time of arrival in RTP timestamp units for packets i & j respectively. S_i and S_j are the RTP timestamps from packets i and j respectively [2].

Results

Packet loss can easily be detected using the gateway emulator, Figure 2, program that inspects the sequence number in order to report this to a specified store location. The emulator is also able to introduce random errors during the transmission of the RTP packets by applying the probability of this error rate as defined from the user interface.

Figures 1, 2 and 3 show the graphical user interfaces (GUI) of the test bed for Client, Gateway and Server, respectively. These tools enable the display of the packet information to the user and they allow the user to take actions using the buttons shown on those figures.

Conclusion

The flexibility of this test bed enables the packet-loss and jitter calculations to be applied in stress testing and network applications monitoring. The visual QoS of the video can be compared after and before the packet drop introduced in the Gateway.

Further Work

This tool can be further modified to accommodate the display of these QoS parameters in graphical manner and to store such data in database for future analysis. Different types of network and RTRM applications can be considered during the implementation of this tool.

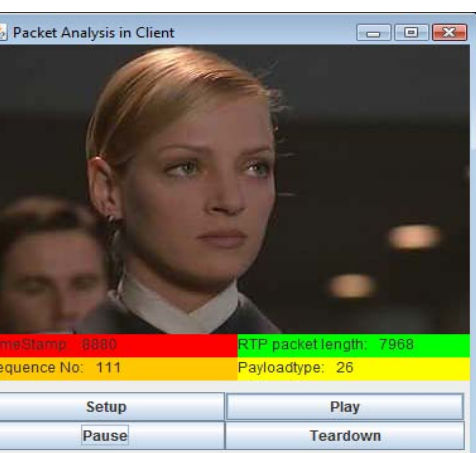


Figure 1: Client GUI

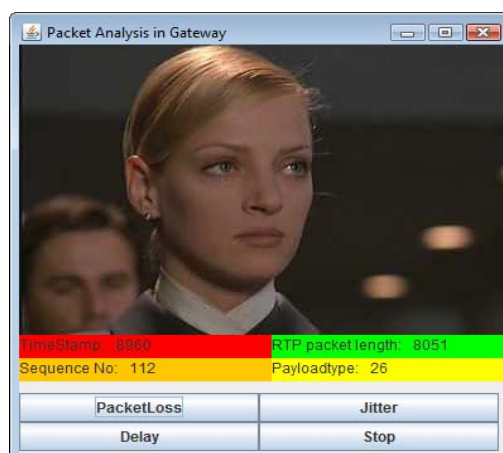


Figure 2: Gateway GUI

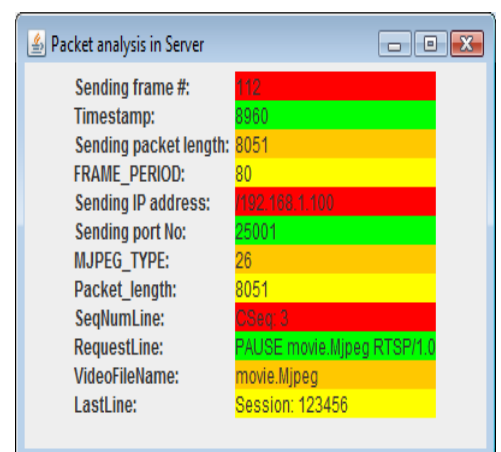


Figure 3: Server GUI

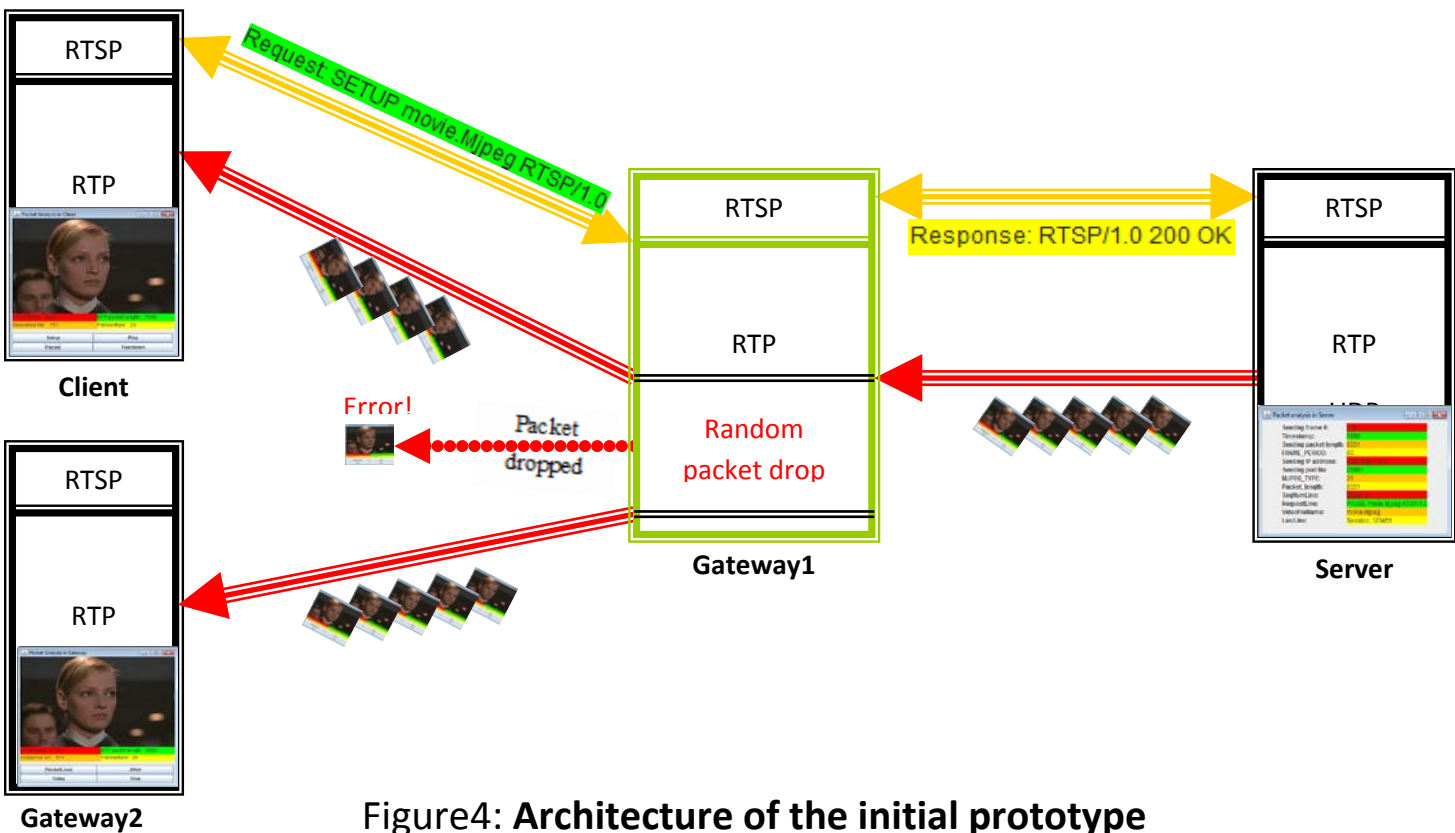


Figure4: Architecture of the initial prototype

References

- [1] RFC 1889 : <http://www.ietf.org/rfc/rfc1889.txt>, access date 02 April 2009
- [2] Wireshark: <http://www.wireshark.org/about.html>

RESCON '09

DAY THREE: SESSIONS



SED Research Student Conference

Brunel University

22-24th June 2009

AN INTELLIGENT SYSTEM FOR PET TUMOUR DETECTION AND QUANTIFICATION

Mhd Saeed Sharif, Abbas Amira

Electronic and Computer Engineering

School of Engineering and Design

Brunel University, Uxbridge, Middlesex, UK

mhd.sharif@brunel.ac.uk

Keywords: Artificial Neural Network, Medical Image Analysis, Positron Emission Tomography.

Introduction

Tumour classification and quantification in positron emission tomography (PET) imaging at early stage of illness are important for radiotherapy planning, tumour diagnosis, and fast recovery. Medical images can be acquired using different medical modalities such as positron emission tomography (PET), computed tomography (CT), magnetic resonance imaging (MRI), and ultrasound. PET is a tomographic technique which is used to measure physiology and function rather than anatomy by imaging elements such as carbon, oxygen and nitrogen which have a high abundance within human body. PET plays a central role in the management of tumour beside the other main components as diagnosis, staging, treatment, prognosis, and follow-up. Due to its high sensitivity and ability to model function, it is effective in targeting specific functional or metabolic signatures that may be associated with various types of diseases [1], [2], [3], [4].

There are many techniques for segmenting medical images, in which some of the approaches have poor accuracy and require a lot of time for analyzing large medical volumes. Artificial intelligence (AI) technologies can provide better accuracy and save decent amount of time. Artificial neural network (ANN), as one of the best AI technologies, has the capability to classify, measure the region of interest precisely, and model the clinical evaluation. ANN is a mathematical model which emulates the activity of biological neural networks in the human brain. It consists of two or several layers each one has many interconnected group of neurons. The main aim of this research is to evaluate the capability of ANN to detect and classify the region of interest (ROI), tumour, in PET images, utilizing thresholding and multiresolution analysis (MRA) approaches to feed the network with the generated features. Promising results have been achieved utilizing phantom and real PET images.

Methodology

The 3D PET image acquired from the scanner goes through the preprocessing block. At this stage histogram equalization and median filter are utilized to enhance the quality of image features and remove most of the noise associated with the image. The enhanced image can be processed using two approaches; the first processing block is the thresholding technique which removes the background and unnecessary information making the image features ready for the ANN. The second approach is the MRA, where the image is transformed into the wavelet domain using Haar wavelet transform (HWT) at different levels. This transform decomposes the image and produce the approximation, horizontal, vertical, and diagonal features. The approximation features are fed to the ANN for classifying and quantifying the tumour. The outputs of both ANNs are compared in the next step and the best outputs are selected. The generated outputs are finally mapped and displayed.

Results and discussion

The results have shown that HWT method has generated better results in comparison with thresholding method; however in both cases the ROI has been clearly detected using ANN. Fig. 1 illustrates the segmented real PET images.

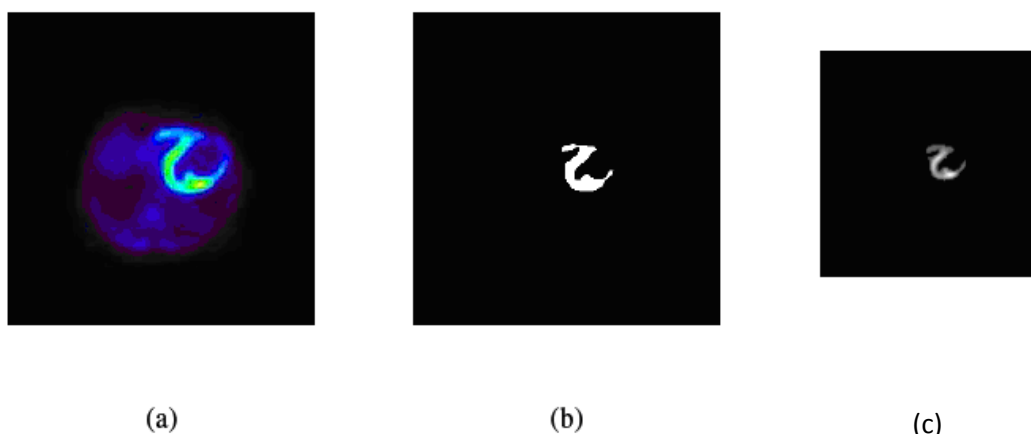


Fig 1: Real PET: (a) Original PET image (256x256), (b) Reconstructed image from ANN and thresholding (256x256), (C) Reconstructed image from ANN and HWT (128X128).

Conclusion

Subjective evaluation for the proposed system outputs has been presented in this paper. It worth mentioning that objective evaluation using phantom images contain simulated tumour was also carried out. The experimental results have shown good performance for the ANN in detecting and segmenting the tumour.

References

[1] D. A. Mankoff, M. Muzi, and H. Zaidi, "Quantitative analysis in nuclear oncologic imaging", in *Quantitative Analysis of Nuclear Medicine Images*. edited by H. Zaidi, Springer, New York, pp. 494-536, 2006.

- [2] D.Montgomery, A. Amira and H.Zaidi, "Oncological PET Volume Segmentation Using a Combined Multiscale and Statistical Model", Medical Physics (The American Association), 34 (2), February 2007.
- [3] P. Dendy, B. Heaton, "Physics for Diagnostic Radiology" , Institute of Physics, 2002.
- [4] A. Webb, "Introduction to Biomedical Imaging", IEEE Press Series in Biomedical Engineering, 2003.



SED Research Student Conference

Brunel University

22-24th June 2009

Simulation of a Novel, Toroidal-Type, CVT

Colin Bell, Romeo Glovnea

Lubrication Laboratory, Mechanical Engineering, School of Engineering and Design, Brunel University, Uxbridge, Middlesex, UK

Colin.Bell@Brunel.ac.uk

Keywords: Traction Drive, Continuously Variable Transmission, Vehicle Modelling

Introduction

The benefits of using a continuously variable transmission (CVT) in an automotive environment have been well documented. In addition to more than a 10% reduction in fuel consumption, and hence emissions (which is of particular relevance in the current global aim for reduction in CO₂ emissions), a vehicle with a CVT can also provide better acceleration and reduced noise [1]. A new, toroidal-type CVT is currently in development, which offers a good balance of efficiency, ratio range, and size.

In an attempt to improve and optimize the design without using a costly 'trial and error' design approach, a fully detailed drive-train simulation has been created, which moves away from the traditional approach of using pre-existing software packages. Everything within this model has been created from first principles, allowing a much higher level of customization and control.

The design for the new CVT is shown in Figure 1, the operating principle of which has been documented in [2]. The radial positions and angles of axis of rotation of each spherical element are altered automatically by simply adjusting the resistive torque applied to the output of the CVT, which in turns changes the transmission ratio. The resistive torque is transformed to a linear force via a ball-screw and balanced by a loading system applied to the toroidal disc. By balancing these two forces the CVT will automatically provide the correct transmission ratio, and hence sufficient torque to balance the resistive torque applied.

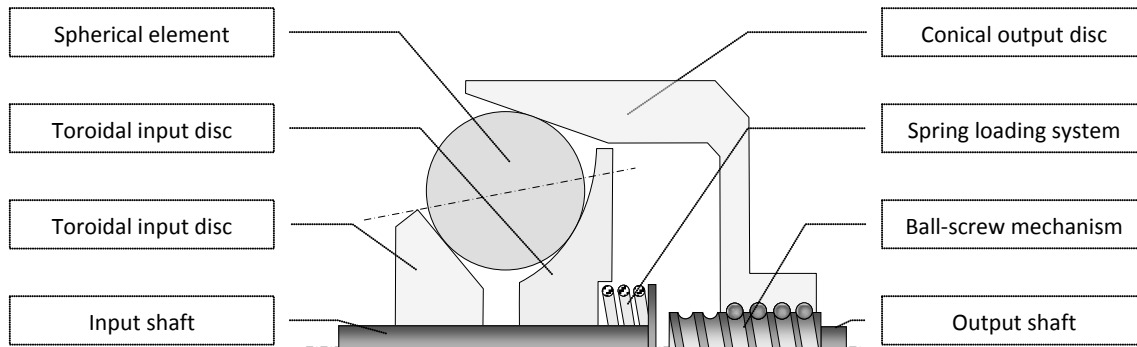


Figure 1: A schematic of the new toroidal CVT design

Methodology/Approach

The simulation is based on analyzing the inertia and acceleration of each individual element within the transmission, whilst elements outside the element, such as the wheels and engine/flywheel are considered to be singular elements with lumped inertias. The traction interaction between adjacent elements are based on previous experimental results from which a relationship between slip and traction has been determined. The tire-road interaction is based on the well documented Pacejka friction model. The torque produced by the engine has been simplified to a quartic function of engine speed, which can be easily adapted to simulate any desired engine size and type. Based on this model a differential equation has been developed that relates the instantaneous acceleration of the wheels to the torque produced by the engine.

Results and discussion

Initially to validate the model the CVT was replaced with a simpler step-gear transmission. As shown in the results in Figure 2a the simulation accurately represents values obtained from real vehicles. Figure 2b shows the results obtained from the full simulation including the CVT. The graph shows that during the initial sudden demand of torque to accelerate from rest, the CVT takes approximately 2 seconds to respond, which is well within the response time offered by similar devices [3].

Vehicle	0-60mph [s]		Top Speed [mph]	
	Real	Sim.	Real	Sim.
2.0l Family saloon (107kW @ 4,500rpm) (190Nm @ 6,000rpm) 1400kg mass	9.5	9.09	135	132.3
1.3l hatchback (43kW @ 2,500rpm) (101Nm @ 5,000rpm) 1200kg mass	18	17.08	95	95.5

Figure 2a: Step-gear results

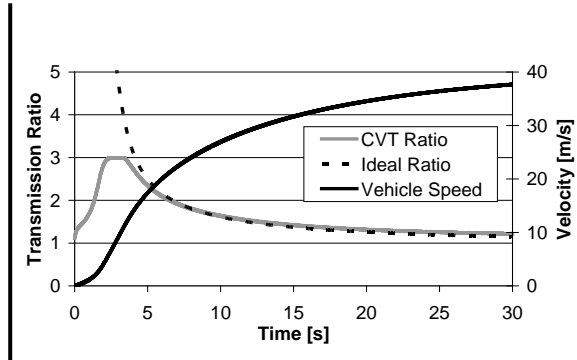


Figure 2b. CVT results

Conclusion

The simulation performed very well when compared to real performances in open-throttle tests on step-gear transmissions. When compared to the discrete-ratio simulation, the CVT offered similar performance when accelerating at full throttle, with the added benefit of a more stable engine speed and smoother acceleration. The CVT simulation proved extremely useful in simulating performance, which allows for future research in optimization of the device without the need for expensive prototypes.

References

- [1] Boos, M. and Mozer, H., Ecotronic: The Continuously Variable ZT Transmission (CVT). *Transmission and Driveline Symposium*. SAE (1997), pp.61-67.
- [2] Cretu, O. S., and Glovnea, R.P., Constant Power Continuously Variable Transmission (CP-CVT): Operating Principal and Analysis, *Journal of Mechanical Design*. Vol.127, No.1. (2005) pp.114-119.
- [3] Fuchs, R., Hasuda, Y. and James, I., "Modeling, Simulation and Validation for the Control Development of a Full-Toroidal IVT" Technical Report (2002), *Torotrak Development Ltd.*, Leyland, UK



SED Research Student Conference

Brunel University

22-24th June 2009

**Efficient Low Power Reconfigurable Architectures
for 3D Medical Image Compression**

Afandi Ahmad, Abbas Amira

Electronic and Computer Engineering, School of Engineering and Design,

Brunel University, Uxbridge, Middlesex, UK

afandi.ahmad@brunel.ac.uk

Keywords : Haar Wavelet Transform (HWT), Field Programmable Gate Array (FPGA), three dimensional (3D) medical image compression

Introduction

Medical image compression poses a complex problem since, for certain image modalities, it is unacceptable to lose information. Higher compression ratios can be achieved using wavelet techniques where 3D wavelet transform is widely applied for medical applications due to its features of perfect reconstruction property and lack of blocking artifacts [1].

Reconfigurable hardware, especially field programmable gate arrays (FPGAs) with various advantages, are widely used in digital signal processing [2], [3]. It can reduce the amount of memory used, computational complexity and power consumption [4], and also lead to significant contribution towards processing large medical volumes. As diverse as the higher demand of processing complexity for 3D medical image compression is, power consumption has become a key design issue in FPGA based architectures [5].

In this research, novel architectures based on different design approaches and arithmetic techniques will be developed for 3D medical image compression. Furthermore, solutions for processing large medical volumes will be investigated and power modelling of the architectures developed will be carried out on different FPGA platforms. The ultimate aim of this research is to examine the most efficient low power reconfigurable architectures for 3D medical image compression.

Methodology

Fig. 1 illustrates a methodology framework of this research including: a 3D wavelet compression and decompression system, the computation process of 3D HWT coefficients using transpose based computation, hardware resources optimisation using block random access memory (BRAM) in Xilinx FPGA device architecture, and different design

approaches and arithmetic techniques for one-dimensional (1D) Haar wavelet transform (HWT) implementation. The research presented in this paper focuses on the design and implementation of low power architecture for 3D HWT.

Results and discussion

The results obtained from the preliminary implementation of the direct mapping method for 1D HWT on different platforms are presented in Table 1. Comparison of the hardware resources utilization, power dissipation and maximum frequency have been made in order to evaluate the implication of design architectures towards the hardware resources utilization and also the design performance.

Chip layouts for each targeted device including Spartan-3L, Virtex-E, Virtex-4 and Virtex-5 are given in Fig. 2. The preliminary results of this study indicate a significant idea regarding the technology advancement of an FPGA. Interestingly, the latest devices offer more hardware resources and also specific FPGA devices are available for low power application. Moreover, it is proven that Spartan-3L as a low power FPGA device consumes less power in comparison with other FPGA devices.

It is worth noting that this preliminary results significantly contributes to future research exploration in order to determine the most efficient low power reconfigurable architectures in 3D medical image compression.

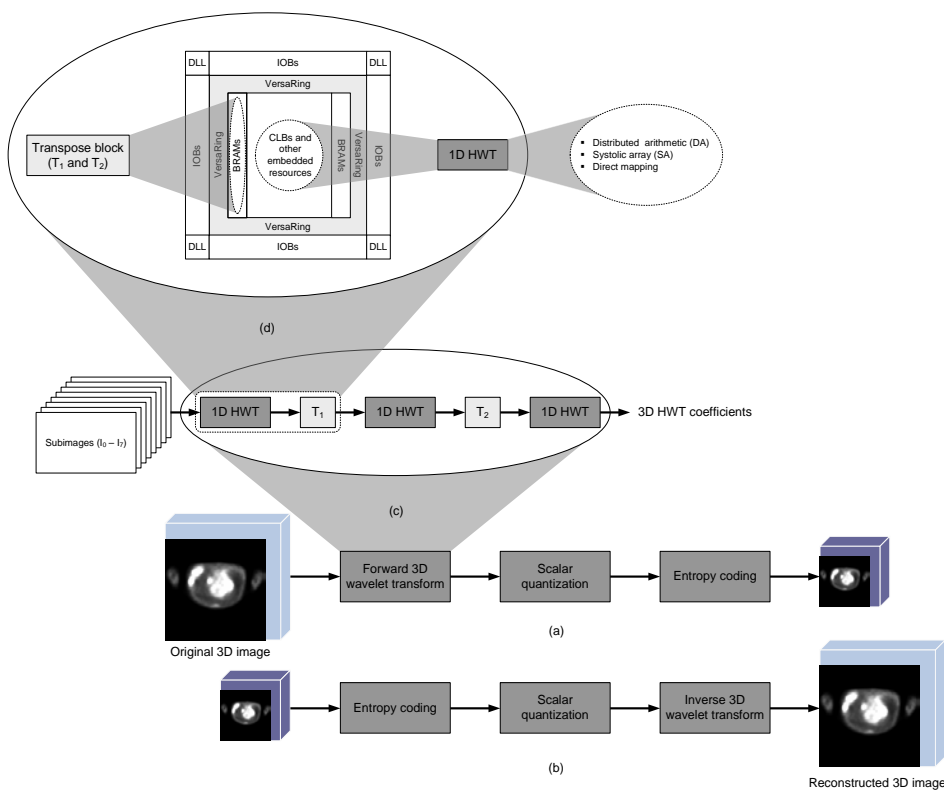


Fig. 1 Research methodology frameworks. (a) and (b) Block diagrams of the 3D wavelet compression/decompression. (c) Block diagram for the computation of 3D HWT coefficients using

transpose based computation. (d) Hardware resources optimisation using BRAM and other embedded resources in Xilinx FPGA device architecture.

Table 3 Comparison of 1D HWT direct mapping implementation results on different platforms.

Parameter	FPGA devices			
	Spartan-3L	Virtex-E	Virtex-4	Virtex-5
% Logic utilization	2	2	3	5
% Number of occupied slices	1	1	3	2
% Number of bonded IOBs	26	15	53	58
Maximum frequency (MHz)	127	108	305	353
Power consumption (mW)	144	367	281	356

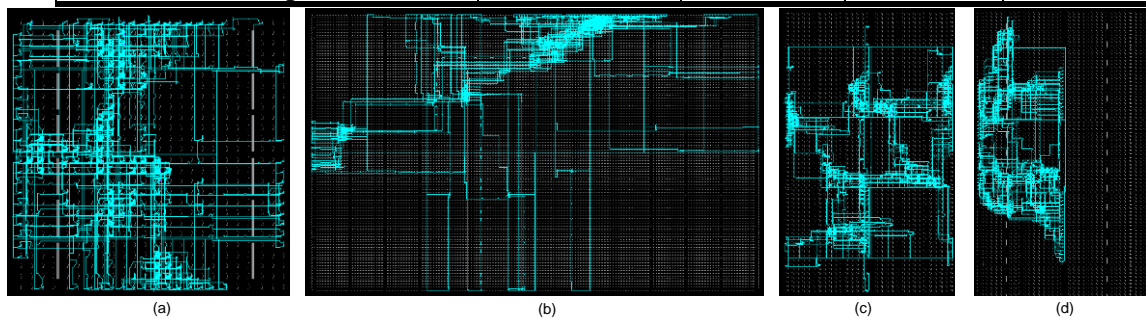


Fig. 2 Chip layout for different devices. (a) Spartan-3L (XC3S1500L-4FG676). (b) Virtex-E (XCV3200E-8FG115). (c) Virtex-4 (XC4VLX15-12SF363). (d) Virtex-5 (XC5VLX30-3FF324).

Conclusion

This paper introduces a framework of efficient low power reconfigurable architectures for 3D medical image compression. On going research is focusing on the integration of 1D HWT in the 3D transpose based decomposition will be carried out with different design architecture strategies including distributed arithmetic (DA) and systolic array (SA). The influence of parallelism and pipelining also will be studied in order to explore the implication towards performance and power consumption in FPGAs.

Moreover, analysis on power consumption for each 1D HWT and transpose blocks will be carried out in comparison with complete 3D transpose based decomposition. This comparison contributes to significant error analysis in order to reveal the most efficient low power reconfigurable architectures for 3D medical image compression.

References

- [1] Y. F. Low and R. Besar, "Optimal Wavelet Filters for Medical Image Compression," *Int. Journal of Wavelets, Multiresolution and Info. Process.*, vol. 1, no. 2, pp. 179–197, 2003.
- [2] L. Deng, K. Sobti, and C. Chakrabarti, "Accurate Models for Estimating Area and Power of FPGA Implementations," in *Proc. IEEE Int. Conf. on Acoustics, Speech and Signal Process. (ICASSP 2008)*, April 2008, pp. 1417–1420.
- [3] P. Porwik and A. Lisowskai, "The Haar Wavelet Transform in Digital Image Processing: Its Status and Achievements," *Machines Graphics and Vision*, vol. 13, no. 1/2, pp. 79–98, 2004.

- [4] S. Chandrasekaran, A. Amira, S. Minghua, and A. Bermak, "Efficient VLSI Architecture and FPGA Implementation of the Finite Ridgelet Transform," *J. Real-time Image Process.*, vol. 3, no. 2, pp. 183–193, May 2008.
- [5] S. Chandrasekaran, "Efficient FPGA Implementation and Power Modelling of Image and Signal Processing IP Cores," Ph.D. Dissertation, Brunel University, 2007.



SED Research Student Conference

Brunel University

22-24th June 2009

Robustness of complex networks to node and cluster damage

Emil Gegov¹, Mark Atherton¹, Hamed Al-Raweshidy²

1. Mechanical Engineering, School of Engineering and Design, Brunel University, Uxbridge, Middlesex, UK

2. Electronic & Computer Engineering, School of Engineering and Design, Brunel University, Uxbridge, Middlesex, UK

emil.gegov@brunel.ac.uk

Keywords: scale-free network, random network, cluster damage

Introduction

One of the main characteristics of complex networks is their ability to sustain a significant amount of damage, while their functionality virtually remains unaffected [1]. For example, communication networks often experience local failures of core components, but this has no effect on the performance of the rest of the network. The same holds for a vast range of biological networks [2]. Simple organisms often develop, survive and reproduce in the presence of extreme environmental changes, internal failures, or even pharmaceutical interference. This is due to the robustness of the underlying metabolic network.

There are three principle mechanisms of network robustness: redundant components, distributed functionality, and self-organization [3]. Redundancy ensures that if a component fails, there is another identical or similar component, which can carry out the function of the former. However, having back-up components is wasteful and costly, so an alternative is to have multiple heterogeneous components with overlapping (distributed) functions. The most complex mechanism, self-organization, involves concepts, such as modularity, decoupling, feedback control and self-adaptation.

The goal of this investigation is to assess the robustness of two popular network structures – ER random networks and BA scale-free networks – to node and cluster damage. There is no previous work on the latter.

Methodology

We investigate two types of network robustness: error and attack tolerance. For the former, components are removed at random. For the latter, components with the highest *betweenness centrality* are removed first, i.e. those, which have the highest proportion of shortest paths going through them. The level of tolerance is measured by two parameters: the average of all shortest paths, and the number of isolated nodes.

For node damage, we proceed by removing nodes iteratively and measuring the two parameters. For cluster damage, the network first needs to be divided into a set of optimum clusters with maximum modularity, as described in [4]. We then represent each cluster by a single node, and cross-cluster links by normal links, in a new *network of clusters*. Finally, we proceed by deleting nodes iteratively to simulate cluster damage.

Results and discussion

To simulate node damage, we used Network Workbench to build and analyse two ER and two BA networks, of 1000 nodes and 1981 links each. All results confirmed previous work on the topic by highlighting the robustness of scale-free networks to random errors, and their vulnerability to targeted attacks. For example, Fig. 1 shows how the number of isolates increases, as nodes are removed from the network. Next, we need to simulate cluster damage and compare the results.

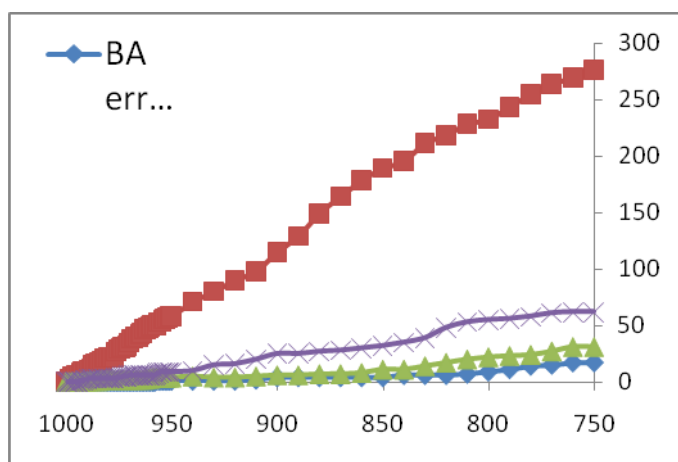


Fig 1. Isolates as a function of nodes

Conclusion

There will be two main contributions to scientific knowledge to follow from this investigation: to shed some light on the effects of cluster damage in complex networks; and to explore the relationship between node and cluster damage.

References

- [1] Albert, R., Jeong, H. & Barabasi, A-L. Error and attack tolerance of complex networks. *Nature* **406**, 378-381 (2000).
- [2] Jeong H. *et al.* The large-scale organisation of metabolic networks. *Nature* **407**, 651-654 (2000).
- [3] Kitano, H. Biological robustness. *Nature Reviews Genetics* **5** (11), 826-837 (2004).
- [4] Newman, M. E. J. & Girvan, M. Finding and evaluating community structure in networks. *Physical Review E* **69**, 026113-1-026113-15 (2004).



SED Research Student Conference

Brunel University

22-24th June 2009

Designing Medical Devices for Lay Use

Abdusselam Selami Cifter¹, Dr. Hua Dong²

1. Inclusive Design Research Group, School of Engineering and Design, Brunel University, Uxbridge, Middlesex, UK a.cifter@brunel.ac.uk
2. Inclusive Design Research Group, School of Engineering and Design, Brunel University, Uxbridge, Middlesex, UK hua.dong@brunel.ac.uk

Keywords: lay-users, professional-users, user characteristics

Abstract

There is an increasing and evolving demand from the end-user market for the adaptation of products originally designed for professional use to the use of lay people. Such products can be found in different market segments, for example home-use medical devices such as blood sugar monitors, digital thermometers, etc. These products were originally designed for professional users (e.g. doctors) to meet their specific needs, and now many of them become available on the mainstream market for lay people (e.g. patients). However there is very little understanding of this adaptation process of which the designers are playing an important part. This paper reports my PhD research about designing medical devices for lay people, specifically focusing on the adaptation process from professional to lay use. It aims to provide support for designers to make the adaptation easier, and to reduce time to market in the product development process.

Introduction

Our lifestyle and expectations from products are changing day by day and advancements in technology bring the opportunity to make products **smaller**, **smarter**, and **cheaper**. Today, products perform various complicated tasks without the need for user interaction except the use of a few buttons and are also affordable by a wide range of user groups. These circumstances have led to the emergence of the adaptation concept from professional use to the use of lay people.

According to Liddle [3], there are three phases of technology adoption: enthusiast phase (Hobby), professional phase (Work) and consumer phase (Life). Enthusiast phase is the invention phase where people like to exploit the technology without giving consideration to the complexities and difficulties on the technology. However, after sometime an enthusiast user may come up with an idea to put that technology in a practical way and then invention starts to become an innovation. This is the professional phase where priorities of developers change and become more focused on costs and prices. In this phase, the design must be

reliable, consistent and above all useful and usable. After the product has built up enough volume through the business phase and technology has become cheaper, the consumer phase starts. In this phase product's language changes dramatically with respect to the priorities of the consumers. The design must be easy to use, pleasurable and must present its functionality in an aesthetic way.

My PhD research is focused on the consumer phase. Designers are central to the adaptation process from the professional phase to the consumer phase. They ensure that products perform a professional level of tasks, yet simplify the interface to the level of lay users. To make this process easier, comprehensive information on the characteristics of lay users should be provided to designers.

Medical devices are chosen as major case studies in this study. Susanne Ludgate [1], Medical Director at the UK Medicines and Healthcare products Regulatory Agency (MHRA), states that "over the past few years there has been a huge increase in the number of medical devices being used by patients at home." However there are still shortcomings during the design development process of these products. According to Gupta [2], although the context of use differs for lay-users, the same regulatory framework is applied to both professional and lay-use medical devices at present. There is a need to develop a more appropriate framework for the context of lay users.

Methodology

To understand the characteristics of lay users and to understand the professional-to-lay-use adaptation process, a series of studies has been planned:

1. Literature review covering topics: professional users, lay users, design process, medical devices and product adaptation.
2. Experimental studies on lay users using digital products. This study involves 10 able-bodied users, 10 older users and 10 users with disabilities.
3. Interviews with industry (designers and manufacturers) to understand their current approach and requirements. 10 companies will be interviewed.
4. Development of the design support based on data gathered from studies 2 and 3.
5. Evaluation of the design support with design students and with professional designers.

Initial Findings

From literature review, it was found that 1) home-use medical devices are a fast growing market but there is little understanding on this segment. 2) The context differs between professional use and lay use. 3) Lay users' needs differ from professional users and they vary

significantly. 4) Very little previous research was found on lay users, and the information was mainly theoretical therefore an experimental study necessary.

The experimental studies carried out (a pilot study involving 6 users and user test with 10 able-bodied and 10 older users) so far suggest that: 1) Previous experience has a big effect on the user behavior, and in some cases misleads the users. 2) Older users experience difficulties in understanding digital interface and they are often unmotivated to use digital devices. 3) Disabled users' abilities vary significantly, and it is worth investigating their interaction with products according to their specified impairments, i.e. physical, sensory and cognitive impairments.

Conclusion

Designing for professional users is different from designing for lay users and designers require comprehensive information about lay-users. This research will provide 1) a better understanding of the professional-to-lay-use adaptation process 2) experimental data on lay-user characteristics 3) accessible information for designers about lay-users 4) practical design guidance on the adaptation process from professional use to the use of lay people.

References

- [1] **Ludgate S** (2003). Why the MHRA Needs Your Help. *The Pharmaceutical Journal*, V.271, No.7278, P.780
- [2] **Gupta, S** (2007). *Design and Delivery of Medical Devices for Home-Use: Drivers and Challenges*. Cambridge, Department of Engineering.
- [3] **Moggridge, B** (2007). *Designing Interactions*. MIT Press, Page 245-251



SED Research Student Conference

Brunel University

22-24th June 2009

FOrecasting Routing TEchnique using Location information for wireless ad hoc networks (FORTEL)

Hadi Nouredine¹, Hamed Al- Raweshidy²

1. Electronic and Computer Engineering, School of Engineering and Design, Brunel University, Uxbridge, Middlesex, UK

2. Wireless Network and Communications Centre, Brunel University, Uxbridge, Middlesex, UK

hadi.nouredine@brunel.ac.uk

Introduction

According to the proactive approach [1], every node maintains a list of routes of all the possible destinations. Hence, a vast amount of control messages is used to discover and maintain those routes, regardless of data meant to be transmitted or not. On the other hand, reactive routing approach [1] reduces the amount of overhead that the proactive protocols require by discovering routes to the destination node on demand, only. A request message is transmitted by the sender to its one hop neighbors which, in turn, forwards it to its neighbors and so on. Consequently, the request messages are propagated in the network despite whether they are propagated towards the destination or away from it. Position based routing approach [2] uses location information, which is considerably small as compared to the routing information, in order to perform the routing from the sender to the destination. Each node retains a location table, in which location information of other nodes of the network is stored. Several works have been proposed regarding position based routing. In particular, some works propose the transmission of the data message to the node, which progresses to the destination, while some others propose the flood of the data message in the direction of the destination. Furthermore, other works apply the reactive concept of routing while reducing the zone where the route request message is propagated. However, the utilization of location information can be more efficient and more critical than confining the request zone or reducing the routing overhead messages. As proposed in the present work, we attempt to transform the route discovery mechanism that usually involves other nodes, into a local process. This process is performed at the source node minimizing, therefore, the discovery time and reducing the routing overhead, network load and the end-to-end delay.

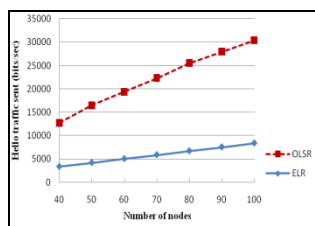
Methodology/Approach

The present approach, along with other objectives, explores the possibility of using the location information of the nodes, which includes the location coordinates and the distance threshold, to relay data packets to the destination. Distance threshold represents the distance

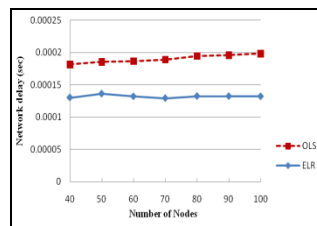
separating the node with its farthest one hop neighbor, with which maintains an acceptable communication link. Assuming that the data rate is uniform throughout the network, each node maintains a location table, which contains the location information of all the other nodes. Relying on the location table, any source node in the network is able to predict and foretell a list of intermediate nodes capable of successfully relaying the message. When a node 'S' wants to send a message 'm' to node 'D', it utilizes the location parameters of the destination to select its first hop neighbors. A node is considered a destination's neighbor, only if its distance to the destination is less than or equal to the destination's distance threshold. The destination and its neighbors will be used to construct the routing tree. The root of the tree is the destination; the branches are its neighbors while the link weights are the distance from the destination to every neighbor. The same logic is followed for each branch of the tree, until the tree construction is completed, which is determined when 'S' becomes a leaf of all possible branches. The selected route is the shortest path, in terms of distance.

Results and discussion

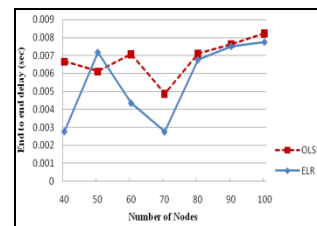
The protocol performance is tested using OPNET 14.5 modeler and is compared to Optimizes Link State Routing protocol (OLSR) in terms of Hello traffic sent (bits/sec), network delay (sec), medium access delay (sec), end-to-end delay (sec) and routing overhead (bits/sec). The simulation was run for 40, 50, 60, 70, 80, 90 and 100 nodes and the average values of the above metrics are considered.



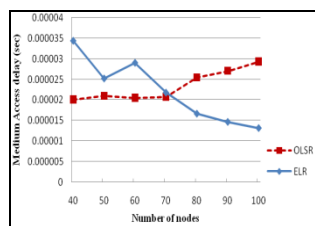
Average hello traffic sent (bits/sec)



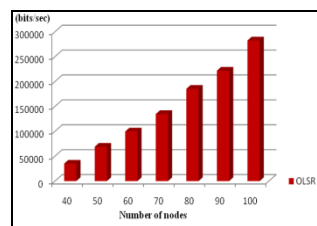
Average network delay (sec)



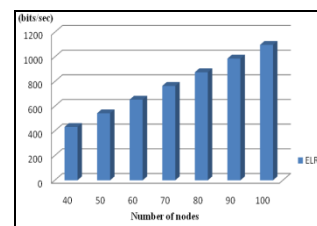
Average end-to-end delay (sec)



Average medium access delay (sec)



OLSR Routing control overhead (bits/sec)



ELR Routing control overhead (bits/sec)

Conclusion

In this paper we have presented a novel technique of route discovery, referred as FORTEL, for wireless ad hoc networks using nodes location information. The simulation results show that FORTEL performs well in fixed node scenarios, as opposed to DSR, in terms of end-to-end delay and routing overhead.

References

- [1] Changling Liu, Jörg Kaiser, “A Survey of Mobile Ad Hoc network Routing Protocols”, University of Ulm, Tech.Report Series, Nr. 2003-08, October 2003.
- [2] M. Mauve, A. Widmer, and H. Hartenstein, “A survey on position-based routing in mobile ad hoc networks”. IEEE Network, 15(6), 30-39, 2001.

Liquid-Vapour Visualization of an evaporating diesel spray using Laser Induced Exciplex Fluorescence Technique

Mohammad Reza Herfatmanesh, Alvaro [Diezrodriguez](#) and Hua Zhao

Mechanical Engineering, School of Engineering and Design, Brunel University, Uxbridge, Middlesex, UK Mohammad.Reza.Herfatmanesh@brunel.ac.uk

Keywords (3): Laser induced exciplex fluorescence, evaporating diesel spray and DI diesel engine

Introduction

Ever increasing concern over global warming, stringent emission legislations and limitations in available fossil fuel resources enforces the need for improvements towards a more efficient and cleaner internal combustion (IC) engines.

The combustion process in an IC engine is a complex phenomenon which is highly influenced by the fuel and air mixing process [1]. The combustion of liquid fuel sprays has a direct influence on the efficiency and the level of emissions produced by an engine. As a result, many advanced non-intrusive laser based diagnostic techniques have been developed in order to gain insight into the combustion process.

The use of engines equipped with optical access enables the characterisation of the injected fuel sprays through laser spectroscopy methods permitting detailed investigation of the combustion process. The majority of engine manufacturers rely on optical methods for the development of the latest production engines present in the market.

Methodology/Approach

Laser induced exciplex fluorescence (LIEF) is a unique technique developed for simultaneous visualisation of liquid and vapour phases. In order to measure liquid and vapour concentrations inside an IC engine, two tracer dopants are added to the fuel. N, N, N', N' – tetramethyl-phenylene-diamine known as TMPD is used as the fluorescent monomer and 1-methyl-naphthalene as the partner to form the exciplex species [2]. These dopants are then dissolved in decane to form the fuel mixture used for this technique.

The fluorescence from the excited monomer (i.e. TMPD^{*}) and the exciplex molecules when they return to the ground state indicate the vapour and liquid concentration respectively. The exciplex species are formed due to reactive collision of the excited monomer with Naphthalene in a dense region such as the liquid phase where the reaction probability is much higher [3]. The emission spectra of the exciplex molecules is red-shifted with respect to that

of the fluorescent monomer, this is due to the binding energy required for the formation of the exciplex molecules, Figure 1.

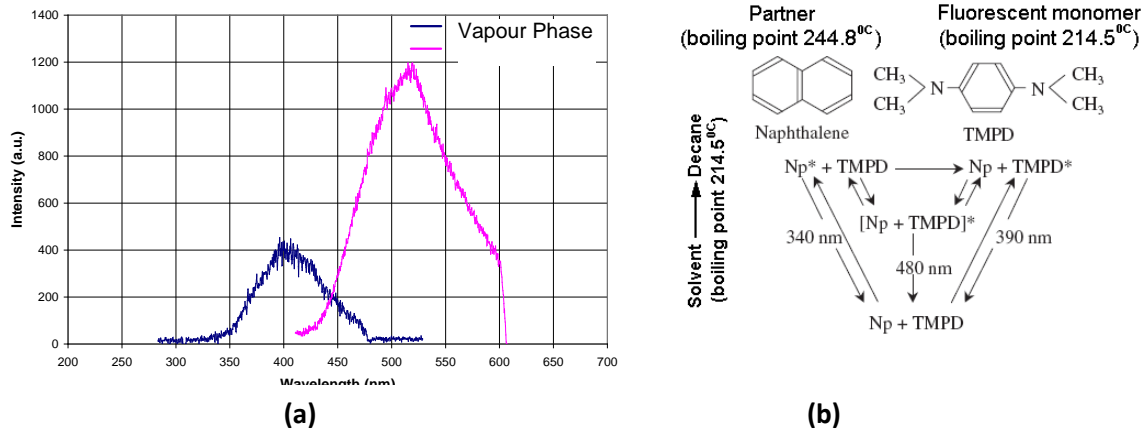


Figure 1. (a) Fluorescence spectra for liquid and vapour phase, (b) Photophysics of TMPD/Naphthalene exciplex system

Therefore it is possible to spectrally separate the fluorescence from the liquid and vapour phases of an evaporating diesel spray through appropriate filters.

A single cylinder optical diesel engine consisting of three side access and a glass piston is used in order to visualise the fuel spray inside the engine, Figure 2.

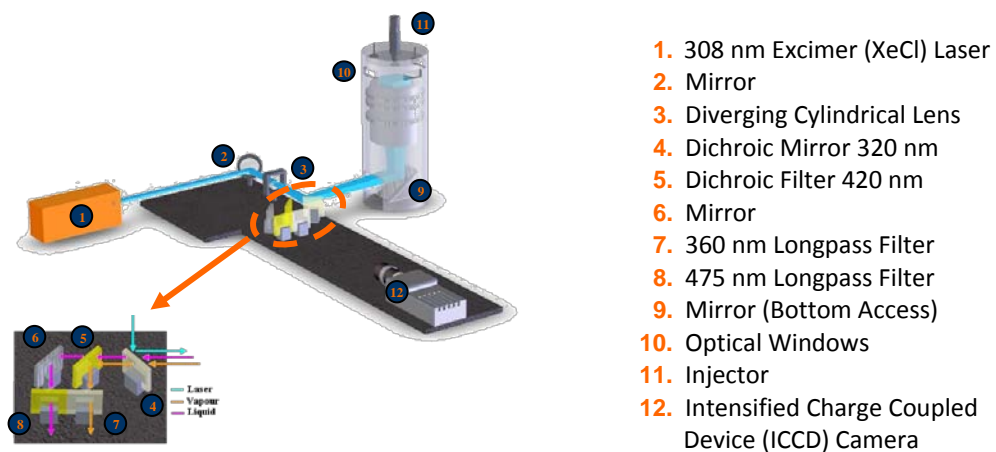


Figure 2. Schematic diagram of the engine and the optical setup

Results and discussion

The results depicted below are obtained by the use of a fuel mixture containing 89% decane, 10% naphthalene and 1 % TMPD. The start of injection takes place at 40 degrees crank angle before top dead centre (CA BTDC) with the injection duration of 500 μ s at 1200 bar.

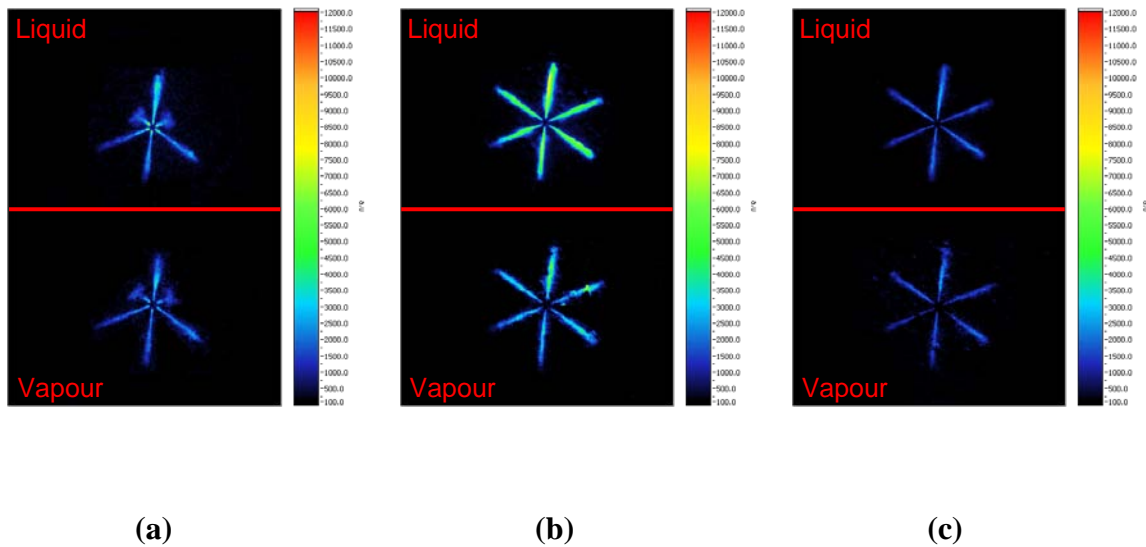


Figure 3. Spatial distribution of liquid and vapour phases of an evaporating diesel spray, (a) 100 μ s After Start of Injection (ASoI), (b) 250 μ s ASoI (c) 400 μ s ASoI

It is evident that at the start of injection the vapour concentration is low due to poor atomization of the spray at this stage, Figure 3. The asymmetry of the fuel sprays at the start of injection is attributed to the inherent characteristics of VCO type fuel injectors.

Conclusion

The spectral separation of liquid and vapour signals through the LIEF technique allows simultaneous visualisation of liquid and vapour phases of an evaporating diesel spray. The fluorescence intensities are directly proportional to the fuel (liquid and vapour) concentration as well as the thermodynamic conditions of the surroundings. Thus quantitative analysis can only be achieved through a comprehensive calibration procedure.

Moreover, the intake manifold pressure and temperature as well as cycle to cycle variations inside an IC engine have a direct influence on the characteristics of an evaporating diesel spray. Therefore time averaging technique should be used to minimize such variations.

It is crucial to obtain a mixture with uniform TMPD concentration since the solubility of TMPD in decane/naphthalene is relatively low at room temperature. In addition, lubricity of the fuel mixture used in this technique is very low compared to standard diesel fuel, therefore premature failure of the fuelling system due to excessive mechanical friction is of great concern.

References

- [1] Schafer R, Schock H and Stuecken T 1994 The Development of an Improved Quantitative Calibration for an Exciplex Liquid/Vapor Fuel Visualization System SPIE Vol. 2122/61
- [2] Melton L A and Verdick J F 1984 Vapor/liquid visualization in fuel sprays *20th Int. Symp. on Combustion* (Combustion Institute) pp 1283–90
- [3] Zhao H and Ladommatos N 1998 Optical Diagnostics for In-cylinder Mixture Formation Measurements in IC engines PII: S0360-1285(98)00002-1

Performance of a Transparent Polymer Film UWB Antenna Under Varying Radius of Curvature

Thomas Peter¹, Rajagopal Nilavalan²

1,2. Electronic and Computer Engineering, School of Engineering and Design, Brunel University, Uxbridge, Middlesex, UK

Thomas.Peter @brunel.ac.uk

Keywords: curved, polymer, film

Introduction

Recent approvals in Europe for the use of UWB technology in Wireless Communication has spurred research on the shape, size and compactness of a UWB antenna especially with regard to its conformity to specific shapes; such conformity helps overcome space constraints, improve aerodynamics or even decrease visibility. It has been shown that compact antennas that exhibit multi-band behaviour can easily be conformed to curved surfaces [1], [2]. However, no complete simulation study has been carried out on the performance of a UWB antenna with varying radius of curvatures. Recent papers demonstrate simulation study done for one radius of curvature and experimentally for up to two radii of curvatures [3], [4], [5]. The simulation study in this paper has been made possible with the improved features of CST2009 software [6] which allows the modelling of the antenna on curved surfaces whether singly or doubly curved.

In this paper, we simulate the performance of a coplanar wave guide (CPW)-fed Flexible Monopole UWB Antenna for Wireless Communications on varying radii of curvatures using CST2009. The study of the relationship of the radius of curvature to the performance of the antenna will help understand why wearable antenna performances deteriorate with the bending of the material it is attached or imprinted on and hopefully help to resolve this.

Methodology/Approach

The proposed CPW-fed Flexible Monopole UWB antenna here is done first using a radiating copper surface on a polymer and later a direct radiating transparent silver based polymer, AgHT-8. The design of the antenna is to cater for the standard ultra wideband bandwidth of 3.1 GHz to 10.6 GHz.

Results and discussion

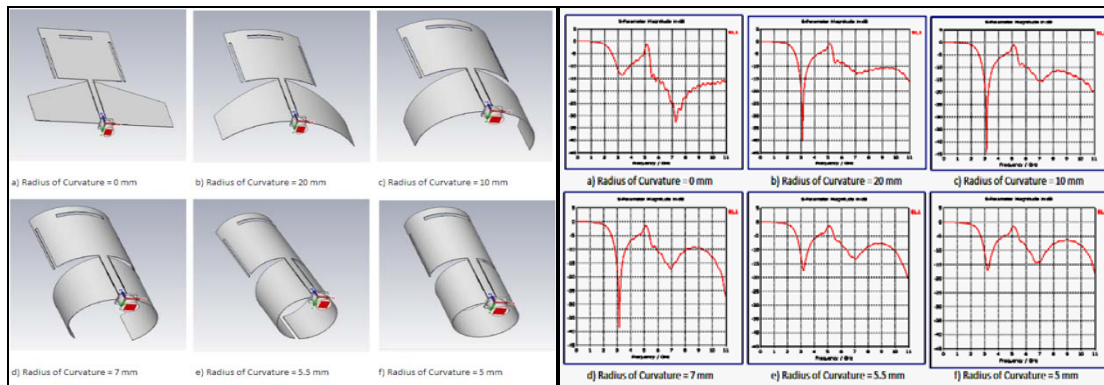


Fig. 1 Shape of antenna on various radii of curvatures

Fig. 2 S11 of the antenna for the various shapes in Fig. 1

Initial findings show that the 10dB bandwidth reduces as the antenna is flexed more. This helps to understand why the performance of a wearable antenna deteriorates as it bends or flexed more. The simulation results provided here are for an antenna with copper film as the radiator on a polymer substrate. Further studies of an antenna designed completely with a transparent polymer radiator and substrate will be done in comparison to study how the performance varies. Positive results could help provide a solution for wearable antennas.

Conclusion

The simulation study shows that performance of a flexible antenna deteriorates as it bends. This is to be verified with experimental results later. Understanding this issue could help us look into using antenna material that will have less impact on performance with bending and consequently improve its performance. The study could also help us to determine the maximum flexure possible for acceptable antenna performance when designing RFID antennas which is also gaining popularity. Providing transparency besides flexibility to both wearable and RFID antennas makes them more discrete and of low visibility; a feature which would be greatly favoured and welcomed by industry.

References:

- [1] B.R.Piper, M.E. Bialkowski, "Electromagnetic Modelling of Conformal Wideband and Multi-Band patch Antennas by Bridging a Solid-Object Modeler with MOM software", *IEEE Antennas and Propagation Magazine*, Vol. 46, No. 5, October 2004.
- [2] C.A. Macon, K.D. Trott, L.C. Kempel, "Practical Approach To Modelling Doubly Curved Conformal Microstrip Antennas", *Progress In Electromagnetics Research, PIER* 40, 295-314, 2003.
- [3] Su Won Bae, Hyung Kuk Yoon, Woo Suk Kang, Young Joong Yoon, Cheon-Hee Lee, "A Flexible Monopole Antenna with Band-notch Function for UWB Systems", *Proceedings of the Asia-Pacific Microwave Conference 2007*.
- [4] Nikolaou, S.; Tentzeris, M.M.; Papapolymerou, J., "Study of a Conformal UWB Elliptical Monopole Antenna on Flexible Organic Substrate Mounted on Cylindrical Surfaces," *Personal, Indoor and Mobile Radio Communications, 2007. PIMRC 2007. IEEE 18th International Symposium on*, vol., no., pp.1-4, 3-7 Sept. 2007

- [5] Santas, J.G.; Alomainy, A.; Yang Hao, "Textile Antennas for On-Body Communications: Techniques and Properties," *Antennas and Propagation, 2007. EuCAP 2007. The Second European Conference on* , vol., no., pp.1-4, 11-16 Nov. 2007.
- [6] CST Microwave Studio 2009, 1998-2006, CST GmbH



SED Research Student Conference

Brunel University

22-24th June 2009

Inclusive Design for Air Travel

Laura Baird

Inclusive Design Research Group, School of Engineering and Design, Brunel University,
Uxbridge, Middlesex, UK

Laura.Baird@Brunel.ac.uk

Keywords: air travel, inclusive design, assistance.

Introduction

This paper addresses the issue of inclusive design in air travel. Inclusive design is defined by the British Standards Institute as "The design of *mainstream* products and/or services that are accessible to, and *usable* by, *as many people* as reasonably possible ... without the need for special adaptation or specialised design." [1]

Over 2 billion passengers per year use commercial airlines worldwide and this figure is set to rise [2]. Of these billions of passengers, it is clear that all varieties of people will be represented, particularly in light of the lower price of air travel, increased migration and multiculturalism. It is also well documented that the worldwide population is ageing [3] and that there is currently a high prevalence of people with disabilities – approximately 20% of the UK population, for example. Consequently, there is a large, wide and growing frequency of people at risk from design exclusion during a typical air travel journey. The needs of these groups must be considered and brought to the attention of designers and managers in the industry. Previous research in inclusive design [4] suggests that this will not only improve the quality of the air travel experience for extreme users, but for all passengers, as well as alleviating the burden on air travel staff.

The aim of this early stage of the research is to gain a comprehensive understanding of the current situation with regard to the inclusivity of air travel. Air travel will be examined from the perspective of the industry, along with that of the passengers, with a view to identifying the problems and needs of both groups in relation to the inclusivity of the journey. The results from these initial investigations will narrow the focus of the research.

Method

Firstly, a subjective framework for the analysis of a typical commercial air travel journey was created by dividing the journey into four distinct stages. An initial analysis of these stages, using the 'exclusion calculator' tool provided by the Inclusive Design Toolkit [5] was carried out to determine the exclusivity of the typical air travel journey. Two sets of exclusion calculations were made.

An analysis of existing regulations concerning passenger rights was made. Key regulations and their impact on the design and management of the air travel journey were identified. Along with this, existing guidelines concerning the inclusivity of air travel were analysed.

Air travel is an industry involving many different parties. In order to create a feasible solution to the problem of exclusivity in air travel, a thorough understanding of these parties and their relationships must be established. For this reason, the main stakeholders involved in the design and management of air travel were identified. Interviews were carried out with individuals from the industry to gain a better understanding of this complex situation.

Results and discussion

The results from the exclusion calculations show that air travel excludes an estimated 1% of the UK population, and 12% of the population are only included through the provision of special assistance (based on population statistics from 1996) [6]. With this in mind, the focus of this research will be on reducing the need for this special assistance through inclusive design.

Regulations are improving passenger rights, and are a step in the right direction, however so far they have had little or no impact on the inclusivity of air travel. A set of guidelines regarding access to air travel for disabled people was developed by the Department for Transport in 2003 [7]. These guidelines are very comprehensive in their scope, however a review carried out by the same body in 2005 showed that little or no difference had been made [8]. Further research must be carried out with the industry to discover why these guidelines are not being utilised.

The analysis of the stakeholders was made from the perspective of the airlines. The main stakeholders are the airlines, the airport authorities, the aircraft manufacturers and the passengers. In general, the more premium the airline, the more input they have in the design of the air cabin. Budget airlines often purchase second hand and sometimes even rent aircraft, allowing for minimal design input of the cabin spaces. With regard to the design and management of the airports, the airport authorities have the most control. The airlines with high passenger volumes are more likely have input into the design of the airport spaces, such as the check-in areas and lounges, than those with low passenger volumes.

Conclusions & current work

There are a few main points to take from the research so far are. There is a problem with regard to the inclusivity of air travel. That although new regulations are increasing passenger rights, they are not increasing the inclusivity of air travel as they are focussed on providing special assistance (which is not inclusive). Current guidelines are not having an impact on the design practices. That for any proposed solutions to have an impact, they must take into consideration the complex relationships and responsibilities of the various stakeholders involved.

With all this in mind, the current research is focussed on gaining a comprehensive understanding of the design management of the stages within the air travel journey. This research takes the form of case studies, questionnaires and interviews. The case studies

involve audits of the physical aspects and interviews of the design managers, and cover the three main booking procedures, three airports and three airlines. A detailed case study of one airline's design practices and design management structure is also being carried out. In addition, the view point of the passengers, in two forms i.e., general passengers and passengers with disabilities, will be evaluated through questionnaires.

References

- [1] British Standards Institute (2005), British Standard 7000-6:2005. Design management systems - Managing inclusive design – Guide
- [2] ICAO (2008), International Civil Aviation Organisation. Available from: www.icao.int [accessed 30-06-08]
- [3] United Nations (2006), Population Prospects: The 2006 Revision. United Nations Population Division
- [4] Baird, L (2007). Claustrophobia and Air Travel. Major Project Report, School of Engineering & Design, Brunel University, West London.
- [5] Clarkson, J, Coleman, R, Hosking, I & Waller, S (2007). Inclusive Design Toolkit. Cambridge Engineering and Design Centre. Also available from: www.inclusivedesigntoolkit.com
- [6] Baird L & Dong H (2009). Inclusive Design for Air Travel. Include 2009, conference proceedings. Royal College of Art, London.
- [7] Department for Transport (2003). Access to Air Travel for Disabled People - Code of Practice. Available from: www.dft.gov.uk [accessed 14-10-08]
- [8] Department for Transport (2005). Review of the Access to Air Travel for Disabled People: 2005 Monitoring study. Available from: www.dft.gov.uk [accessed 14-10-08]

PRE-CLINICAL ASSESSMENT OF A SMART PIEZO-ACTUATED LIMB LENGTHENING DEVICE

* MacInnes R.A.^{1,2}, Taylor A.², Hobson P. R.¹, Brown C.J¹

1. School of Engineering and Design, Brunel University, Uxbridge, Middlesex, UK

2. Finsbury Development Ltd., Leatherhead, UK

rhona.macinnes@brunel.ac.uk

Keywords: Tissue Limb Lengthening Forces Modeling

Introduction

Limb lengthening by distraction osteogenesis (DO) is a technique used for the clinical treatment of limb length discrepancies arising from congenital causes, trauma or infection of the bone. It can also be used bilaterally in the case of dwarfism. DO uses the phenomenon that tissue, when subjected to stress during elongation, will proliferate forming a callus which after a consolidation period, becomes bone of normal strength. Lengthening can be achieved using an external fixator and if no other deformity correction is required a monolateral fixator can be used in place of the traditional and more cumbersome Ilizarov circular frame. The procedure is associated with problems such as pain arising from large incremental distractions, unknown state of the callus during distraction and consolidation and various sources of distraction resistance [1]. A new smart monolateral lengthening device is under development to that will benefit both patient and clinician.

Methodology/Approach

A battery powered piezo-actuator with a maximum extension of 0.1 mm is used as the driving force for device elongation alongside a one way mechanism, preventing backward motion of a telescopic shaft within its housing. A microcontroller is used to regulate the voltage, charging and discharging the actuator as required, thus a range of rates and frequencies of distraction are available.

Total elongation can be measured using the rotation of the nuts on the shaft. Incremental displacement per cycle is used alongside strain based load measurement to determine the stiffness of the tissue during distraction, which has been seen to be an indicator of the condition of tissue [2]. The device has the potential for adapting the distraction regime according to changes in the tissue stiffness seen over the period of lengthening.

The test material is in compression to negate the use of adhesives but the loading on the device is compression as *in-vivo*. In axial testing the device sits between the two parallel plates (one fixed, one sliding). Non-axial testing requires the use of pin clamps which are fixed to the plates and the device (pin length and diameter can be varied). Voltage, load,

displacement per cycle and total displacement are logged using a PICO data logger for analysis.

Maximum displacement per cycle is reduced by frictional forces and compliant interfaces, as well as the stiffness of the tissue itself. Once the actuator has reached maximum voltage, the load is transferred from the actuator to the housing to prevent backwards motion. During this transfer there is some ‘setback’ of the shaft relative to the housing which must be minimised.

Materials used for initial testing were rubber and a herex – a bone (substitute) which exhibit properties close to linear elastic. It is clear from literature [2,3] that the time-dependant properties of tissue play an important role in the stress state of the tissue and thus the pain experienced by the patient over time. A controllable viscoelastic environment has been designed to allow the peak and relaxation time to be manipulated. A fluid based system with dashpot uses the bulk modulus of water to provide increased pressure that can be slowly released through a controllable needle valve to exhaust. In series or parallel with a spring of known stiffness a Maxwell or Kelvin Voigt model is set up, with k and c values dependant on physical variables of the system.

Numerical modelling of the viscoelastic system is replicated in Matlab’s Simulink. This program is also used to model the device, including contact and friction. The model will be validated using the experimental methods described above and is useful for altering distraction rates and mechanical environments provided by tissues that are more difficult to develop experimentally.

Results and discussion

The prototype is run at various speeds (0.3-30 microns/min) to analyse characteristics of the device including maximum load attainable, setback at various loads and its response to time dependant materials. Tests proved the device could distract at clinically relevant loads. A typical output graph is given (figure 1) showing piezo voltage, load and displacement against a rubber material. The accumulated dvrt signal is linear while the geartooth counter is stepped due to the cyclic nature of the one way mechanism. Any difference between these two signals is due to setback within the device.

The time-based output from the numerical simulation is shown in figure 2, representing

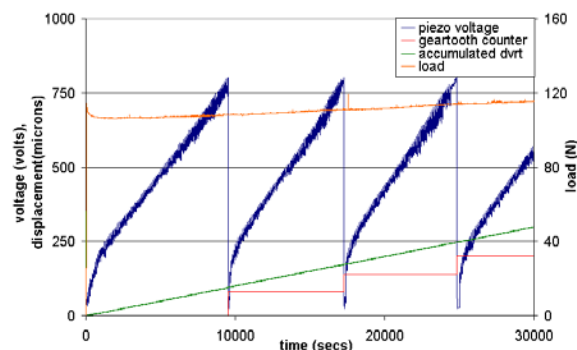


Figure 1: Device running at 0.6micron/min

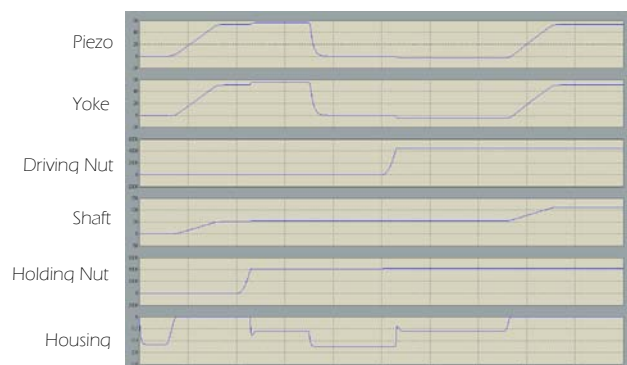


Figure 2: Time-based Simulink output showing displacement (microns) of device components

the displacement of each component of the device.

In this case, there is a pause between cycles therefore the shaft movement appears stepped.

Literature suggests that peak loads in the tissues during distraction are commonly around 200-600N can reach up to 1300N [2,3,4]. High frequency distraction has been shown to reduce tension accumulation [4]. If forces are extreme the control system will limit extension, therefore the aim is to achieve distraction up to loads of approximately 600N with the device.

Under ASTM guidelines, lengthening devices are treated as external fixators. It is proposed that due to the dynamic nature of this new device, a more thorough approach to testing is required, involving materials with non-linear and time dependant characteristics to simulate the hard and soft tissue response including load relaxation and healing behaviour. The experimental viscoelastic setup requires validation, as does the numerical model. This validation process is in progress, using previously collected data from other authors as well as new data from tissue studies using the automated device.

Conclusion

Load-displacement characteristics of tissue during distraction are being simulated to allow for pre-clinical assessment of a new device in comparison to other fixators. In use, the device will not only keep the tissues at a more constant load to reduce pain and increase tissue quality but can additionally be used as a valuable research tool to find the optimum distraction regime for lengthening.

References

- [1] Paley, D. (1990) Problems, obstacles, and complications of limb lengthening by the Ilizarov technique. *Clinical Orthopaedics and Related Research*. Vol 250, pages 81-104
- [2] Gardner T.N., Evans M., Simpson H., Kenwright J. Force-displacement behaviour of biological tissue during distraction osteogenesis, (1998) *Medical Engineering and Physics*, Vol.20, No.9, pages 708-715
- [3] Simpson, A.H.R.W. The forces which develop in the tissues during leg lengthening, A clinical study, (1996) *The Journal of Bone and Joint Surgery*. Vol 78-B, No.6, pages 979-983
- [4] Aarnes, G.T., Steen, H., Ludvigsen, P., Kristiansen, L.P., Reikerås, O. High frequency distraction improves tissue adaptation during leg lengthening in humans ,(2002) *Journal of Orthopaedic Research*, 20 4, Pages 789-792.
- [5] Goodship, A.E., Kenwright, J. The influence of induced micromovement upon the healing of experimental tibial fractures, (1985) *The Journal of Bone and Joint Surgery* Vol 67-B, No.4, pages 650-655

A Review of Short-term Electricity Price Forecasting Techniques in Deregulated Electricity Markets

Linlin. Hu, Dr. G.A. Taylor, Dr. H.B. Wan

Brunel Institute of Power Systems, School of Engineering and Design, Brunel University,
 Uxbridge, Middlesex, UK

Linlin.Hu@brunel.ac.uk

Keywords: Power Markets, Short-term Electricity Price Forecasting, Support Vector Machine

Introduction

Electricity price forecasting has become an important area of research globally since the introduction of the deregulated whole-sale electricity markets. All whole-sale market participants, such as generators, power suppliers, investors and traders, require accurate electricity price forecasts in order to maximize their profitability. Unlike load forecasting, electricity price forecasting is much more complex because of the unique characteristics, uncertainties in operation as well as the bidding strategies of the market participants. During the last two decades, many techniques and models have been developed for forecasting whole-sale electricity prices, especially for the short-term price forecasting. This paper reviews established approaches to electricity price forecasting and provides an insight into the development of future electricity price forecast methods for readers who are working in the academia or industry.



Figure1. Influenced factors of electricity prices

Methodology/Approach

Through observation of short-term electricity price series, power price movements exhibit several seasonal cycles, mean reversion and spikes [1]. Because electrical energy can not be

stored and needs constant balance between demand and supply, the price of electricity is volatile in nature, which causes high risks to market participants. Moreover, other factors may also cause the price to change, such as, weather conditions and transmission congestion in the power system. Main influential factors on electricity price are listed in Figure 1. For different forecasting models, different inputs are used to represent factors that are considered to have a significant impact on electricity price forecasting. Time-series approaches (ARIMA and HMM) analyze historical data, such as load, price and fuel cost. Artificial Neural Networks (ANNs) are more flexible and consider additional factors such as weather conditions, unit operation cost, system constraints and so on. However, based on a recent survey of case studies [2], including more factors in such models does not necessarily mean that the predictive results will be better. The reason for this is that some additional factors are also unavailable and may need forecasting as well. Therefore, the selection of a suitable forecast technique with proper input factors is vitally important for accurately forecasting electricity price.

Results and Discussion

Development of techniques for electricity price forecast is still an important area in research. Several papers have proposed taxonomy of the forecasting methods. In [3], approaches are classified in two sets: time-series and simulation. Depending on the original tree, an extended classification of forecasting methods is presented in Figure 2.

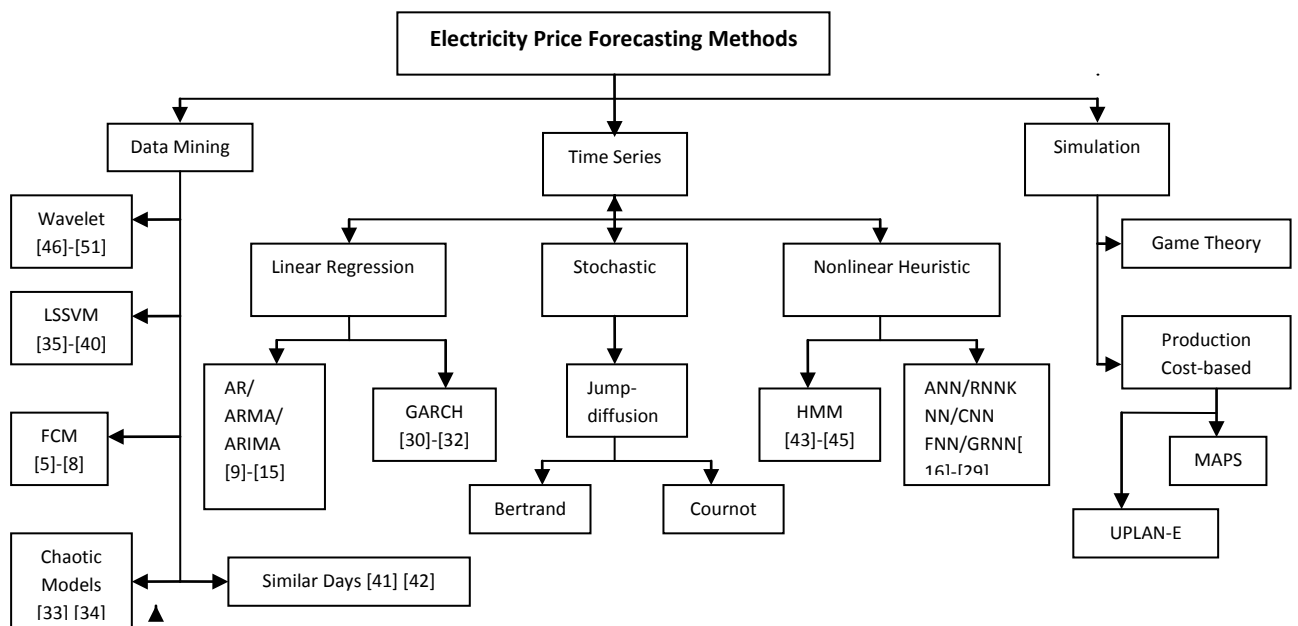


Figure 2. Price forecasting methods classification

In Figure 2, a new branch of data mining methodology has been added to the tree and more typical forecasting methods are included along with the survey papers. In this survey, many publications indicate ANN has become a more popular approach for price forecasting. Meanwhile, hybrid models that combine two or more forecasting methods to overcome the individual limitations are becoming a novel direction for researchers [4].

Conclusion

This paper analyses the characteristics of electricity price series and summarizes the influencing factors of price behaviour. An extended classification of price forecasting methods is proposed. It is noticeable that specific simulation models have inherent disadvantages, which are also discussed in order to make improvements on the model and find a way forward to develop novel approaches. A summary of hybrid methods that combine different models to offset the weaknesses of individual models is presented. Hybrid approaches based on wavelet network models and SVM are reviewed in detail. Based on comparisons of different techniques, this paper highlights the main features of electricity price forecasting methods and indicates the future development of methodologies for accurate electricity price forecasting.

Key References

- [1] Hamed Valizadeh Haghi, and S. M. Moghaddas Tafreshi, "An Overview and Verification of Electricity Price Forecasting Models," *International Power Engineering Conference (IPEC)* 2007.
- [2] Xian Zhang, and Xifan Wang, "Overview on Short-term Electricity Price Forecasting," *Automation of Electric Power Systems*, Vol.30, No.3, Feb.10, 2006
- [3] T. Niimura, "Forecasting Techniques for Deregulated Electricity Market Prices," *IEEE* 2006.
- [4] Carolian Garcia-Martos, Julio Rodriguez, and Maria Jesus Sanchez, "Mixed Models for Short-Run Forecasting of Electricity Prices: Application for the Spanish Market," *IEEE Transaction on Power Systems*, Vol.22, No.2, May 2007

Note: The rest of references [5]-[51] will be included in the full paper.



SED Research Student Conference

Brunel University

22-24th June 2009

Elastohydrodynamic Film Thickness in Variable Conditions

Konstantinos G. Kalogiannis , Romeo P. Glovnea

Lubrication Laboratory

Mechanical Engineering, School of Engineering and Design, Brunel University, Uxbridge,
Middlesex, UK

konstantinos.kalogiannis@brunel.ac.uk

Keywords: elastohydrodynamic lubrication, film thickness, vibrations

Introduction

Many machine components, which work in the Elastohydrodynamic (EHD) lubrication regime, including transportation bearings, reciprocating engines and geared transmissions experience transient conditions due to variation of load, surface geometry, entrainment speed or a combination of these. It is very important to understand how these vibrations affect the functioning of the bearings supporting the main spindle, in order to maintain the desired precision and accuracy of the cutting process.

EHD lubrication under transient conditions is a subject that has received merited attention during the past two decades. From an experimental point of view, this problem has been approached using the optical interferometry technique [1-5]. The aim of this study is to investigate the behaviour of EHD films during lateral oscillatory motion as experienced in the applications stated above.

Methodology/ Approach

The method for measuring the EHD film thickness, used in this study is optical interferometry [6]. Optical interferometry is the only technique which not only can measure accurately the film thickness in elastohydrodynamic contacts, but also is able to map the entire area of the contact, thus allowing the study of local film thickness variation.

In the current arrangement as seen in Figure 1, the contact EHD is formed between a transparent disc and a ball, loaded against each other whilst being driven by independent motors at a desired load of 45N. The disc is coated with a thin chromium layer and a silica layer, on the face contacting the ball.

White light is shown onto the contact through a specially built microscope. The interferometric fringes formed by the rays reflected by the chromium layer and by the ball's surface are captured by a high speed CCD camera at a rate of 2500 frames per second. The lubricant used in these tests, polyalphaolefin (PAO), has a dynamic viscosity of 0.0087 Pa.s at 60°C. The entrainment speed was 3 m/s. The frequency of the lateral oscillations of the ball was set at 50Hz and 100Hz.

Results and discussion

Figure 2 shows typical coloured fringes of an EHD contact. Each colour represents a certain wavelength, which shows separation between two solid surfaces, which means that a map of the film thickness can be extracted from these images. It is well known that the elastohydrodynamic film thickness is established in the inlet of the contact and depends on the entrainment speed, lubricant viscosity and piezoviscosity coefficient inlet geometry and on a much lesser extent on the load. In this case the direction of flow is going downwards as observed in Figure 2. A

constriction is then formed at the exit of the contact which resembles a 'horseshoe' shape, where the minimum film thickness can be found. The central region of the contact area indicates a thicker layer of film caused by the squeeze effect (i.e. due to the increase of pressure as the lubricant builds up at this position). As the lubricated surfaces recede from each other a negative squeeze occurs and therefore negative pressures are predicted within this region. This is observed in the Figure 3 in the form of the lubricant film cavitation within the diverging part of the clearance. In the current arrangement, the Hertzian pressure can reach up to 1.6 GPa and a contact diameter of up to 236 microns.

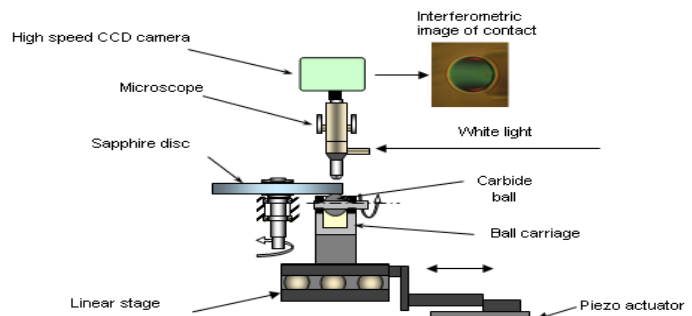


Figure 1. The experimental

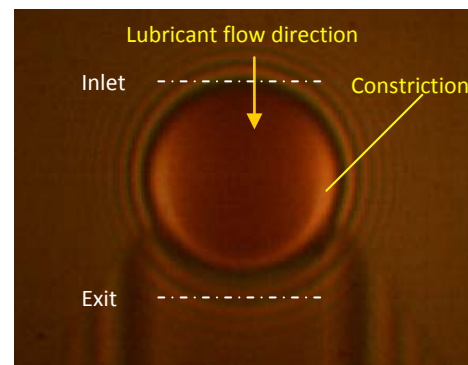


Figure 2. Coloured fringes of the EHD contact

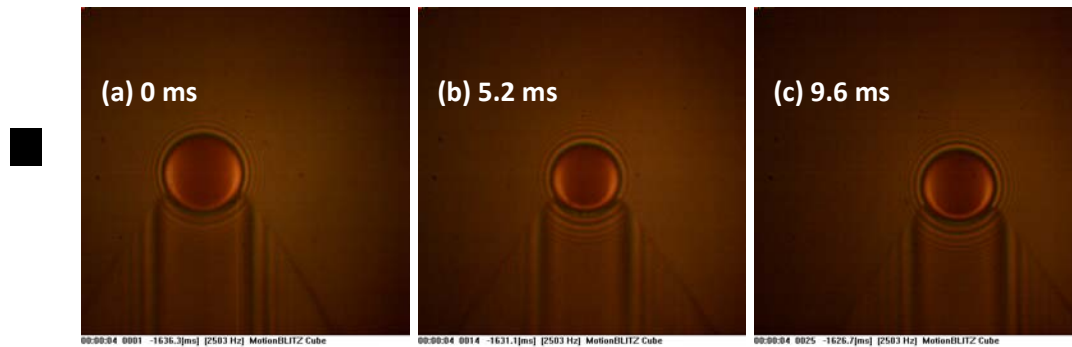


Figure 3. Film thickness profiles along the rolling direction at 50 Hz at different intervals (a) 0 ms, (b) 5.2 ms and (c) 9.6 ms

The images shown in Figures 3a to 3c show profiles of the film thickness along the rolling direction at 50Hz, at various time intervals which have been chosen to show clarity of movement of the contact region between the ball and disc. It is observed that the contact area oscillates from left to right as the time interval changes, with one cycle being completed in 19.6ms. During the cycle, variation of the geometry of the contact (i.e. coloured fringes) does not appear which demonstrates a consistent loading of 45N.

By increasing the frequency in a subsequent experiment to 100 Hz at constant amplitude, it was observed that the speed of the lateral oscillation of the contact region increased, with one cycle being completed in 9.7 ms. Moreover, the film thickness also increases at the centre of the contact region by increasing the frequency.

Conclusion

This abstract shows initial results of a wider study on the behaviour of elastohydrodynamic contacts under lateral oscillations. Optical interferometry coupled with high speed imaging, have been used to measure film thickness in contacts at 45 N.

Results show that the moving speed of the contact area gets larger by increasing the frequency of vibration applied to the ball carriage in the lateral direction by a piezo -actuator.

References

- [1] N. Ren, D. Zhu and S.Z. Wen, 1991, "Experimental method for quantitative analysis of transient EHL," **Trib. Int.**, **24**, pp. 225-30
- [2] H. Nishikawa, K. Handa, K. Teshima, K. Mashuda and M. Kaneta, 1995, "Behaviour of EHL films in cyclic squeeze motion," **JSME**, Vol. 38, No.3, pp.577-85
- [3] J. Sugimura, W.R. Jr. Jones and H.A. Spikes, 1998, "EHD film thickness in Non-Steady state contacts," **ASME Trans J. of Tribology**, Vol.120, pp. 442-452
- [4] M. Kaneta, Y. Kanzaki, K. Kameichi and H. Nishikawa, 1990, "Non-Newtonian response of elastohydrodynamic oil films," **Proc. Jpn. Int. Trib. Conf.**, **3**, pp.1695-700
- [5] C.H. Venner, M. Kaneta and A.A. Lubrecht, 2000, "Surface roughness in elastohydrodynamically lubricated contacts," **Proc. 26th Leeds-Lyon Symp**, Elsevier Science, pp. 25-35

- [6] A. Cameron, and R. Gohar, 1966, "Theoretical and Experimental Studies of the Oil Film in Lubricated Point Contacts," **Proc. Roy. Soc. London A291**, pp. 520-536.



SED Research Student Conference

Brunel University

22-24th June 2009

Reconfigurable Patch Antenna for Cognitive Radio and Wireless Mobile Applications

H. F. AbuTarboush, R. Nilavalan, and H. S. Al-Raweshidy

Wireless Network and Communication Research Centre (WNCC), Brunel University, West
London, UB3 8PH

Hattan.AbuTarboush@brunel.ac.uk

Keywords: Patch Antenna, Reconfigurable Antenna, wideband Tunability Range

Reconfigurable five bands single feed Microstrip Patch Antenna (MSA) is proposed capable of operation between 1 to 3 GHz cellular and wireless radio frequency bands. The antenna connected to one line by four switches (Varactor diodes). Each patch generates a single band. By placing a variable capacitor and an inductor at the antenna input, the impedance matching frequency of the antenna can be varied. The results show a tunable frequency range from 1 to 3 GHz serving 12 applications.

Introduction

The rapid development of electronics and wireless communication has led to great demand for mobile devices that can operate using different standards such as GSM850, GSM900, GPS, DCS, PCS, UMTS, WLAN and WiMAX. In addition, the average consumer also demands smaller form factors for their mobile devices. These two requirements have attracted research on the design of small size and multiband antennas. The advantage of microstrip antenna makes them popular in many applications requiring small size antenna, patch antenna is promising to be a good candidate for the future technology such as cognitive radio system or any other system due to the flexibility of the structure as it can be easily incorporate into the communication equipments.

There are two different categories for reconfigurable antenna; the first category is frequency reconfigurable. The aim of tuning the frequency of the antenna is to have single multifunctional antenna in a small terminal for many services. In [1] a tuning method has been introduced to tune dual band for mobile applications. In [2] reconfigurable dual-band antenna for wireless applications has been reported with very wide range tenability. In [3] reconfigurable patch antenna for satellite and terrestrial application has been reported. From all the above papers, the radiation patterns of these antennas remain unchanged when the frequencies tuned from one band to another. The second type of reconfigurable antenna is radiation patterns reconfigurability, the frequency band remain unchanged while the radiation pattern changes upon the system requirements. The antenna can steer their radiation patterns beams to different direction. These types of reconfigurability have been reported recently in [4-8].

Antenna Structure and Results

The proposed antenna has a very simple structure to manufacture. The antenna is designed in a two-layered printed circuit board (PCB) fed by a 50Ω microstrip line. It consists of four patches, four varactor diodes, one lumped capacitor and bias networks as shown in Fig.1. The four patches designed to generate single band from 1 to 3 GHz. The conventional rectangular patch antenna was designed as the basic structure to operate at 2.4 GHz which is compatible with indoor wireless applications using the given below equations (1) to (4). Then, the total size of the patch was divided and optimized into four patches to generate single band. A varactor diode was placed on the feeding of each patch to control the current generated from the patches.

$$W = \frac{C}{2f_r} \left(\frac{\epsilon_r + 1}{2} \right)^{-\frac{1}{2}} \quad (1)$$

$$L = \frac{C}{2f_r \sqrt{\epsilon_{eff}}} - 2\Delta L \quad (2)$$

$$\epsilon_{eff} = \frac{\epsilon_r + 1}{2} + \frac{\epsilon_r - 1}{2} \left(1 + \frac{12h}{w} \right)^{-\frac{1}{2}} \quad (3)$$

$$\Delta L = 0.412 \times h \left(\frac{\epsilon_{eff} + 0.3}{\epsilon_{eff} - 0.258} \right) \left(\frac{\frac{w}{h} + 0.264}{\frac{w}{h} + 0.8} \right) \quad (4)$$

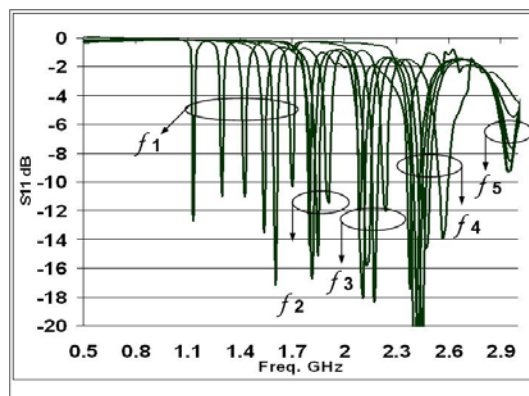
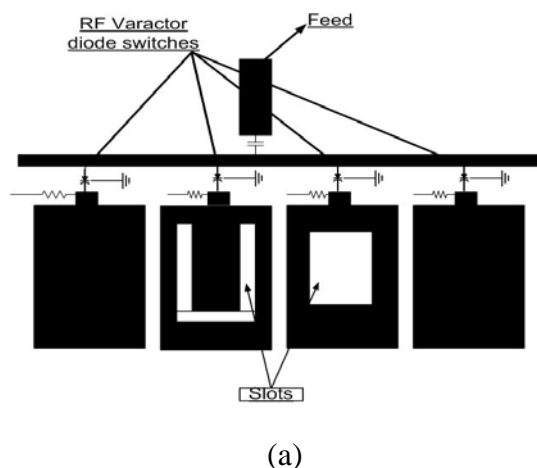


Fig. 1. (a) The structure of the proposed Antenna (b) The measured return Loss

Conclusion

A new technique for designing multi-band reconfigurable antenna is proposed. The frequency response for each band can be tuned by changing the voltages from 0 to 22V. The proposed antenna can be used in more than 12 applications between 1 to 3 GHz. The structure of this antenna is very practical and easy to manufacture. The total size of the ground plane is 50mm X 50mm.

References

- [1] M. Ali, A. T. M. Sayem and V. K. Kunda, "A Reconfigurable Stacked Microstrip Patch Antenna for Satellite and Terrestrial Links," Vehicular Technology, IEEE Transactions on, vol. 56, pp. 426-435, 2007.

- [2] N. Behdad and K. Sarabandi, "Dual-band reconfigurable antenna with a very wide tunability range," *Antennas and Propagation, IEEE Transactions on*, vol. 54, pp. 409-416, 2006.
- [3] S. -. Hsu and Kai Chang, "A Novel Reconfigurable Microstrip Antenna With Switchable Circular Polarization," *Antennas and Wireless Propagation Letters, IEEE*, vol. 6, pp. 160-162, 2007.
- [4] N. Jin, Fan Yang and Y. Rahmat-Samii, "A novel patch antenna with switchable slot (PASS): dual-frequency operation with reversed circular polarizations," *Antennas and Propagation, IEEE Transactions on*, vol. 54, pp. 1031-1034, 2006.
- [5] M. Komulainen, M. Berg, H. Jantunen, E. T. Salonen and C. Free, "A Frequency Tuning Method for a Planar Inverted-F Antenna," *Antennas and Propagation, IEEE Transactions on*, vol. 56, pp. 944-950, 2008.
- [6] Rui-Hung Chen and J. -. Row, "Single-Fed Microstrip Patch Antenna With Switchable Polarization," *Antennas and Propagation, IEEE Transactions on*, vol. 56, pp. 922-926, 2008.
- [7] Shing-Hau Chen, Jeen-Sheen Row and Kin-Lu Wong, "Reconfigurable Square-Ring Patch Antenna With Pattern Diversity," *Antennas and Propagation, IEEE Transactions on*, vol. 55, pp. 472-475, 2007.
- [8] S. Zhang, G. H. Huff, J. Feng and J. T. Bernhard, "A pattern reconfigurable microstrip parasitic array," *Antennas and Propagation, IEEE Transactions on*, vol. 52, pp. 2773-2776, 200.

Operational Analysis of Security Constrained Optimal Reactive Power Flow Solutions

Peter Macfie¹, Paul Hurlock¹, Gary Taylor², Malcolm Irving²

1. National Grid Control Centre, Wokingham, Berkshire, UK

2. BIPS, Brunel University, Uxbridge, Middlesex, UK

peter.macfie@brunel.ac.uk

Keywords (3): Power transmission control, losses, dispatching, power industry, power system modelling, power system security, reactive power, reactive power control, voltage, voltage control.

Introduction

Loss minimisation studies on the Great Britain (GB) transmission network indicate an average theoretical loss reduction of 2.3%. This energy is equivalent to annual emissions of around 74,000 tonnes of carbon dioxide. These studies are based on Security Constrained Optimal Reactive Power Flow (SC-ORPF) calculations, constrained by 800 credible contingencies and voltage limits consistent with the GB Security and Quality of Supply Standards (SQSS). This work demonstrates the value of a multi-staged approach to the transmission loss minimisation problem, both in terms of reducing the overall objective function and removing constraint violations created by discretization. The work reveals additional key findings. Firstly, when starting from a secure GB network operating point, the loss minimisation process encounters few binding contingencies (contingency cases with binding constraints). Secondly, the loss minimisation solutions reduce leading and lagging reactive generation volumes by an average of 13.1%.

Methodology/Approach

A commercial sequential linear programming (SLP) algorithm was selected to solve the main problem, as this is one of the few approaches that can solve this type of optimisation problem within operational timescale requirements [1].

The modelled control variables within the SC-ORPF are:

- Generator voltage targets.
- Static VAR compensator (SVC) voltage targets.
- Discrete shunt capacitors on/off
- Discrete shunt reactors on/off.

Results and discussion

Figure 1 shows the MW losses SC-ORPF results for five day-ahead planning networks from five different staged optimisation approaches, loss reduction % is shown on the x-axis. The figure compares four optimisation approaches in terms of their overall success at reducing the MW losses objective. Additional data is overlaid showing the 1 stage optimisation voltage violations, note that the other solutions from the multi-staged OPF techniques did not contain any voltage limit or voltage change violations. The maximum number of critical contingencies encountered in any of the optimisations is also shown.

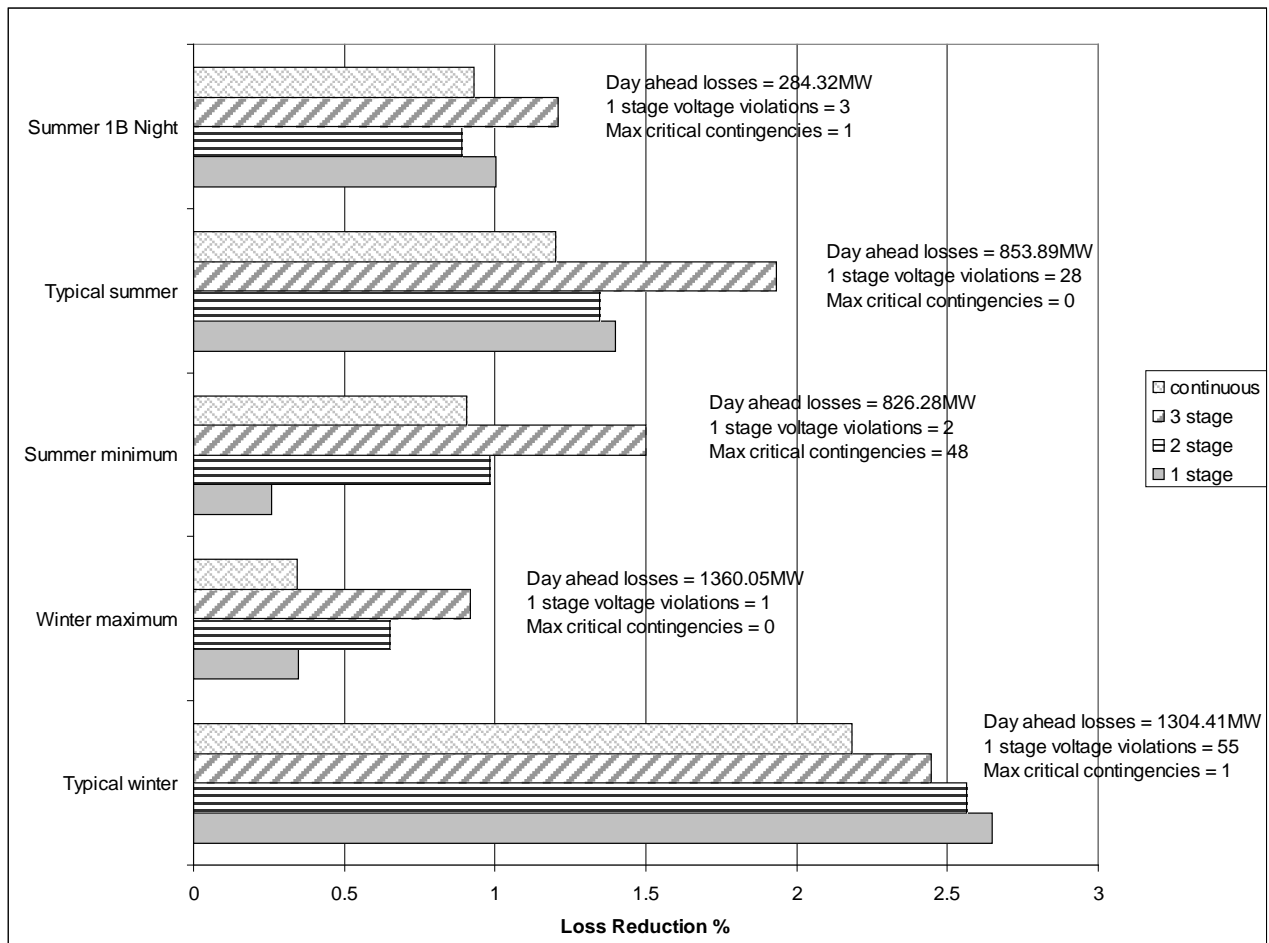


Figure 9. Presents % MW loss optimisation results for the five day-ahead planning networks.

Conclusion

As shown in Figure 1 security constrained optimisation with the MW loss objective has achieved a theoretical MW loss reduction of between 1.1% and 3.5%, with an average of 2.3%. The optimisation has also achieved a simultaneous reduction in reactive generation of between -0.5% and 25.0% with an average of 13.1%.

References

- [1] N. Dandachi, 'Improved algorithm for the voltage/VAR management on the NGC system', IEE Colloquium, Issue 24, pp4/1 – pp 4/6, 1997.



SED Research Student Conference

Brunel University

22nd-24th June 2009

An Analysis of Organisations that have purchased BS 8887-1 (2006)

Alexander Plant

Supervisors: Professor David Harrison, Dr. Brian Griffiths and Dr. Busayawan Ariyaturn

Cleaner Electronics Research Group, School of Engineering and Design, Brunel University,
Uxbridge, Middlesex, UK

Alexander.Plant@brunel.ac.uk

Keywords: Sustainability, SIC, DfE

Introduction

The British Standards Institute's 'Technical Product Realisation' triumvirate of standards encompasses the three interrelated disciplines of product specification (BS 8888), manufacturing (BS 8887) and verification (BS 8889). BS 8887-1 (2006) is titled 'Design for manufacture, assembly, disassembly and end-of life processing' (MADE) [1]. It builds on the earlier design for manufacture standard PD6470. BS 8887-1 is a generic standard and is the first in a series. It is intended to be applicable to a large range of manufactured goods. One of the benefits of the standard is that it facilitates the inclusion of design for the environment principles within product specifications. This is particularly advantageous in light of the growing trend towards global manufacturing, as the standard can be applied to products rather than industrial sites. BS 8887-1 provides designers with practical advice and information about the implications of decisions such as product component fixing methods and material choices with regard to end-of-life processing, and the quality of the resulting secondary materials. It is important because it is the first attempt by a national standards body to address these issues. Its application will help to improve the profitability of recycling activities and thus help to reduce both waste and demand for virgin materials. "Since [the standard] was published, it has been a bestseller and thus indicative of a design need" [2].

The aim of this study was to identify the types of the organizations that have bought BS 8887-1 and group them according to their industry sector. This was done with the objective of assessing industry responsiveness to this voluntary standard, and to look for any relationship between industry specific environmental legislation and adoption of BS 8887-1. The scope has been limited to organizations that have ordered the standard directly and excludes those that may have downloaded it from British Standards Online (BSOL), as this information is not available. The study is original as there has been no previous work in this area and very few academic papers published about BS 8887-1. Its value is in identifying which industries are taking the greatest interest in this official best practice guide, thus

providing an indicator of the desire to progress towards sustainability within various sectors as well as suggesting where market penetration could be improved.

Methodology/Approach

The BSI has supported this study by providing a confidential list of companies and organisations that have purchased BS 8887-1, upon the agreed understanding that this information shall not be disclosed. The first step in analysing the data was to count the frequency of sales per month since publication and to represent this as a graph (Fig. 1). This shows sales up until July 2008. A recent update revealed a further four sales. These were undated, but suggest a natural continuation of the trend.

For the sector analysis, the standard industrial classification (SIC) code for each listed company was added. The information was gathered from Companies House and the FAME database. For other organisations such as some public sector institutions, SIC codes were estimated according to descriptions of their activities presented online. Repeat orders were omitted so as not to bias the results, thus leaving a final list of 118 unique entries.

SIC codes categorise organisations into *Section, Subsection, Division, Group, Class and Subclass*. By dividing the codes in a spreadsheet in accordance with their structure, the frequency occurrence was calculated. This allowed the data to be considered from both general and granular perspectives.

Results and Discussion

The *Sales Distribution over Time* graph (Fig. 1) shows a high initial demand that gradually reduces to a steady rate of one or two per month suggesting an ongoing need.

Recent legislative measures to reduce the environmental impact of consumer products include regulations governing: *Waste Electrical & Electronic Equipment, End of Life Vehicles, Packaging & Packaging Waste, Restriction of Hazardous Substances and Energy-Using Products*. As these directives particularly affect

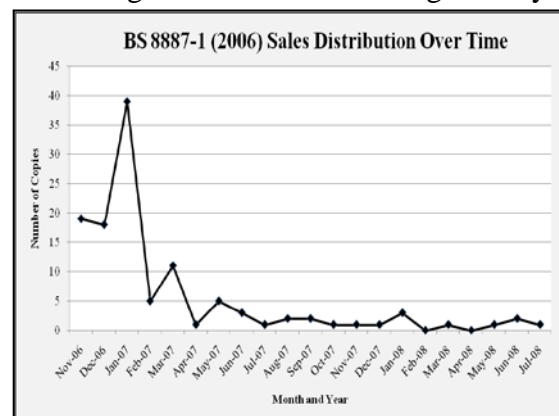


Figure 1

the electronics, automotive and packaging business, it would seem logical to expect multiple instances of SIC codes for these sectors within the results. This hypothesis is partially supported by the high proportion of orders from the electronics sector, accounting for 21 sales from division 31 and 32 (see Fig. 2). However there were surprisingly few from car manufacturers or automotive parts companies, with only three from division 34 and just a couple of other auto-electrical producers. This may be because car manufacturers perhaps generally subscribe to BSOL, thereby potentially skewing the results. Surprisingly, a high proportion of the orders were from medical companies, eight being from SIC 33.10. Possibly, these historically innovative companies are proactively developing sustainable design strategies. Traditional precision engineering companies were also well represented.

None of the orders were from companies whose primary activity was the production of packaging.

Of the non-manufacturing sections, 'K' (*Real Estate, Renting & Business Activities*), was the largest with 20 orders. The majority of the entries were in SIC 74.87 (*Other Business Activities*). The remainder of section 'K' primarily consists of R & D organizations and design consultancies.

Pleasingly, education (Section

M) ranks as the third highest with schools, colleges and universities supporting the standard and presumably teaching students about sustainable design and BS 8887-1.

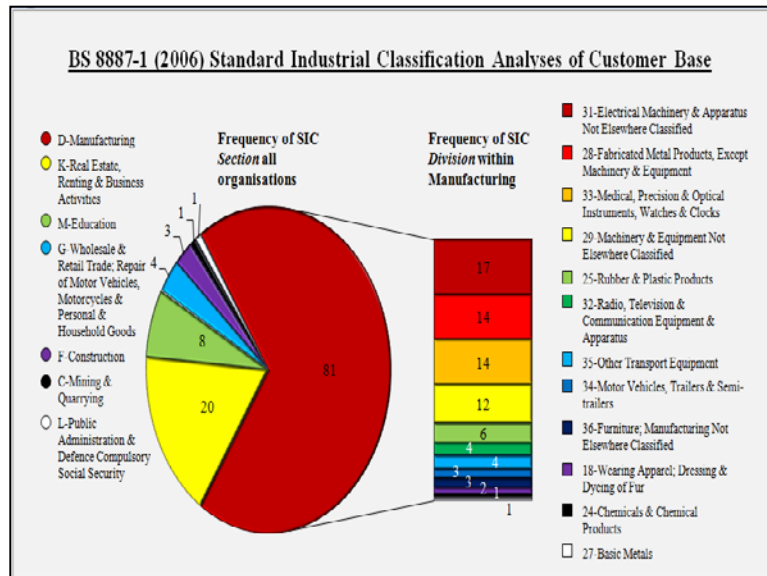


Figure 2

Conclusion

BS 8887-1 has enjoyed high acceptance in manufacturing, especially amongst producers of electrical and electronic products. This sector has been the subject multiple pieces of environmental legislation that may have been a motivating influence. The education sector has also shown encouraging levels of interest.

References

- [1] British Standards Institution (2006) *Design for Manufacture, Assembly, Disassembly and End-of life Processing (MADE) – Part 1: General Concepts, Process and Requirements*, (BS 8887-1).
- [2] Griffiths, B. (2008) "The New Suite of 'Design for Manufacture' British Standards", *Journal of the Institution of Engineering Designers*, **34**, 6, pp. 21-24.
